Tropical Water Quality Hub

National Environmental Science Programme

Final Report

Bund wall removal increases saltwater intrusion and controls invasive aquatic weeds on a coastal floodplain

Nathan Waltham, Maria Fernanda Adame, Fazlul Karim, Brett Abbott and Jim Wallace



JAMES COOK UNIVERSITY AUSTRALIA

Bund wall removal increases saltwater intrusion and controls invasive aquatic weeds on a coastal floodplain

Nathan Waltham[1], Maria Fernanda Adame[2], Fazlul Karim[3], Brett Abbott[3], Jim Wallace[1]

[1] TropWATER, Centre for Tropical Water and Aquatic Ecosystem Research, James Cook University, Australia
[2] Australian Rivers Institute, Griffith University, Australia
[3] CSIRO Land and Water, Australia





Supported by the Australian Government's
National Environmental Science Program
Project 3.3.2 Science evaluation of coastal wetland systems repair projects across GBR catchments

© James Cook University, 2020



Creative Commons Attribution
Bund wall removal increases saltwater intrusion and controls invasive aquatic weeds on a coastal floodplain is licensed by James Cook University for use under a Creative Commons Attribution 4.0 Australia licence. For licence conditions see: https://creativecommons.org/licenses/by/4.0/

National Library of Australia Cataloguing-in-Publication entry:
978-1-925514-58-2

This report should be cited as:
Waltham, N. J., Adame, M. F., Karim, F., Abbott, B., Wallace, J. (2020) *Bund wall removal increases saltwater intrusion and controls invasive aquatic weeds on a coastal floodplain.* Report to the National Environmental Science Program. Reef and Rainforest Research Centre Limited, Cairns (83pp.).

Published by the Reef and Rainforest Research Centre on behalf of the Australian Government's National Environmental Science Program (NESP) Tropical Water Quality (TWQ) Hub.

The Tropical Water Quality Hub is part of the Australian Government's National Environmental Science Program and is administered by the Reef and Rainforest Research Centre Limited (RRRC). The NESP TWQ Hub addresses water quality and coastal management in the World Heritage listed Great Barrier Reef, its catchments and other tropical waters, through the generation and transfer of world-class research and shared knowledge.

This publication is copyright. The Copyright Act 1968 permits fair dealing for study, research, information or educational purposes subject to inclusion of a sufficient acknowledgement of the source.

The views and opinions expressed in this publication are those of the authors and do not necessarily reflect those of the Australian Government.

While reasonable effort has been made to ensure that the contents of this publication are factually correct, the Commonwealth does not accept responsibility for the accuracy or completeness of the contents, and shall not be liable for any loss or damage that may be occasioned directly or indirectly through the use of, or reliance on, the contents of this publication.

Cover photographs: (Front) Boolgooroo lagoon, Mungalla; (Back) Wetland bore water quality monitoring at Mungalla. Images supplied by Nathan Waltham.

This report is available for download from the NESP Tropical Water Quality Hub website:
http://www.nesptropical.edu.au

CONTENTS

Contents i
List of Tables iii
List of Figures iv
Acronyms vi
Abbreviations vi
Acknowledgements vii
Executive Summary 1
1.0 Introduction 3
1.1 Mungalla wetland complex 7
1.1.1 Rainfall and hydrology at the Mungalla wetland complex rainfall and hydrology - snapshot 9
2.0 Methods 10
2.1 Hydrodynamic modelling 10
2.1.1 Model framework 10
2.1.2 Model inputs 10
2.1.3 Scenario modelling 11
2.2 Physicochemical monitoring 11
2.2.1 Logger network 11
2.2.2 Logger data analysis 12
2.3 Vegetation monitoring 12
2.4 Fish surveys 12
3.0 Results 14
3.1 Hydrodynamics 14
3.2 Physicochemical monitoring 18
3.3 Vegetation monitoring 22
3.3.2 Pre-bund removal on Boolgooroo 22
3.3.3 Post-bund removal (Boolgooroo lagoon) 22
3.3.4 Post-bund removal (Annabone) 23
3.4 Fish surveys 26
4.0 Discussion 28
5.0 Conclusions and recommendations 31
References 33
Appendix 1: Rainfall and Hydrology 37
A1.1 Rainfall 37

A1.2 Streamflow and catchment runoff 40
A1.3 Tide and wetland inundation 41
A1.3.1 Frequency of high tides 42
Appendix 2: Hydrodynamic model development 44
A2.1 Modelling tools 44
A2.1.2 Regular grid model 44
A2.1.2 Flexible grid model 45
A2.2 Model inputs 45
A2.2.1 Topography 45
A2.2.2 Surface roughness 46
A2.2.3 Inflow 47
A2.2.4 Seaside boundary 47
A2.3 Model configuration 47
A2.3.1 Regular grid model [MIKE 21] 47
A2.3.2 Flexible grid model [MIKE 21 FM] 48
A2.4 Model calibration 48
Appendix 3: Vegetation composition change 52
Appendix 4: Saline groundwater trial 54
Appendix 5: Grazing damage observations 55
Appendix 6: Observation of mangrove stress 57
Appendix 7: Nitrogen removal by tropical floodplain wetlands through denitrification 60
Appendix 8: Carbon and Nitrogen Sequestration of Melaleuca Floodplain Wetlands in Tropical Australia 70

LIST OF TABLES

Table 1: Summary of tidal inundation simulation scenarios using a MIKE21 hydrodynamic model at the Mungalla wetland complex 11
Table 2: Effect of tide height on seawater intrusion and inundation depth at Mungalla wetland. Presented is the distance of tidal ingress (m), extent inundated at various depths (ha), the volume of seawater ingress (m^3), and the mass of salt introduced to the wetland (tonnes). 15
Table 3: Effect of on shore wind on seawater intrusion and inundation depth in the wetland. Also shown are the total volume of seawater entering the wetland and the weight of salt it content. 16
Table 4: Effect of low atmospheric pressure (950 hPa) on inundation and seawater intrusion 17
Table 5: Effect of sea-level rise on inundation and seawater intrusion into the wetland. 18
Table 6: Simple contrasts for water quality measurements - above and below bund location and before and after bund removal combinations (2014-2016 = After) (Abbott et al., 2020). 19
Table 7: Simple contrasts for water quality measurements - before and after bund removal combinations Before = 2012-13, After = 2014-16, After2 = 2017-18 .19
Table 8: Fish assemblage recorded in Mungalla wetland, before and after bund wall removal works 26
Table 9: Summary wet season (Nov – March) statistics of rainfall recorded at Victoria Point Sugar Mill station 37
Table 10: Summary dry season (April – October) statistics of rainfall recorded at Victoria Point Sugar Mill station 37
Table 11: Number of tides per year greater than 3.7 to 4.1 m at Forrest Beach (3 km from the Mungalla wetland).....43
Table 12: Major tide constituents at Lucinda (based on 1 year of tide data) 49
Table 13: Area inhabited by vegetation groups (%): pre- (2012/13) and post (2014 - 2017) bund removal -tidal inundation 52
Table 14: Area inhabited by vegetation groups (%): pre- (2012/13) and post (2014 - 2017) bund removal - no tidal intrusion. 53

LIST OF FIGURES

Figure 1: Conceptual diagram of bund wall in coastal wetlands (Source, Paul Groves, Great Barrier Reef Marine Park Authority) 6
Figure 2: Location of wetlands within Mungalla station in the lower Herbert River catchment, Queensland, Northern Australia. The Mungalla wetlands are hatched in dark grey, the Boolgooroo region of the wetland complex is shown in yellow. Also shown are the locations of the logger sites above and below the earth bund which was removed on 6th October 2013. Reproduced from Abbott et al (2020). 8
Figure 3: Excavator breaching the earth wall in August 2013 (Photo credits M. Nicholas) 9
Figure 4: (A) Aquatic plant community upstream of the earth wall (approximately July 2013) with extensive invasive freshwater weeds, and B) same photo location after the removal of the earth wall section (approximately September 2015) (Photo credits M. Nicholas)..... 9
Figure 5: Predicted seawater inundation at the Mungalla wetland for a 4.3 m tide with (a) and without (b) the tidal bund in place. 14
Figure 6: Seawater inundation and depth predicted at the Mungalla wetland for (a) 4.1 m tide and (b) 4.3 m tide.....14
Figure 7: Wetland inundation scenarios for different tides and on shore winds, (a) 4.3 m tide and 5 m/s wind speed, (b) 4.3 m tide and 10 m/s wind speed 16
Figure 8: Wetland inundation for a low-pressure system (950 hPa): (a) 0.6 surge coincides with a 3.7 m tide, (b) 0.6 surge coincides with a 4.3 m tide. 17
Figure 9: Maximum extent of wetland inundation for a combined 3.7 m tide and a SLR of (a) 50 cm and (b) 80 cm. 18
Figure 10: The percentage of time depth exceeded any given threshold within the Boolgooroo wetland, vertical dotted line shows the threshold depth for reduction of tidal inflow due freshwater outflow (hydrologic pressure) at 40 cm.....20
Figure 11: The percentage of time EC exceeded any given EC threshold during pre and post bund removal years within the Boolgooroo wetland. Horizontal dashed lines show boundaries between fresh, brackish, saline and briny water from left to right. 20
Figure 12: Proportion of temperature above any given threshold, vertical dotted line shows the exceedance threshold for aquatic biota. Presented here is the acute effect temperature threshold of fly specked hardyhead of 31.4^{o}C (Burrows & Butler, 2012). 21
Figure 13: The percentage of time DO exceed any given DO threshold in the Boolgooroo wetland. Vertical dashed lines represent critical values of DO affecting fish species, a) acute trigger value, b) chronic trigger value and b) to c) optimal DO for fish species. From dissolved oxygen guidelines for freshwater habitats of Northern Australia (Butler & Burrows, 2007). 21
Figure 14: Time-series of classified imagery for Boolgooroo lagoon – area inundated by tidal water after bund removal (updated from Abbott et al., 2020). 24
Figure 15: Time-series of classified imagery for Annabone and north Boolgooroo – area not inundated by tidal water (updated from Abbott et al., 2020). 25

Figure 16: Barramundi (*Lates calcarifer*) captured in Boolgooroo upstream of bund wall after its removal 27
Figure 17: BOM wet-season (Nov - March) rainfall data recorded at Victoria Point Sugar Mill (station number 32045) ranked in order of decreasing total rainfall (mm). Blue bars show total rainfall over the past few years, red bars cover wet season during this survey 38
Figure 18: BOM dry-season (April - October) rainfall data recorded at Victoria Point Sugar Mill (station number 32045) ranked in order of decreasing total rainfall (mm). Blue bars show total rainfall over the past few years, red bars cover dry season during this survey 39
Figure 19: Annual flow in the Stone River at Running Creek upstream of the Mungalla wetland 40
Figure 20: Mean monthly flow distribution at Running Creek in the Stone River based on observed flow records for the period of 1980 to 2014. 41
Figure 21: An example of typical tidal cycles at Forrest Beach. Data are presented with respect to lowest astronomical tide (LAT) datum. 42
Figure 22: Observed tides at Forrest Beach since 2012 that are greater than 3.7 m. Data are presented with respect to lowest astronomical tide (LAT) datum (AHD is 1.844 m above LAT and 0.053 m below MSL) 42
Figure 23: Mungalla topography model showing Annabone and Boolgooroo lagoons, logger sites and bund wall 46
Figure 24: An example of flexible mesh hydrodynamic modelling grids with different mesh zones for rivers, riparian zones and the adjacent land subject to inundation. .48
Figure 25: Comparison between observed (blue) and predicted (red) tide level at Lucinda. The black line shows the prediction error (Note: MSL at Lucinda is 0.053 m above AHD) 49
Figure 26: Comparison between high and low tides at Lucinda (observed) and Forrest Beach (simulated) for January 2012 50
Figure 27: Comparison between observed (green dots) and simulated (orange line) water depths in the Mungalla wetland at (a) 250 m and (b) 50 m below the bund, and (c) 250 m and (d) 450 m above the bund for the tide in January 2014 (calibration). 51
Figure 28: Comparison between observed (green dots) and simulated (orange line) water depths at 250 m below the bund for the tides of 3.9 m in August 2014 and 4.0 m in February 2015 (verification). 51
Figure 29: Example of the feral pig damage to Mungalla tidal wetland region across saltmarsh meadow 56
Figure 30: Example of the cattle access and trampling of important marine aquatic plants. Fencing cattle from accessing coastal wetland areas is necessary in order to prevent further damage and further loss of the ecosystem services provided 56
Figure 31: Second bund wall site located in Mungalla. Yellow polygon shows where feral pig impact was greatest, green polygons show where erosion of saltmarsh vegetation greatest because of increased sea level rise, and ponded tidal water downstream of the second bund wall illustrating altered hydrology following construction of the bund wall, and its breach some years ago 58
Figure 32: Example of a mangrove in Mungalla wetland under stress from changing local conditions 59

ACRONYMS

ANZECC……. Australia and New Zealand Environment Conservation Council
ANOVA ..... Analysis of Variance
DEHP ..... Department of Environment and Heritage Protection
DEM..... Digital Elevation Model
DES..... Department of Environment and Science
DO ..... Dissolved Oxygen
EC..... Electrical Conductivity
GBR..... Great Barrier Reef
HES..... High Ecological System
JCU..... James Cook University
LAT ……. Lowest Astronomical Tide
NALC……... Nywaigi Aboriginal Land Corporation
NE..... North East
NESP ..... National Environmental Science Program
TWQ..... Tropical Water Quality
WONS……. Weed of National Significance

ABBREVIATIONS

cm.....centimetre
ha.....hectare
hc3.....heteroscedasticity-corrected coefficient covariance matrix
m.....metre
mb .....standard atmospheric pressure
mm.....millimetre

ACKNOWLEDGEMENTS

We acknowledge the contribution of stakeholders who have provided advice and input into the project, with specific reference to:

- We acknowledge the National Environmental Science Program (NESP) Tropical Water Quality (TWQ) Hub funding provided by the Australian Government.
- We thank Jacob Cassady from Nywaigi Aboriginal Corporation for Development for permission to access the wetland, and continued support and advice during the project.
- Mike Ronan and Andrew Meiklejohn from Queensland Wetlands Team (Department of Environment and Science, DES). Carla Wegscheidl (DES) and Professor Pearson, James Cook University (JCU) provided constructive comments on an early draft of this report.
- Mike Nicholas provided valuable insight into the history and early restoration efforts for the site.
- Dr Lynise Wearne, Merv Pyott, and Belinda Bickley from Greening Australia also provided technical support and assistance during field work
- Dr Adam Canning assisted with edits and improvements to the final version of this report.

EXECUTIVE SUMMARY

The construction of earth (bund) walls/banks to collect and retain freshwater for the purposes of supporting stock during late dry season has occurred in many places along the Great Barrier Reef (GBR) coastline. They occur over a variety of habitats including wetlands, floodplains or directly across tidal low-lying plains to limit or prevent tidal intrusion and encourage pasture growth. These areas often contain semi-aquatic invasive weeds – namely Para grass (*Urochloa mutica*), Aleman grass (*Echinochloa polystachya*) and Hymenachne (*Hymenachne amplexicaulis*) which have been introduced to provide a late dry season food source for cattle – in an attempt to drought-proof farms particularly in low rainfall areas. These developments potentially have major effects on viability of fisheries habitat - for example on the central Queensland plains it has been estimated that more than 16,000 ha of ponded areas occur adjacent to important fish nursery areas.

We demonstrated that the presence of the earth bund prevented seawater entering the Mungalla wetland, even for the highest tides of 4.3 m. When it was removed (Oct 2012) tides higher than 3.7 m entered the wetland, inundating progressively larger areas as the tide height rose to 4.3 m, when ~ 12.5 % of the wetland was flooded to a depth of ~ 0.5 m. Large volumes of seawater (up to 118060 m^3) containing up to 4132 tonnes of salt entered the wetland, but much of this would have drained from the wetland as the high tides receded. When onshore winds coincide with high tides there can be substantial increases in wetland inundation. Whereas moderate breezes (up to 5 m/s) cause little increase in inundated area, strong winds (~10 m/s) increases the inundated area by 200 % and the volume of water entering the wetland by over 400 %. Under these conditions the highly weed infested part of the wetland (Annabone) would also be inundated with seawater. The marked difference at these two wind speeds is because wave height increases rapidly with wind speed. When high tides and low atmospheric pressure cyclonic conditions coincide, the result is a greater penetration of seawater into the wetland. The low pressure, with a 3.7 m tide, causes inundation similar to that under a 4.3 m tide with normal atmospheric pressure. A more serious scenario is when low pressure coincides with the higher 4.3 m tide, when 353 ha (~80%) of the wetland is inundated to a depth of up to 1.1 m. In this scenario seawater penetrates the wetland to 2370 m above the bund. Simulation of sea level rise shows that seawater will enter the wetland (above the bund) on tides that previously did not reach it. For example, whereas a 3.7 m tide does not currently enter the wetland it will cause significant flooding by 2060 and beyond. This also implies that tides lower than this, down to 3.2 m, will also reach the wetland and these occur much more frequently. For example, a 3.2 m tide occurs 122 days per year compared to only 16 days per year for a 3.7 m tide. The rare high tides of 4.3 m, which occur ~ once every 5 years would cause massive ingress of seawater (3,414,365 m^3) with deep flooding (over 1.4 m), and bring a huge tonnage of salt into the wetland (119,503 tonnes).

The water quality data presented here confirms the major improvements to system repair that have been achieved in the Mungalla wetland resulting from the removal of the earth bund constructed over 80 years ago. Most notably, dissolved oxygen and pH improved in the wetland, towards ranges more likely to reduce acute and chronic exposure risks to fish. These improvements were achieved entirely by restoring the tidal nature of the wetland, a condition that will likely not require future on-going maintenance (e.g., spraying and mechanical dredging costs) if no further bunding is put in place. Improvements in connectivity with the downstream

estuary and in water quality have also resulted in fish species being now able to access the wetland area upstream of the bund.

Removal of bund walls that were constructed to prevent tidal ingress to low-lying areas to allow establishment of ponded pastures in northern Queensland are of increasing interest to managers and scientists as potential restoration opportunities that maximise the benefits on the investment. However, little explicit data exists on the environmental services that can be achieved, and also lost, as a result of this restoration activity exists. This report represents the most comprehensive investigation, using multiple lines of evidence, to assist in both understanding the scale of the opportunity and consequences, and also the timeframes and works needed to achieve and protect the restoration goals set by local community groups involved in the project (or landholders). There may also be negative impacts of removing the bund as a result of the creation of clearer, weed free, water and more rapid drainage of coastal wetlands, including increased risk of exposure to high water temperatures for aquatic species, lost habitat for freshwater species including freshwater turtles, birds and invertebrates. The loss of these freshwater values needs full consideration for any bund wall removal project. Although saltwater intrusion and elimination of freshwater weeds occurred in the initial, low rainfall years after bund wall removal, when average or above average rainfall returned, freshwater invasive plants returned, or were replaced with more saltwater-tolerant plant species. This contrast between wet and dry years has important consequences for the successful management of the wetland, but with projected sea level rise the difference may become less obvious as more tides will reach the wetland. Overall, the Nywaigi people have been heavily impacted by urban and agricultural development and suffered disconnection from their lands for close to 100 years. This wetland restoration project continues to be an important opportunity for Nywaigi people to re-establish links with their coastal country – however, this objective will require on-going maintenance of the site to keep it free of weeds, and invasive animals, in addition to stock management on-site.

1.0 INTRODUCTION

Coastal floodplain wetlands provide essential habitat for a range of flora and fauna that hold cultural, social and economic values that deliver diverse amenity and ecosystem services (M Elliott & Whitfield, 2011; Michael Elliott et al., 2016; Gorski et al., 2011; Waltham & Fixler, 2017). Their low-lying position makes them vulnerable to runoff from urban, agricultural and industrial sites (Barbier et al., 2011; Creighton et al., 2015), sea level rise from climate change (Lee et al., 2019; Rogers et al., 2019), and drainage and reclamation (Coleman et al., 2008). Global floodplain wetland loss is estimated at 95 km^2/yr and unlikely to slow (Coleman et al., 2008; Davidson, 2014). There is, however, an increasing global movement to halt this loss and degradation, and to commence large-scale programs to repair and restore coastal wetland ecosystem habitat and connectivity (Barbier, 2013; Van Coppenolle & Temmerman, 2019). The United Nations General Assembly declared 2021-2030 as the Decade of Ecosystem Restoration, embedded within multiple global Sustainable Development Goals, including the universal provision of clean water access, the sustainable management of land and water ecosystems, and climate action (United Nations General Assembly, 2015).

Australia also faces a legacy of lost and degraded coastal wetland habitat, driven largely from agricultural and urban development over the last 200 years (Creighton et al., 2016). Not only does the loss of coastal wetlands impact the biological communities they support, it also impacts ecosystems they are connected to, as they provide habitat for migratory species, regulate flows, reduce sedimentation and reduce nitrogen runoff (Bainbridge et al., 2009; Brodie & Waterhouse, 2012; Waterhouse et al., 2016). Such that the loss of Queensland's coastal wetlands has contributed to a reduction in the Great Barrier Reef's (GBR) resilience to future development and climate pressures (DEHP 2016). In response to this, a raft of management strategies and legislation has been developed that seek to protect against further degradation and encourage restoration of coastal wetlands (Box 1).

The push for restoration has been met with optimism by scientists (Waltham et al., 2020); however, to date, many restoration projects have been unable to demonstrate success, in part, due to the lack of scientific guidance and data collection (Paschke et al., 2019; Waltham et al., 2019; Weinstein et al., 2019). For instance, removing non-native macrophytes is common regardless of whether the goal of the restoration project is to improve water quality or to increase biodiversity (Zedler & Callaway, 2000). If biodiversity outcomes are expected, the removal of non-native macrophytes could be important, as they reduce oxygen availability in the water column, which results in reduced fish habitat (Perna et al., 2012; Waltham & Fixler, 2017). However, macrophyte removal efforts might be conducted differently if the goal is improvement of water quality, as denitrification will decrease if the macrophytes are removed (Alldred & Baines, 2016). Therefore, a 'one size fits all' approach can often lead to inappropriate restoration outcomes that are poorly aligned with project objectives. Inappropriate applications of restoration methods can be prevented by examining their outcomes where they have been applied previously and then using those learnings to assess the suitability at future restoration sites.

The removal of tidal bunds to restore coastal habitats has become an attractive option for coastal restoration managers in Australia, including the GBR catchments, yet like many other restoration methods, the efficacy and outcomes of this technique have not been assessed in

Australia (Challen & Long, 2004; Kelleway et al., 2017). Tidal bund walls were initially constructed in many places along the GBR coastline to provide stock with ponded pasture as late dry season forage. The exclusion of saline sea water permitted the growth of freshwater macrophytes, namely Para grass (*Urochloa mutica*), Aleman grass (*Echinochloa polystachya*) and Olive hymenachne *(Hymenachne amplexicaulis*), allow the health and condition of livestock to be maintained throughout the dry season – saving on brought-in supplementary feed and improving farm resilience to drought (Challen & Long, 2004; Hyland, 2002). Whilst they provide on-farm benefit, the ponded pastures carry out a range of environmental processes; whether those processes are deemed positive or negative is context dependent. Understanding these processes, and the processes of an altered system where tidal bunds have been removed to allow seawater ingress, would be critical in deciding whether tidal bund removal is a suitable restoration technique for future coastal wetland repair projects.

There are a number of environmental processes resulting from ponded pasture construction (Figure 1). The most apparent is that the earth wall becomes a direct barrier to movement of fish and other aquatic fauna, effectively limiting available habitat areas to complete lifecycles (e.g. mangrove jack). On the central Queensland plains it has been estimated that more than 16,000 ha of ponded areas occur adjacent to important fish nursery areas (Houston & Duivenvoorden, 2002). With excessive aquatic plant growth/high organic load and warm water conditions associated with the bund walls, the stagnant waters can become anoxic (Burrows et al., 2012). During rainfall these waters (termed black water) contribute to massive fish kills not only in the pond itself (Butler & Burrows, 2007), but extend downstream into estuaries causing more regional problems including fish kills, and impact on marine plants (Burrows et al., 2012; Burrows & Perna, 2005). Another service ponded pastures provide is that they trap sediment, potentially more course sediment particles, in much the same way that the natural wetland vegetation would without the walls – this service might be also seen as a negative given that the supply of sediment to estuaries from catchments is decreased, causing erosion of banks and channels downstream (Figure 1). The provision and loss of these processes will inevitably be a determinant on whether bund removal for restoration is a suitable technique for a particular repair project.

The application of the tidal bund removal restoration within the GBR catchments may reduce the risk of black water flow events from reaching coastal areas and causing fish kills (Perna et al., 2012; Waltham & Fixler, 2017), improve the natural control of invasive freshwater plants rather than using chemical control methods (Abbott et al., 2020), increase opportunities for mangrove and saltmarsh expansion and blue carbon additionality (Kelleway et al., 2017; Lovelock & Duarte, 2019), and increase fisheries habitat extension and passage (Waltham et al., 2019). Despite these perceived restoration achievements following bund wall removal, data supporting the efficacy of this restoration technique has not been assessed and presented in a single resource document. Here we combine an extensive program of high frequency logging of water depth and quality before and after bund wall removal, hydrodynamic modelling, vegetation mapping, carbon additionality measures and ecological assessment in order to examine the components and processes lost and achieved by the restoration action of bund wall removal at the Mungalla wetland complex within the GBR catchment. We also examined how the services of this wetland might change in future scenarios, for example, under sea level rise. Finally, we present recommendations to improve the success of future tidal bund removal restoration projects.

Box 1. GBR wetlands management framework.

Legislation governing Australia's Great Barrier Reef (GBR), a World Heritage Area and National Marine Park, reflect a desire for coastal wetland restoration. In response to the loss of coastal wetlands that are reducing the GBR's resilience to future disturbance, the overarching framework for managing the GBR, the *Reef 2050 Long-term Sustainability Plan* (Reef 2050 Plan hereafter), and its subordinate *Wetlands in the Great Barrier Reef Catchments Management Strategy 2016-2021* (Reef wetlands strategy) and *The Reef 2050 Water Quality Improvement Plan 2017-2022* (Reef WQ Plan), all recognise the need to maintain and improve the net extent and condition of wetlands, within a whole-of-system catchment management approach. In addition to the Reef 2050 Plan framework, there are numerous laws regulating the development or disturbance of coastal habitats, including the Australian Government's *Environment Protection and Biodiversity Conservation Act 1999* and the Queensland Government's *Environmental Protection Act 1994*, *Fisheries Act 1994*, *Marine Parks Act 2004*, *Planning Act 2016*, *Vegetation Management Act 1999* and *Water Act 2000*. While the *Queensland Environmental Offsets Act 2014* provides a framework to facilitate environmental offsets that may lead to restoration of degraded habitats or creation of wetlands with demonstrable benefits.

Whole-of-system catchment management is an integrated approach to catchment management and the protection, maintenance and restoration of wetland systems (catchment strategy). The approach integrates information on natural and human values of a wetland with catchment functioning. Most wetlands have multiple values and managing wetlands effectively involves balancing these values to achieve the best outcomes economically, socially and environmentally. Restoring wetland services first requires defining the values desired, for example, bird habitat, fish habitat, water quality, carbon abatement, hydrology, or cultural. These values will differ between stakeholders and locations. Ecosystem repair strategies seem to be most effective when values of all stakeholders are incorporated, a process best facilitated through discussions to set objectives early in the project lifecycle. Often there will be trade-offs between values, for example, wetlands designed for high nitrogen attenuation are often poor for carbon abatement. The nature of the catchment can heavily influence the ability of a wetland to support given values, integrating desired values with catchment functioning is, therefore, critical to successful restoration. Once the values are set and agreed to by relevant stakeholders, wetland restoration projects can then be prioritised and implemented in a way that supports the identified values and catchment constraints, maximising the likelihood of a successful restoration that is generally accepted.

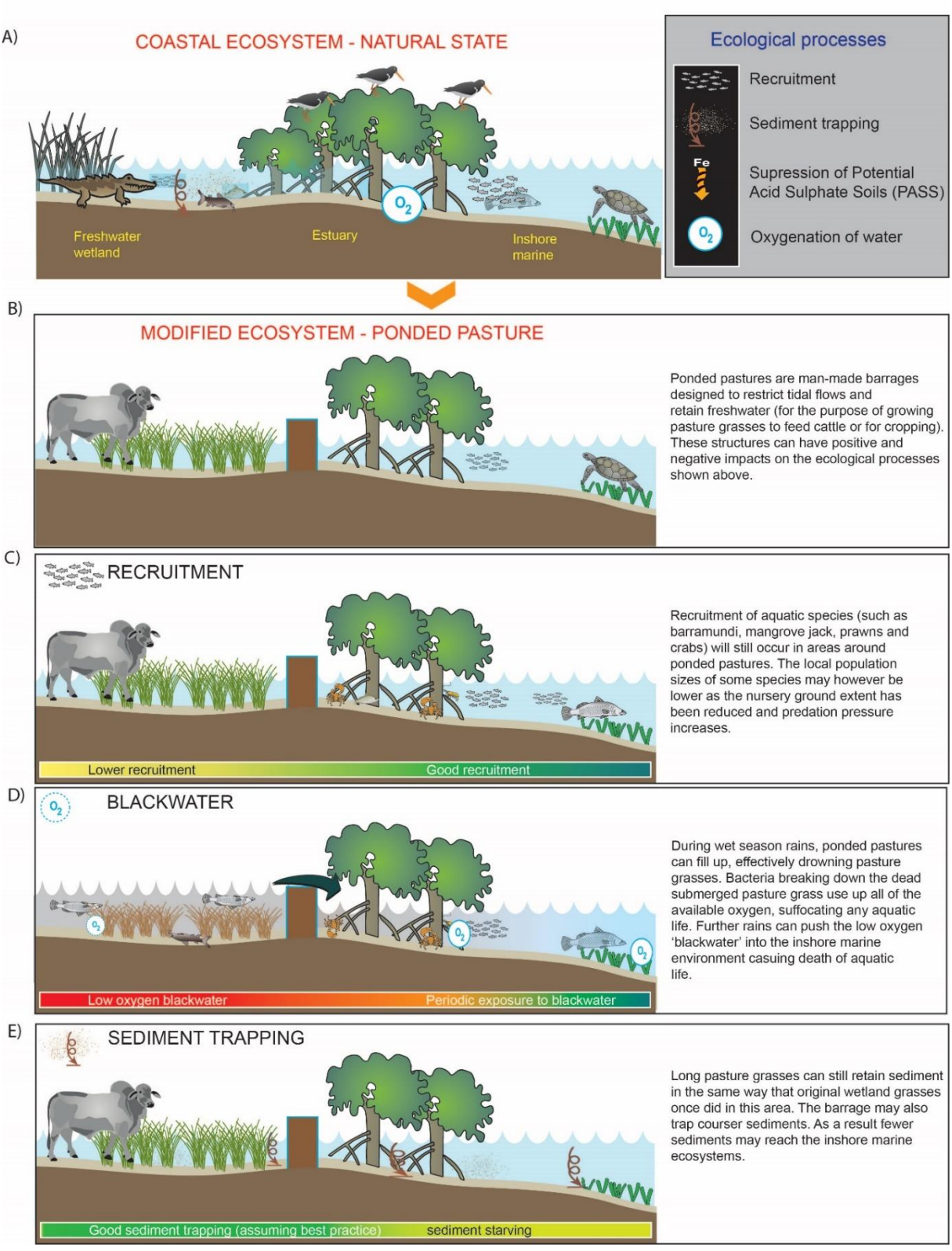


Figure 1: Conceptual diagram of bund wall in coastal wetlands (Source, Paul Groves, Great Barrier Reef Marine Park Authority)

1.1 Mungalla wetland complex

Mungalla Station (-18.707º, 146.261º) is an 830 hectare (ha) property located on Palm Creek in the lower Herbert valley east of Ingham in north Queensland. The Mungalla property is centrally located within the ancestral lands of the Nywaigi people (Grice et al., 2012). The Nywaigi people have been heavily impacted by urban and agricultural development and suffered disconnection from their lands for close to 100 years. In 1999 Mungalla was reclaimed by purchase on behalf of the Nywaigi Aboriginal Land Corporation (NALC) providing an opportunity for Nywaigi people to re-establish links with their coastal country (Abbott et al., 2020).

The site is mapped as a High Ecological System (HES) with very high conservation values (WetlandInfo, accessed November 2019). The property includes a large area (~ 160 ha) of coastal wetland which historically (pre-European settlement) was estuarine towards the coast merging into palustrine wetlands further inland (Figure 2). These estuarine wetlands would have previously supported *Melaleuca* and mangrove forests on the seaward edge with saline to hyper-saline vegetated saltmarsh landward. Further inland, saltmarsh would have merged into intertidal grass-sedge wetlands dominated by Bulkuru (*Eleocharis dulcis*) with fringing *Melaleuca* freshwater forest (Blackman et al., 1999). Bunding of the Mungalla grass-sedge wetlands, landward of the saltmarsh, was completed in the mid-1940s, as a trackway to provide access across the wetlands. Shortly after, Para grass (*Urochloa mutica*) was introduced into the freshwater ponded area on the landward side of the bund wall. More recently, two other ponded pasture species have been introduced - Olive hymenachne (*Hymenachne amplexicaulis*) and Aleman grass (*Echinochloa polystachya*). These two species were released into Queensland in 1988 despite warnings about possible weedy invasion by the Queensland Environmental Protection Agency (Csurhes et al., 1999; Csurhes & Edwards, 1998). Subsequently the two grasses have been recognised as weeds locally, with Olive hymenachne being declared a weed of national significance (WONS) only 10 years after release (Wearne et al., 2010). Two other nationally declared weeds are present in the wetlands, Salvinia (*Salvinia molesta*), and Water hyacinth (*Eichhornia crassipes*), both of which are spread by spore/seed or fragment travel downstream.

In 2008, CSIRO in conjunction with the Nywaigi Traditional Owners, wetland scientists and managers (James Cook University and Queensland local/state agencies) developed a wetlands management strategy, including the urgent need for restoration of cultural and environmental values within the Mungalla wetlands complex. In 2012 and 2013, CSIRO, assisted by hydrodynamic modelling (Karim et al., 2012), removed a section of the earth wall to allow saltwater intrusion (Figure 3), which dramatically changed the vegetation community from a freshwater dominated invasive weed community to an open water system (Figure 4), with fewer hypoxic events and altered fish assemblage (Abbott et al., 2020).

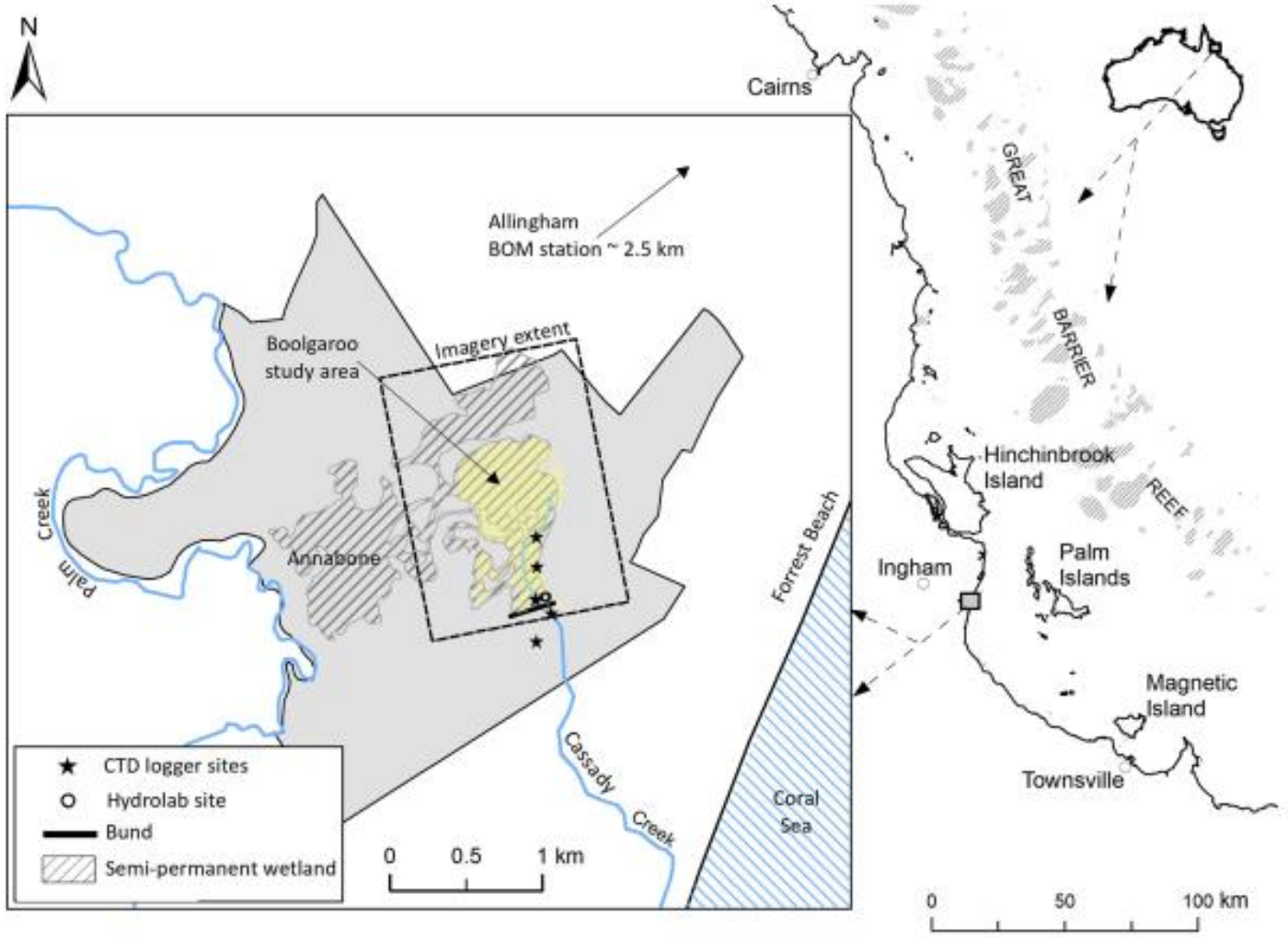


Figure 2: Location of wetlands within Mungalla station in the lower Herbert River catchment, Queensland, Northern Australia. The Mungalla wetlands are hatched in dark grey, the Boolgooroo region of the wetland complex is shown in yellow. Also shown are the locations of the logger sites above and below the earth bund which was removed on 6th October 2013. Reproduced from Abbott et al (2020).



Figure 3: Excavator breaching the earth wall in August 2013 (Photo credits M. Nicholas)

A) B)



Figure 4: (A) Aquatic plant community upstream of the earth wall (approximately July 2013) with extensive invasive freshwater weeds, and B) same photo location after the removal of the earth wall section (approximately September 2015) (Photo credits M. Nicholas)

1.1.1 Rainfall and hydrology at the Mungalla wetland complex rainfall and hydrology - snapshot

Approximately 93% of the freshwater inflow occurs during the wet season, though there is large annual variation. Wet season rainfall at the Mungalla wetland complex, estimated at the nearby Victoria Point Sugar Mill station, is on average 1593 mm annually, ranging from 651 mm for the 5th percentile through to 2603 for the 95th percentile. Analysis of tide data suggests there are approximately 19 days per year when the tide height is greater 3.7 m and, therefore, of sufficient height to reach the Boolgooroo wetland. High tide events typically occur for 2-3 consecutive days, yielding an inundation event frequency of 6-10 times per year. Detailed analysis is in Appendix 1: Rainfall and Hydrology.

2.0 METHODS

2.1 Hydrodynamic modelling

2.1.1 Model framework

A MIKE 21 two-dimensional flexible grid flow model (MIKE 21 FM) was used to simulate tidal inundation under various scenarios at the Mungalla wetland complex. Previous hydrodynamic modelling at Mungalla used a two-dimensional regular grid (Karim et al., 2014); however, flexible mesh (also called irregular grid) models have been shown to have superior accuracy and computational time over regular grid models (Mackay et al., 2015). Detailed model development, including calibration procedures, is presented in Appendix 2.

2.1.2 Model inputs

Topography

Topographic data was sourced from a 30 m resolution hydrologically corrected SRTM (Shuttle Radar Topography Mission) dataset for the entire catchment and a Laser altimetry (LiDAR) derived fine resolution (1 m) data set covering the Mungalla wetlands and surrounding areas. Coastal bathymetry was sourced from Geoscience Australia's 250 m resolution Bathymetric Grid of Australia. Re-sampling these data sets yielded a 10 m resolution digital elevation model (DEM) was produced for the hydrodynamic modelling domain covering an area of 66 km^2. A field survey was also conducted in November 2018 to measure the bathymetry of the two main wetlands, Annabone and Boolgooroo (Figure 2).

Surface roughness

Hydraulic roughness of the land surface, represented using Manning's roughness coefficient, was derived using Geoscience Australia's dynamic land cover map. Key land use types were substituted with plausible roughness coefficients to produce a roughness map. Initial roughness coefficients were sourced from published literature (Chow, 1959; Karim et al., 2012), and later refined during calibration.

Inflow

Two inflow boundaries were used, one upstream with receiving freshwater from Palm and Lucy Creeks, and another downstream with tidal inflow. Both Palm and Lucy Creeks are ephemeral streams, Palm Creek is a distributary of the Herbert River and is relatively large (~100 m wide and ~6 m deep) compared with Lucy Creek (~20 m wide and 2 m deep). A simple rainfall-runoff model was calibrated to estimate inflow through the Palm and Lucy Creeks (DHI, 2012). Initial model parameters were obtained from Karim et al. (2012) and the parameters were recalibrated for the Stone River catchment, a sub-catchment of the Herbert River.

Seaside boundary

Tide data was sourced from the nearest gauge at Lucinda (~20 km NE) from Maritime Safety Queensland for the period of 2001 to 2015. Observed tide data for the period of September 2011 to August 2012 were used to estimate 60 tidal constituents at Lucinda which were then used to simulate tide levels at the Mungalla coast (Forrest Beach) using the inbuilt tide analysis

package in MIKE 21 (DHI, 2012). The constituents were estimated using the ISO (Institute of Ocean Science, Canada) method based on Rayleigh criterion. Once the constituents (that include 45 astronomical main constituents and 24 shallow water constituents) were estimated, high and low waters were estimated and compared with the observed tides at Lucinda. Tide levels at Mungalla were then predicted using the estimated constituents.

2.1.3 Scenario modelling

Eleven tidal inundation scenarios were modelled for the study area, simulating various combinations of bund wall presence-absence, wind speeds, tide heights, atmospheric pressure conditions and sea level rises (Table 1). For each scenario, the extent and volume of saline water intrusion into the wetland was estimated. The additional wave height for a given onshore wind speed was derived using the Beaufort scale. To estimate low atmospheric conditions, it was assumed that sea level increased by ~1 cm per mb pressure below the standard atmospheric pressure of 1013 mb, as suggested in the literature (Gaspar & Ponte, 1997). A reduction to 950 mb in cyclonic conditions may increase the sea level by ~0.6 m.

Table 1: Summary of tidal inundation simulation scenarios using a MIKE21 hydrodynamic model at the Mungalla wetland complex

Scenario	Bund wall	Tide height (m)	Wind speed (m/s)	Atmospheric pressure (mb)	Wave height increase (m)	Sea level rise (m)
1	Present	4.3	0	1013	0	0
2	Absent	4.3	0	1013	0	0
3	Absent	4.1	0	1013	0	0
4	Absent	3.9	0	1013	0	0
5	Absent	3.7	0	1013	0	0
6	Absent	4.3	5	1013	0.7	0
7	Absent	4.3	10	1013	2.1	0
8	Absent	4.3	0	950	0.6	0
9	Absent	3.7	0	950	0.6	0
10	Absent	3.9	0	1013	0	0.5
11	Absent	3.9	0	1013	0	0.8

2.2 Physicochemical monitoring

2.2.1 Logger network

Wetland water depth, temperature and electrical conductivity (EC) were monitored by loggers (CTD-Diver, Eijkelkamp Soil & Water, The Netherlands) located in five permanent positions in the wetland, beginning on 24 October 2012 until 2016 (though some loggers remained in place to December 2018). The locations were 450 m, 250 m and 50 m above, and, 50 m and 250 m below the bund wall (Figure 2). The loggers captured data from the bottom of the water column (10 cm above the soil surface) every 15 minutes and were downloaded as part of monthly routine maintenance visits. An additional water quality logger (Hydrolab, OTT Hydromet,

Colorado, USA) was used above the bund at the 50 m location, adjacent to the Diver logger (Figure 2). The Hydrolab logger recorded values of EC, depth, pH and dissolved oxygen (DO) concentration every 30 minutes at 0.1 m above the soil surface.

2.2.2 Logger data analysis

To examine the effect of bund removal and location (above and below the bund) on depth, EC and temperature, two-way analysis of variance (ANOVA) was carried out. Similarly, one-way ANOVA were run to examine the effects of bund removal on pH and DO (pH and DO were not measured at the below bund location). Data for both analyses were aggregated to daily averages from the 15 and 30-minute raw data. Normality of data residuals was assessed through inspection of residual and Q-Q plots and although there was some deviation it is not problematic given sample sizes (n = 7445, CTD-Diver and n = 1218, Hydrolab), there also appeared to be some heteroscedasticity. As a result, analysis was run using a heteroscedasticity-corrected coefficient covariance matrix (hc3). ANOVA data presented are mean ± standard deviation, unless otherwise stated. The percentage of time that depth, temperature, EC and DO exceeded any given threshold within the Boolgooroo wetland over the monitoring period was also plotted.

2.3 Vegetation monitoring

Vegetation monitoring and mapping in the wetland was carried out using Worldview-3 8-band satellite imagery (DigitalGlobe Inc. Longmont, CO, USA) pan sharpened to a resolution of 0.31m. Imagery was collected once each year between August and September over the Mungalla station region, then cropped to an extent around the Boolgooroo and Annabone wetlands (Figure 2). Classification of the imagery into major vegetation types was carried out using object-based image classification techniques (Knight et al., 2015), using nearest neighbour supervised classification, and manual classification in more difficult areas. Complexity of the wetland area required separate classification of small regions, incorporating different segmentation levels within the object-based process, which were later merged. To aid the supervised and manual classification, dominant species were recorded at 50 fixed ground truthing sites across the imagery extent each year. In addition, high-resolution aerial photography was obtained with a Go-Pro camera attached to the underside of a helicopter flying along several transects that ran parallel and across the wetland site from west to east and at an elevation of approximately 100 m. Images were geo-referenced to preselected ground control points (geo-located with a differential GPS). Major vegetation groups were clearly identified visually from the high-resolution aerial photography, which was used as further ‘ground truth’ of the World-3 imagery classification. A comparison of final classification imagery was carried out between consecutive collection dates (Aug/Sep 2012-2018), to identify differences in the area inhabited by these major vegetation groups.

2.4 Fish surveys

Fish assemblages were surveyed completed using a Smith-Root 2.5 GPP generator boat-mounted electrofishing unit. This involved use of a single pass electro-fishing techniques following a standardised protocol (5-7 five minute shots, depending on size of water body), with effort standardised to number of individuals caught per minute of fishing time. All fish

were measured (standard length in mm) and identified following Allen et al. (2002). Sampling was non-destructive with all fish returned to the water, apart from non-native species which were retained and euthanised in accordance with Queensland Law.

3.0 RESULTS

3.1 Hydrodynamics

The tidal bund wall appeared to be an effective barrier to seawater ingress for all tides simulated, including for a 4.3 m tide (the largest recorded). However, if the bund was absent then the hydrodynamic model predicted that ~55 ha of wetland would have been inundated (Figure 5 & Table 2). Without the bund, seawater is estimated to penetrate 180 m beyond the bund location with a 3.9 m tide, approximately 780 m for a 4.1 m tide, and 1150 m for a 4.3 m tide – though all unable to reach the Annabone region of the complex (Figure 6 & Table 2).

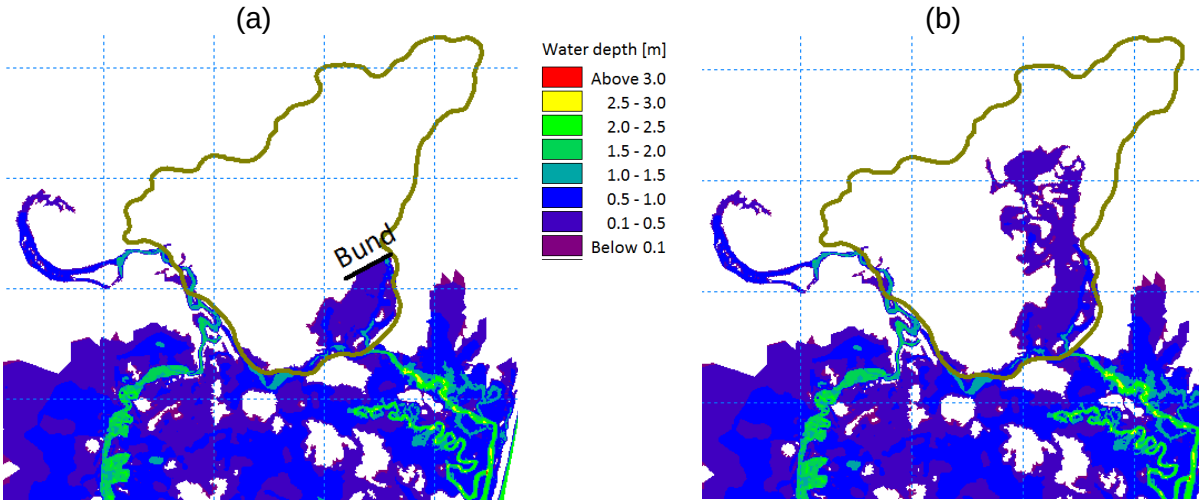


Figure 5: Predicted seawater inundation at the Mungalla wetland for a 4.3 m tide with (a) and without (b) the tidal bund in place.

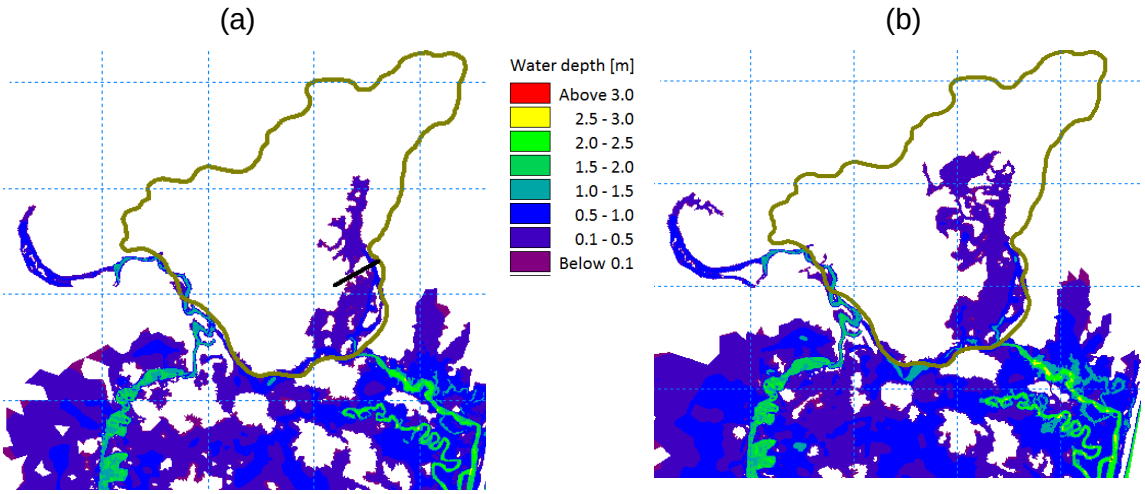


Figure 6: Seawater inundation and depth predicted at the Mungalla wetland for (a) 4.1 m tide and (b) 4.3 m tide.

Table 2: Effect of tide height on seawater intrusion and inundation depth at Mungalla wetland. Presented is the distance of tidal ingress (m), extent inundated at various depths (ha), the volume of seawater ingress (m^3), and the mass of salt introduced to the wetland (tonnes).

Tide height (m)	3.7	3.9	4.1	4.3
Distance above bund (m)	15	180	780	1150
Area (ha) with depth 0 to 0.1 m	0.13	1.98	4.33	8.33
Area (ha) with depth 0.1 to 0.2 m	0.04	2.13	7.02	19.25
Area (ha) with depth 0.2 to 0.3 m	0.00	0.25	5.05	14.64
Area (ha) with depth 0.3 to 0.4 m	0.00	0.00	0.41	9.18
Area (ha) with depth > 0.4 m	0.00	0.00	0.00	3.62
Total Area (ha) inundated	0.17	4.36	16.81	55.02
Volume of seawater ingress (m^3)	125	4810	26,755	118,060
Influx salt mass in wetland (tonnes)	4.4	168	936	4132

Moderate onshore breezes (5 m/s) were estimated to produce a wave height of 0.7 m. When added to the high tide simulations of 3.7 and 4.3 m, the increased area inundated was small, only 0.1 and 1.5 ha respectively. Strong onshore breezes (10 m/s), however, produced waves ~2.1 m high, which when coincided with high tide simulations of 3.7 and 4.3 m, is predicted to cause seawater inundation well into the Annabone area. The addition of a strong onshore breeze to an otherwise normal 4.3 m tide was predicted to increase inundation extent by 200% (110 ha) and maximum depth from 0.5 to 0.7 m (Figure 7 & Table 3).

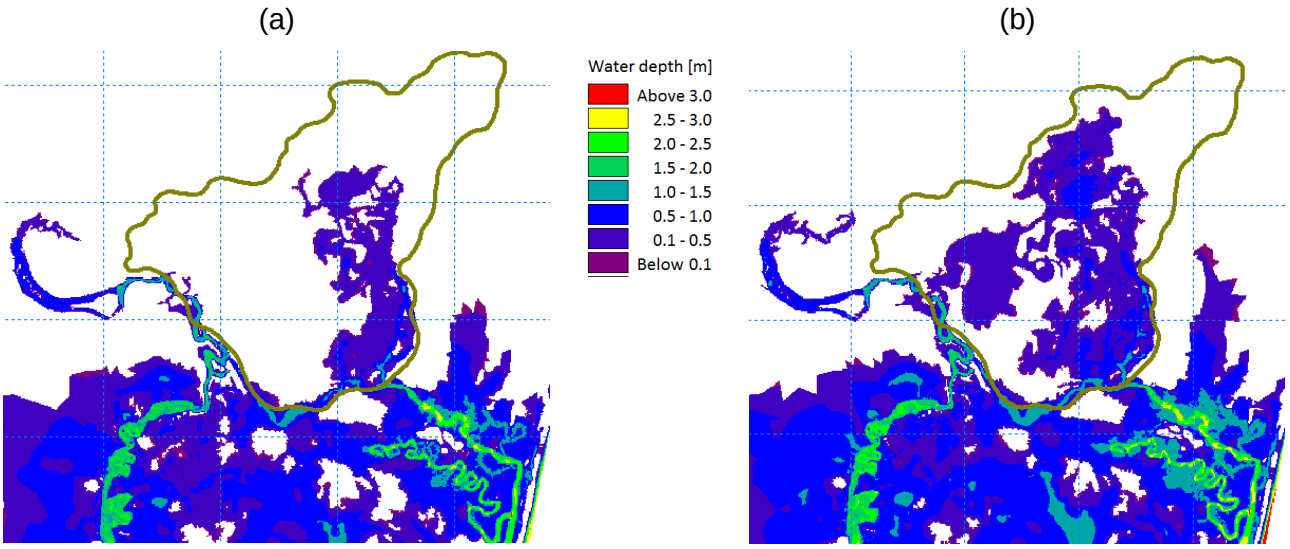


Figure 7: Wetland inundation scenarios for different tides and on shore winds, (a) 4.3 m tide and 5 m/s wind speed, (b) 4.3 m tide and 10 m/s wind speed

Table 3: Effect of on shore wind on seawater intrusion and inundation depth in the wetland. Also shown are the total volume of seawater entering the wetland and the weight of salt it content.

Tide height (m)	3.7m tide			4.3 m tide		
	No wind	Wind: 5 m/s	Wind: 10 m/s	No wind	Wind: 5 m/s	Wind: 10 m/s
Distance above bund (m)	15	25	120	1150	1190	1750
Area (ha) with depth 0 to 0.1 m	0.13	0.18	1.26	8.33	8.43	17.64
Area (ha) with depth 0.1 to 0.2 m	0.04	0.07	1.18	19.25	18.28	35.46
Area (ha) with depth 0.2 to 0.3 m	0.00	0.00	0.19	14.64	16.04	32.08
Area (ha) with depth 0.3 to 0.4 m	0.00	0.00	0.00	9.18	9.85	33.86
Area (ha) with depth 0.4 to 0.5 m	0.00	0.00	0.00	3.62	3.91	30.02
Area (ha) with depth 0.5 to 0.6 m	0.00	0.00	0.00	00	00.0	12.76
Area (ha) with depth > 0.6 m	0.00	0.00	0.00	00	00.0	3.52
Total Area (ha) inundated	0.17	0.25	2.63	55.02	56.51	165.34
Volume of seawater ingress (m^3)	125	195	2875	118,060	123,805	488,870
Weight of salt in wetland (tonnes)	4.4	6.8	101	4132	4333	17,110

The coincidence of low atmospheric pressure (predicted to increase sea level by ~0.6 m) and high tides of 3.7 and 4.3 m is predicted to inundate approximately 55 and 353 ha respectively, and ingress approximately 1155 m and 2370 m respectively (Figure 8 & Table 4).

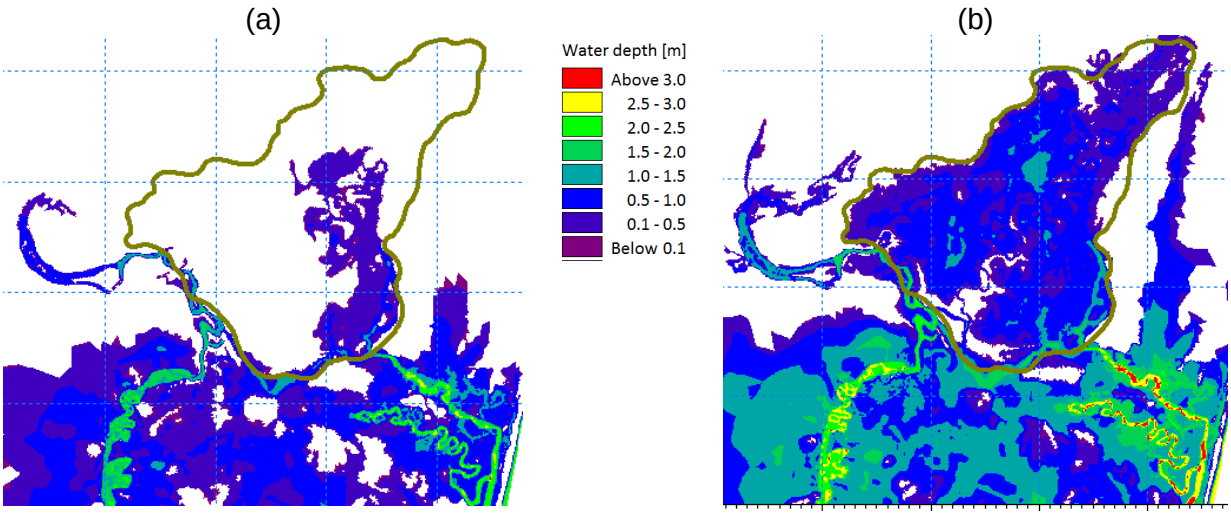


Figure 8: Wetland inundation for a low-pressure system (950 hPa): (a) 0.6 surge coincides with a 3.7 m tide, (b) 0.6 surge coincides with a 4.3 m tide.

Table 4: Effect of low atmospheric pressure (950 hPa) on inundation and seawater intrusion

Atmospheric Pressure (hPa)	**1013**	**950**	**1013**	**950**
Tide height (m)	**3.7**	**3.7**	**4.3**	**4.3**
Distance above bund (m)	15	1155	1150	2370
Area (ha) with depth 0 to 0.1 m	0.13	8.50	8.33	13.41
Area (ha) with depth 0.1 to 0.2 m	0.04	19.28	19.25	24.77
Area (ha) with depth 0.2 to 0.3 m	0.00	14.68	14.64	34.46
Area (ha) with depth 0.3 to 0.4 m	0.00	9.21	9.18	43.90
Area (ha) with depth 0.4 to 0.5 m	0.00	3.62	3.62	47.01
Area (ha) with depth 0.5 to 0.6 m	0.00	0.00	0.00	45.01
Area (ha) with depth 0.6 to 0.7 m	0.00	0.00	0.00	41.21
Area (ha) with depth 0.7 to 0.8 m	0.00	0.00	0.00	29.00
Area (ha) with depth 0.8 to 0.9 m	0.00	0.00	0.00	25.06
Area (ha) with depth 0.9 to 1.0 m	0.00	0.00	0.00	34.43
Area (ha) with depth 1.0 to 1.1 m	0.00	0.00	0.00	13.08
Area (ha) with depth > 1.1 m	0.00	0.00	0.00	1.97
Total Area (ha) inundated	0.17	55.29	55.02	353.31
Volume of seawater ingress (m^3)	125	118,395	118,060	1,928,215
Weight of salt in wetland (tonnes)	4.4	4144	4132	67,488

The addition of sea level rise to high tides substantially increased the extent of inundation predicted. A sea level rise of 0.5 m meant that a 3.7 m tide which would not normally penetrate the wetland, could inundate ~ 53 ha. Whereas a rise of 0.8 m coinciding with a 4.3 m tide is estimated to inundate ~423 ha (Figure 9, Table 5).

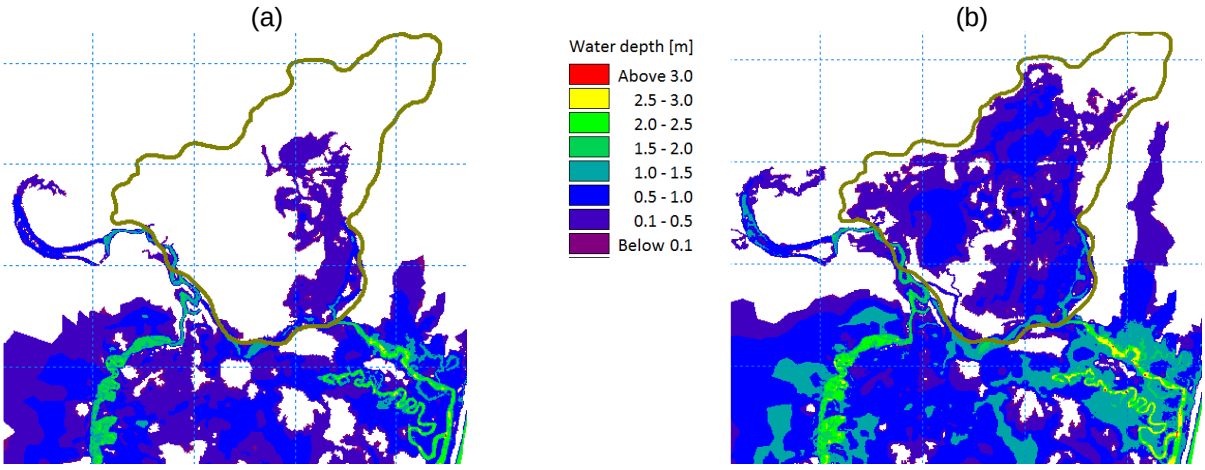


Figure 9: Maximum extent of wetland inundation for a combined 3.7 m tide and a SLR of (a) 50 cm and (b) 80 cm.

Table 5: Effect of sea-level rise on inundation and seawater intrusion into the wetland.

Tide height (m)	3.7 m tide		4.3 m tide	
	0.5m SLR	0.8m SLR	0.5m SLR	0.8m SLR
Distance above bund (m)	1010	1750	2340	2560
Area (ha) with depth 0 to 0.1 m	8.63	19.14	12.49	6.28
Area (ha) with depth 0.1 to 0.2 m	19.12	37.56	25.21	12.29
Area (ha) with depth 0.2 to 0.3 m	14.33	40.95	34.89	17.35
Area (ha) with depth 0.3 to 0.4 m	8.50	43.03	46.07	29.05
Area (ha) with depth 0.4 to 0.5 m	3.22	30.82	46.75	22.41
Area (ha) with depth 0.5 to 0.6 m	0.00	28.06	45.54	25.76
Area (ha) with depth 0.6 to 0.7 m	0.00	31.93	38.46	35.87
Area (ha) with depth 0.7 to 0.8 m	0.00	18.99	28.30	49.38
Area (ha) with depth 0.8 to 0.9 m	0.00	3.82	24.70	48.72
Area (ha) with depth 0.9 to 1.0 m	0.00	0.00	33.99	47.41
Area (ha) with depth 1.0 to 1.1 m	0.00	0.00	9.86	37.61
Area (ha) with depth 1.1 to 1.2 m	0.00	0.00	0.00	27.34
Area (ha) with depth 1.2 to 1.4 m	0.00	0.00	0.00	55.10
Area (ha) with depth > 1.4 m	0.00	0.00	0.00	7.97
Total Area (ha) inundated	53.80	254.30	346.26	422.54
Volume of seawater ingress (m^3)	113,060	994,350	1,852,000	3,414,365
Weight of salt in wetland (tonnes)	3957	34,802	64,820	119,503

3.2 Physicochemical monitoring

Two-way ANOVA for measurements of depth, EC and temperature all showed statistically significant interaction between period (before and after bund removal) and location (above and below bund) $F_{1,7744} = 223.87$, $p < 0.001$, $\eta_p^2 = 0.023$, $F_{1,7744} = 15.692$, $p < 0.001$, $\eta_p^2 = 0.003$, and $F_{1,7744} = 33.11$, $p < 0.001$, $\eta_p^2 = 0.004$ respectively. Given the interactions, simple contrasts were run that compared the difference between means for the before and after (both 2014-16 and 2016-18) bund removal periods, above and below bund location combinations (Tables 6 & 7). Additionally, one way ANOVA for measurements of both DO and pH revealed a statistically significant difference between period for means of DO, $F_{1,1217} = 271.36$, $p < .001$, $\eta_p^2 = .03I$ and pH $F_{1,1217} = 187.21$, $p < .001$, $\eta_p^2 = .027$. Contrast results comparing difference

between period for mean DO and pH also appear in Table 6. Depth measurements:—The above bund location was deeper than the below bund location before bund removal (46.80cm ± 26.35cm vs. 39.43cm ± 26.45cm). However, following bund removal and outflow of confined water from the above bund location this relationship reversed (25.25cm ± 24.16cm vs. 40.04cm ± 31.90cm). Looking at the above and below locations individually, there was no significant change in mean water depth within Cassady creek following bund removal with mean depth remaining stable at 39.43cm ± 26.45cm before, and 40.04cm ± 31.90cm after bund removal. However, the change in water depth following bund removal was significant within the Boolgooroo wetland decreasing from a mean depth of 46.80cm ± 26.35cm to 25.25cm ± 24.16cm. Figures 10-13 show the percentage of time that depth, temperature, EC and DO exceeded any given threshold within the Boolgooroo wetland over the relevant monitoring period.

Table 6: Simple contrasts for water quality measurements - above and below bund location and before and after bund removal combinations (2014-2016 = After) (Abbott et al., 2020).

Dependent variable	Location	Period	Contrast	Mean difference	Std. Error	*t*	*p*
Depth	Above		After - Before	-21.55	0.92	23.37	<0.001
	Below		After - Before	0.60	1.15	0.52	1.000
		After	Above - Below	-14.79	0.73	-20.22	<0.001
		Before	Above - Below	7.37	1.28	5.75	<0.001
EC	Above		After - Before	2.92	0.46	6.43	<0.001
	Below		After - Before	-0.39	0.57	-0.69	1.000
		After	Above - Below	-10.21	0.36	-28.32	<0.001
		Before	Above - Below	-13.52	0.63	-21.42	<0.001
Temperature	Above		After - Before	2.66	0.11	23.38	<0.001
	Below		After - Before	1.61	0.14	11.33	<0.001
		After	Above - Below	-0.2	0.09	-2.188	0.115
		Before	Above - Below	-1.249	0.16	-7.91	<0.001
Dissolved Oxygen (%)	Above		After - Before	17	1.17	14.53	<0.001
pH	Above		After - Before	0.53	0.04	12.61	<0.001

Table 7: Simple contrasts for water quality measurements - before and after bund removal combinations Before = 2012-13, After = 2014-16, After2 = 2017-18

Dependent variable	Period Contrast	Mean difference	Std. Error	*t*	*p*
Depth	After2 - Before	-6.32	1.61	-3.93	<0.001
	After2 – After	20.67	1.22	16.92	<0.001
EC	After2 - Before	2.21	0.56	3.96	<0.001
	After2 – After	-2.16	0.43	-5.1	<0.001
Temperature	After2 - Before	0.83	0.24	3.42	0.002
	After2 – After	-1.65	0.18	-8.98	<0.001

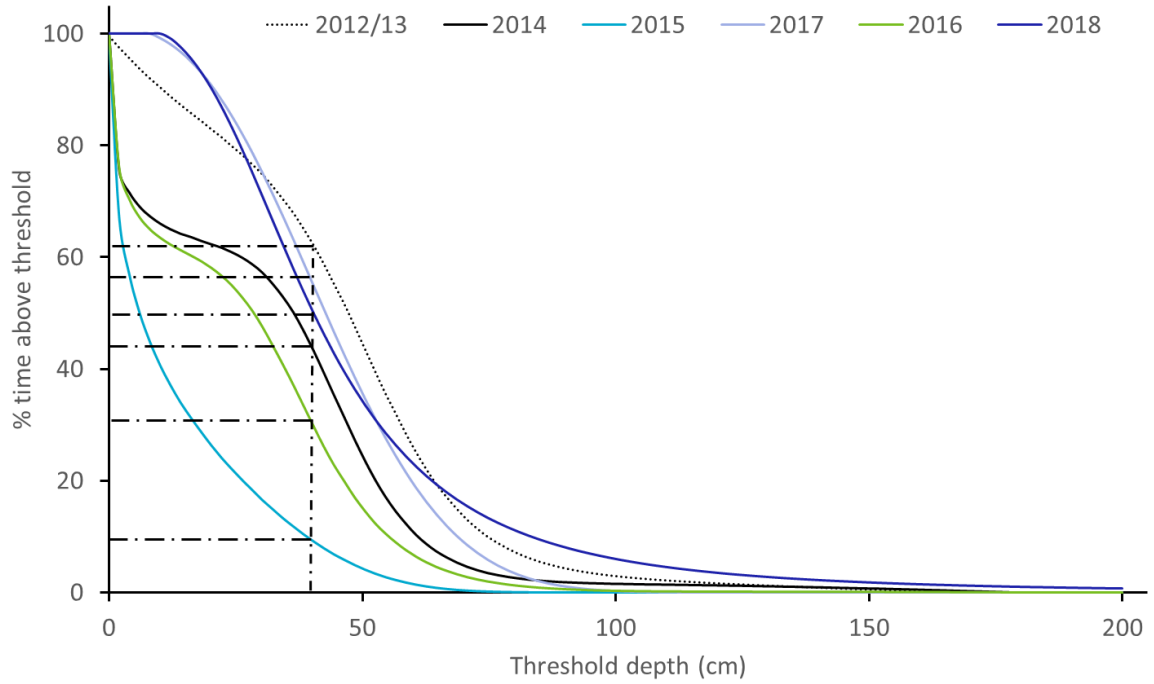


Figure 10: The percentage of time depth exceeded any given threshold within the Boolgooroo wetland, vertical dotted line shows the threshold depth for reduction of tidal inflow due freshwater outflow (hydrologic pressure) at 40 cm.

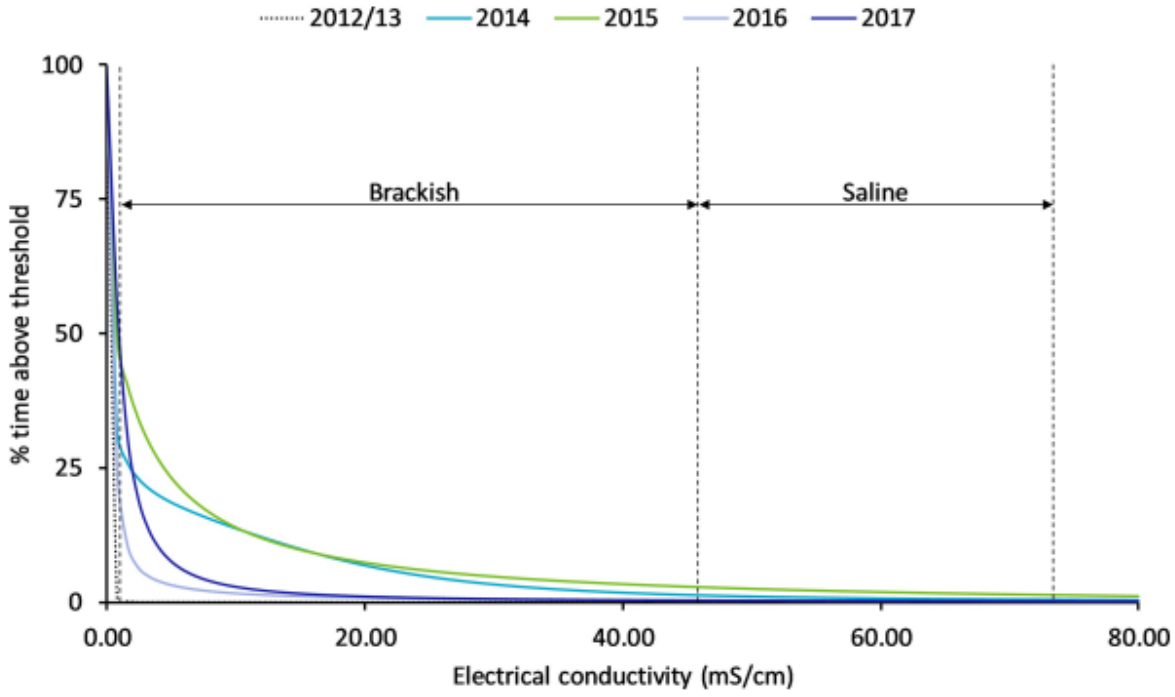


Figure 11: The percentage of time EC exceeded any given EC threshold during pre and post bund removal years within the Boolgooroo wetland. Horizontal dashed lines show boundaries between fresh, brackish, saline and briny water from left to right.

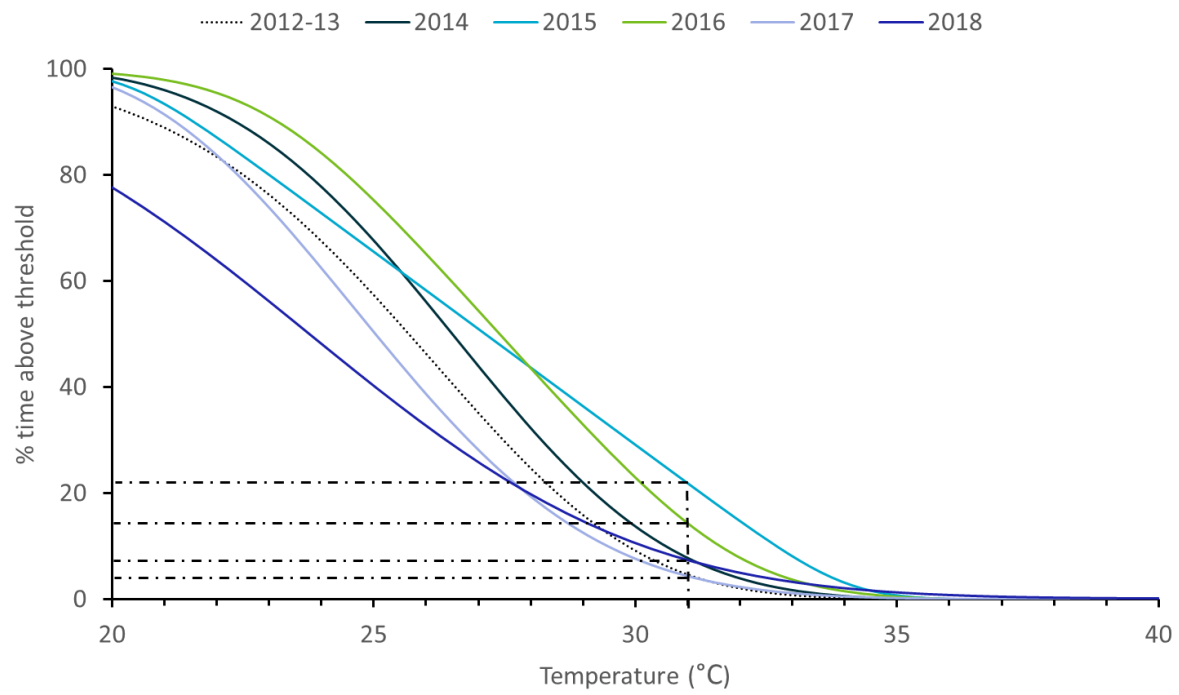


Figure 12: Proportion of temperature above any given threshold, vertical dotted line shows the exceedance threshold for aquatic biota. Presented here is the acute effect temperature threshold of fly specked hardyhead of 31.4ºC (Burrows & Butler, 2012).

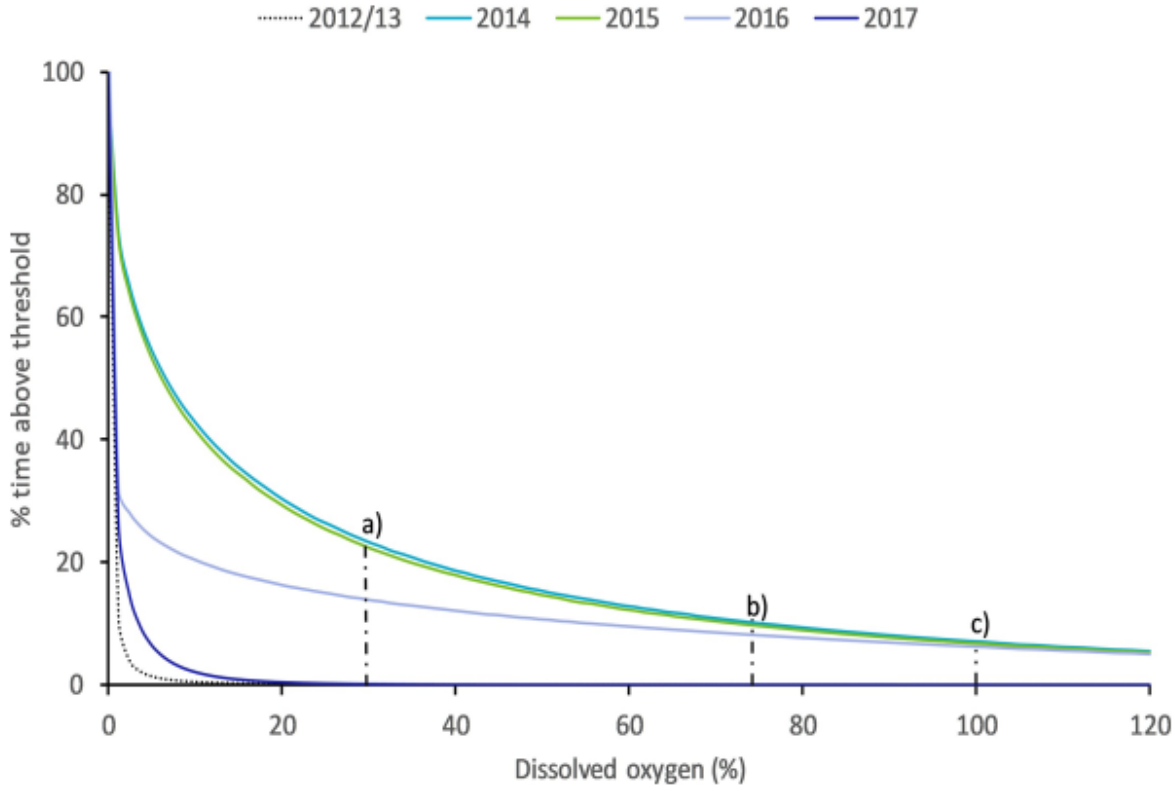


Figure 13: The percentage of time DO exceed any given DO threshold in the Boolgooroo wetland. Vertical dashed lines represent critical values of DO affecting fish species, a) acute trigger value, b) chronic trigger value and b) to c) optimal DO for fish species. From dissolved oxygen guidelines for freshwater habitats of Northern Australia (Butler & Burrows, 2007).

3.3 Vegetation monitoring

3.3.2 Pre-bund removal on Boolgooroo

Prior to bund removal (2012/13), with no changes in EC above the bund within the Boolgooroo lagoon area, over two thirds of the wetland were inhabited with ponded pastures and exotic floating vegetation (Figure 14 & Figure 15, Appendix 3). A small percentage was inhabited by the native Water lily (*Nymphaea gigantean*) during 2012 which increased into open waters during 2013. Over half of the area was covered with weeds of national significance (WONS), dominated by Olive hymenachne (*Hymenachne amplexicaulis*) and Water hyacinth (*Eichhornia crassipes*). On average, open water made up less than one fifth of the Boolgooroo area. Likewise, the Annabone wetland contained high proportions of aquatic weed, primarily made up of Olive hymenachne and Para grass (*Urochloa mutica*) during this period. Open water was higher here than within Boolgooroo most likely due to an aerial spraying campaign that took place in early 2012 across the Annabone area. The open water proportion of ~30 % persisted until late 2014. The Boolgooroo and Annabone areas were similar – in terms of weed infestation - prior to commencement of the treatment (bund removal and reinstatement of tidal inundation) within the Boolgooroo lagoon (Figure 14 & Figure 15, Appendix 3).

3.3.3 Post-bund removal (Boolgooroo lagoon)

Following bund removal (6 October 2013) on Boolgooroo lagoon, vegetation composition remained unchanged for the following three months (Figure 14, Appendix 3). At the end of January 2014, the wetland experienced the first tidal intrusion, with rapid yellowing of ponded grasses and weeds noticeable several days afterwards. By the August 2014 survey, coverage of ponded grasses and other exotic species reduced to below 20%, and a two-third reduction in water lily (*Nymphaea gigantean*), within the tide affected area. In 2015, there was a small increase in two of the ponded pastures – Aleman grass (*Echinochloa polystachya*) and Para grass – primarily on the wetland margins in areas previously inhabited by Olive hymenachne. Olive hymenachne was reduced to ~5% with Salvinia (*Salvinia molesta*) and Water hyacinth being undetectable on the remote sensing imagery. There was an increase in native aquatic plants driven by the appearance of Bulkuru (*Eleocharis dulcis*) within the lower half of the site as well as an increase in Water lily (*N. gigantean*) in the upper site. Duck weed (*Spirodela punctata*) was also present (~3.5%) in some of the shallower areas originally inhabited by Olive hymenachne. In 2016, Salvinia had returned *(*~40% coverage), occupying some of the area previously inhabited by Bulkuru and Water lily, the latter covered ~13% of the Boolgooroo area. Other than several individual plants, appreciable coverage of Bulkuru was undetected. In the upper reaches, Aleman grass and Para grass were reduced slightly from the margins and replaced by Olive hymenachne. In the final two years of the study (2017-18), Salvinia reduced substantially to marginal locations, with Water lily having moved into the areas that it previously occupied in the upper Boolgooroo, and Bulkuru reappearing in the lower Boolgooroo. Club rush (*Schoenoplectus litoralis*), a saltmarsh species, covered a small area directly above eastern end of the bund location. Olive hymenachne reduced to ~5% covered, similar to the 2015 levels. The extent of Para grass and Alemen grass increased into areas previously occupied by Olive hymenachne in 2016 (Figure 14, Appendix 3).

3.3.4 Post-bund removal (Annabone)

Ponded pastures in the Annabone wetland, following herbicide spraying in 2012, increased in extent to almost 100% coverage by 2018 (2015 to 2018) (Figure 15 & Appendix 3), with Olive hymenachne occupying the central (wet) areas of the wetland and Para grass on wetland the margins. The native water lily appeared briefly in 2013 while open water was available, before replacement by Olive hymenachne (Figure 15 & Appendix 3).

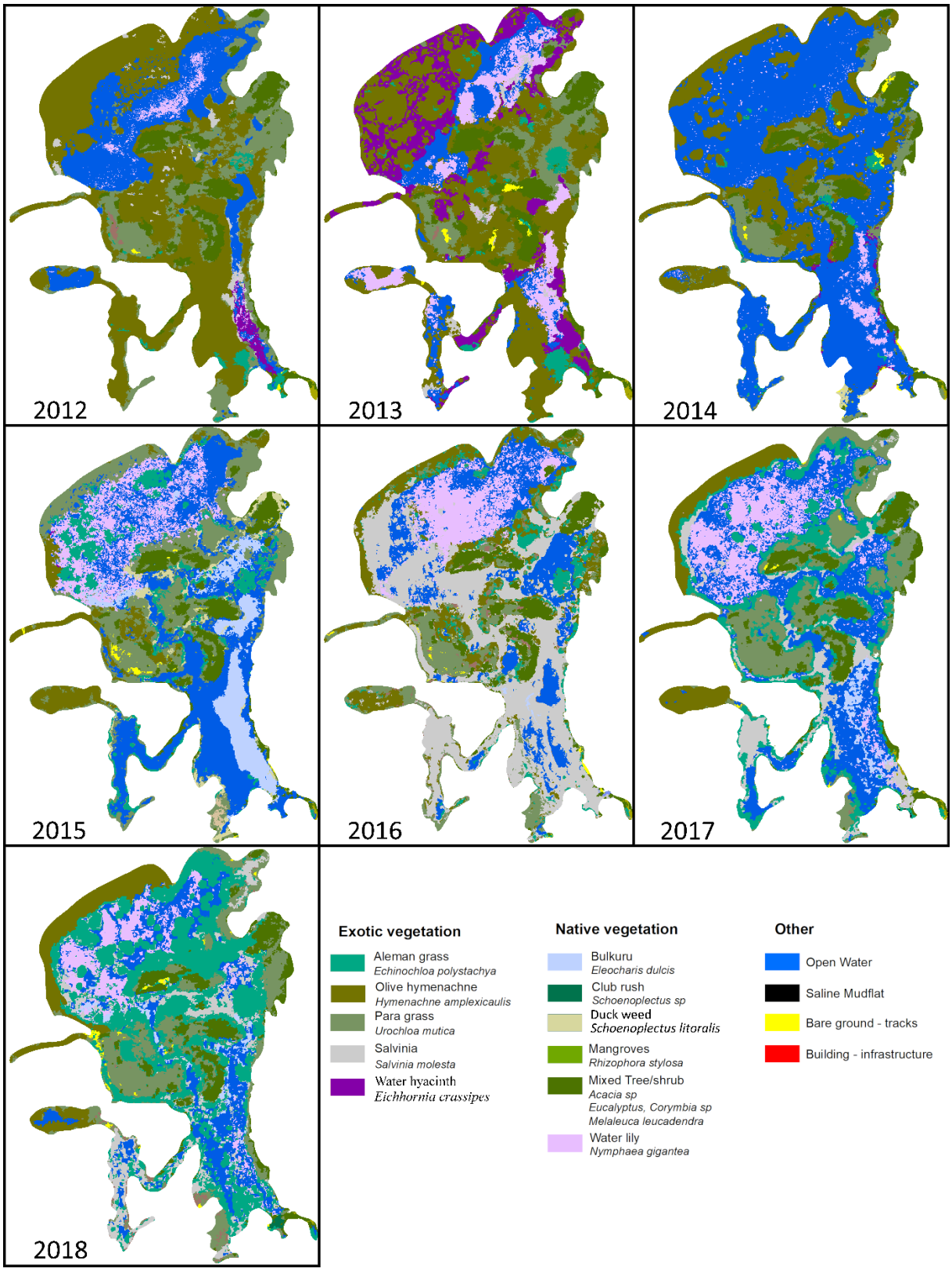


Figure 14: Time-series of classified imagery for Boolgooroo lagoon – area inundated by tidal water after bund removal (updated from Abbott et al., 2020).

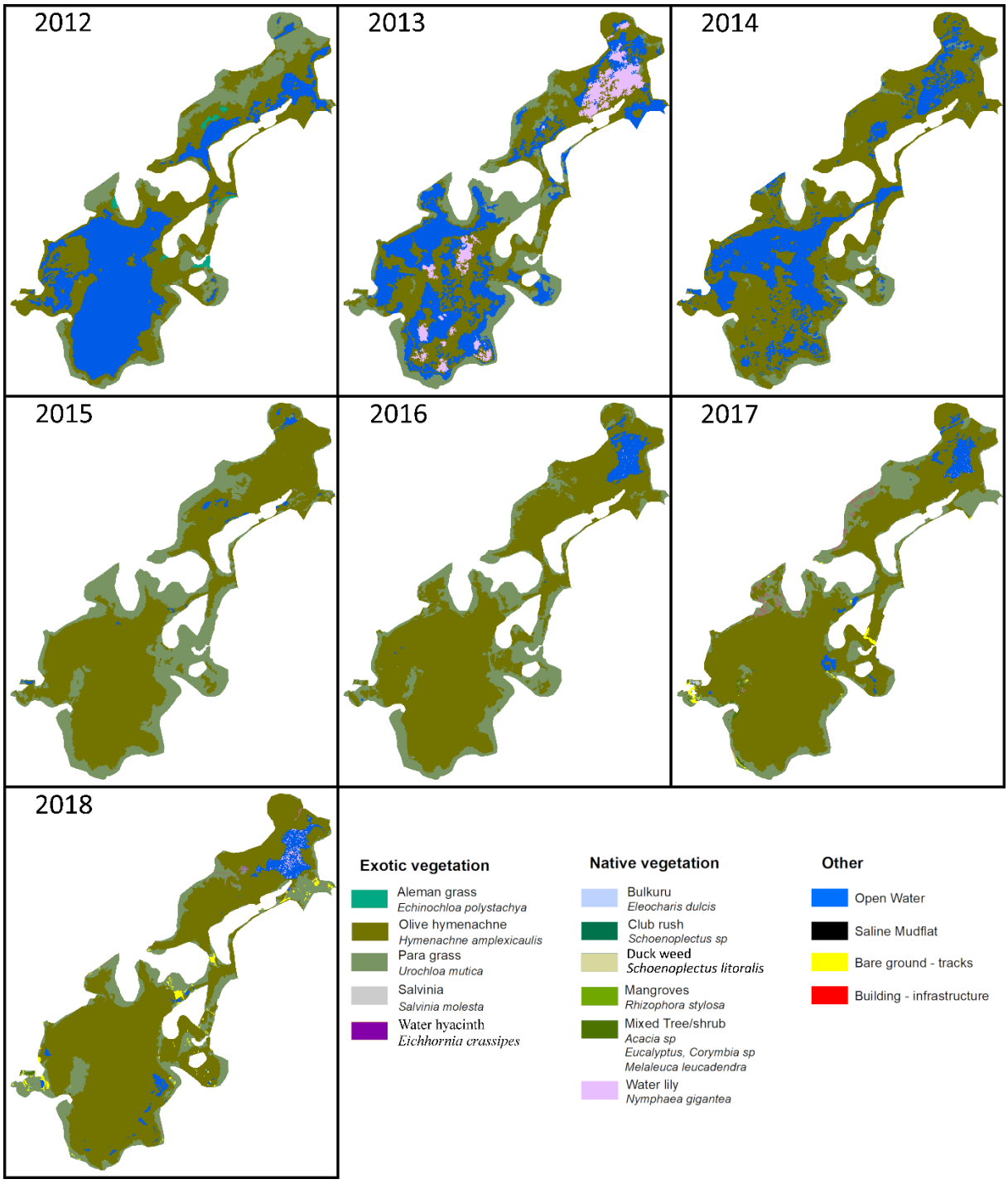


Figure 15: Time-series of classified imagery for Annabone and north Boolgooroo – area not inundated by tidal water (updated from Abbott et al., 2020).

3.4 Fish surveys

The fish assemblage prior to the bund wall removal consisted of three species, including one invasive species and two locally common species (Butler et al., 2009). Post bund removal fish surveys, conducted in May 2016, recorded these three species and an additional six species (Table 8). The most notable records post removal were Barramundi (*Lates calcarifer*) (Figure 16), Silver biddy (*Gerres subfasciatus*) and Banded scat (*Selenotoca multifasciata*); each of these species are diadromous, and require access to wetlands to complete critical life cycle stages.

Table 8: Fish assemblage recorded in Mungalla wetland, before and after bund wall removal works

Common name Species	Pre bund removal survey (2009)	Post bund removal survey (6/5/16)	5/4/17	7/9/17	7/2/18
Power on (sec)		**750**	**1800**	**1050**	**1560**
Mosquitofish *Gambusia holbrooki*	P	P	P	P	P
Glass perch Ambassis sp.					P
Hardyhead *Craterocephalus stercusmuscarum*		P			
Empire gudgeon* *Hypseleotris compressa*	P	P	P	P	P
Tarpon *Megalops cyprinoides**		P	P		P
Rainbowfish *Melanotaenia splendida*	P	P		P	P
Barramundi* *Lates calcarifer*		P			
Silverbiddy* *Gerres subfasciatus*		P			
Banded scat* *Selenotoca multifasciata*		P			
Snakehead gudgeon *Giurus margaritacea*			P		
Long finned eel* *Anguilla reinhardtii*		P		P	
Total species	3	9	4	4	5

*diadromous movement ecology



Figure 16: Barramundi (*Lates calcarifer*) captured in Boolgooroo upstream of bund wall after its removal

4.0 DISCUSSION

Bund wall removal in low-lying coastal areas has become an attractive and inexpensive option for coastal restoration by allowing ingression of saltwater to reduce freshwater weeds and increase hydrological connectivity for fish (Bell-James & Lovelock, 2019; Kelleway et al., 2017). Whilst practiced and studied overseas, the examination of bund wall removal from ponded pastures across the Great Barrier Reef (GBR) catchment has been absent. Encouraging saltwater ingression may be a more enduring and successful restoration technique in some situations than previously used methods, such as physical weed removal. This case study examined the alterations in hydrology, water chemistry, vegetation and fish communities following bund wall removal at the Mungalla wetland complex.

With the bund wall in place, low oxygen levels at the bottom of the water column were likely due to the presence of dense weed mats that severely limited light penetration to the bottom of the wetland and the high organic loading from prolific weed growth. The wetland complex was entirely freshwater, with water levels representing a balance between inputs from rainfall, runoff or from Palm Creek, and losses to evaporation and groundwater. Seawater could reach the bund wall but was unable to penetrate it. These hydrological conditions permitted the dominance of weeds, as our assessment observed half the area was covered with Olive hymenachne (*Hymenachne amplexicaulis*) and Water hyacinth (*Eichhornia crassipes*) directly before bund removal. Butler et al (2009) also observed fish and birds largely occupying the scant weed free areas, hypothesising that the weed dominated areas provided unsuitable habitat for most species of fish and birds.

Following bund removal, seawater penetration first began in late January and early February 2014. Water levels were low (~10 to 40 cm) prior to inundation, and electrical conductivity rapidly increased to levels comparable to that of seawater, indicating the first exposure of the freshwater weeds to highly saline water. Periodic inundations (~4 times per year) have continued to be recorded. The frequency and duration of seawater ingress to the wetland, as indicated by the continuous conductivity logging, was well in excess of that required to cause permanent damage to freshwater weeds. Experimental salinity tolerance tests carried out by (Reid et al., 2018) found that the growth and survival of Aleman grass (*Echinochloa polystachya*), Olive hymenachne, Para grass (*Urochloa mutica*) and Water hyacinth were all affected by salinity, even when exposed to only 30 % seawater for as short as a single day. Salinity tolerance varied between the four weed species with water hyacinth most sensitive and unable to tolerate more than 3 days in 30 % of seawater. Para grass (*U. mutica*) was least sensitive to salinity and cold tolerate up to 70 % of seawater. However, all of the weeds examined stopped photosynthesis when exposed to longer than 7 days in 100% seawater. The impact of seawater on freshwater weeds was clearly observed in the Boolgooroo area, within days after saltwater inundation, where Aleman grass, Para grass, Olive hymenachne and Water hyacinth were all substantially reduced from dominating to a minor presence. There was also an accompanying increase in native aquatic plants, with Water Lily and Bulkuru increasing in the upper and lower parts respectively. The native species generally took advantage of the disappearance of exotic species and newly available open water. In contrast, the Annabone area remained dominated by Olive hymenachne and Para grass throughout the study duration. However, whilst it is evident that tidal bund removal can be an effective tool for managing freshwater weeds, there were instances where it was insufficient alone.

Our investigation revealed that the extent of Aleman grass is increasing, largely occupying areas previously dominated by Olive hymenachne. Aleman grass occupies similar habitat Olive hymenachne, but is relatively more tolerant of salinity and deeper waters. There is also a notion that Aleman grass does not produce viable seed with its spread often associated with cattle transfer between ponded pasture sites (T. Sydes per comm). Continued freshwater weed growth may also be determined by rainfall patterns and the extent to which freshwater held in the wetland pushes back on seawater ingression. At current sea levels, the wetland-ocean connection is greatest during periods of extended low rainfall, allowing for saline conditions over a greater extent, assisting the reduction of freshwater aquatic weeds and recovery of natives. However, in average rainfall years or above, freshwater dominates the wetland and supports weed growth. This oscillation between freshwater and salt tolerant species in the wetland is concomitant with the preceding year's weather conditions (Abbott et al., 2020). The management response will need to depend on the desired outcomes. If the desired outcome is denitrification then retaining the weeds may be necessary to effectively treat nutrient-laded water (a process that would be aided with a high residence time). Alternatively, if supporting the on-going return of native flora and fauna is the aim, then chemical spraying of weeds may be required in wet years.

The combination of improved connectivity, reduced hypoxic conditions and improved habitat (from weed reduction), likely explains the increased richness in fish species observed. Immediately following bund removal, fish species richness tripled from three to nine, including the highly-valued Barramundi. This fish is diadromous and requires connectivity to wetlands to complete their life cycle. Whilst the increased species richness is still low by local standard (Arthington et al., 2015), and were insufficient to formally test statistically, initial evidence suggests bund removal may have improved the fish assemblages.

Despite improved connectivity, oxygenation and biological communities, bund removal may have had negative impacts on the interactions between temperature, depth and drainage. When depths were 40-50 cm, temperatures at the bottom of the water column rarely exceeded values that could be detrimental to fish. Water temperatures recorded above the Mungalla bund did not exceed 34^{o} C either before or after removal (2013 & 2014 respectively). Therefore, bund removal *per se* did not affect the wetland thermal regime. However, when water depths were shallower (0-40 cm), as in the 2015 wet season, due to the very low rainfall, temperatures exceeded 31^{o} C over 60% of the time, 34^{o} C for 35% of the time and even reached 40^{o} C on occasion. These higher temperatures could have increased acute exposure to aquatic species as many tropical fish (Burrows & Butler, 2012), and crustaceans (Stewart et al., 2013; Waltham, 2018), cannot survive prolonged acute and exposure to such thermal regimes. The reduced shading from the weed reduction may have also exacerbated the probability of high temperatures at shallow depths and increased the amplitude of the diurnal temperature oscillation post bund removal.

The bund removal also almost doubled the drainage rate (180% increase) during the rapid drainage phase after rainfall, increasing the duration at shallow depths. For example, the wetland would drain from (say) 170 cm to 60 cm in just 14 days with the bund in place, but in only seven days with it removed. However, once the depth is below 60 cm, drainage is very slow and, in the absence of rain, further level changes are mainly due to evaporation. If the evaporation rate is 6 mm/d at this time, then the wetland would completely dry out after

approximately ten days. Large diurnal oscillations in water temperature occur once depth falls below ~40 cm, approximately three days after rapid drainage stops, thus prolonging the duration of high thermal risk. The actual duration of thermal risk would depend on the frequency and volume of rainfall, but removing the bund significantly increased the potential for exposure to undesirably high water temperatures. The increased drainage rate then exacerbates the risk of intolerable thermal exposure from reduced weed coverage and increased open water.

The extent of future inundation will likely be influenced by tide height, wind, atmospheric conditions and sea level rise. Wetland inundation is likely to increase substantially when high tides and onshore winds coincide. It is estimated that moderate breezes (up to 5 m/s) will cause little increase in inundation extent; whereas strong winds (~10 m/s) may increase inundation extent by 200% and the volume of water entering the wetland by over 400%. Under these conditions, the freshwater and weed dominated Annabone part of the wetland would also be inundated with seawater. The marked difference at these two wind speeds is because wave height increases rapidly with wind speed. If low atmospheric pressure (950 hPa) cyclonic conditions were to coincide with a high tide of 4.3 m, then seawater would penetrate ~2370 m inland of the bund site and inundate ~80% (353 ha) of the wetland up to 1.1 m deep. Sea level rise would further exacerbate inundation extent and frequency. For example, a 3.7 m tide, occurring ~16 days per year, and causing very little inundation, would inundate ~54 ha of the wetland with a 0.5 m sea level rise and ~254 ha with a 0.8 m sea level rise. Whilst the hydrodynamic modelling applied here is specific to the Mungalla wetlands, the method is applicable in any coastal wetland, allowing the assessment of inundation extent, frequency and connectivity changes prior to restoration works commencing.

5.0 CONCLUSIONS AND RECOMMENDATIONS

Bund walls were constructed to prevent tidal ingress to low lying areas in order to establish ponded pastures along much of the Queensland coastline. They are becoming of increasing interest to managers and scientists as potential restoration opportunities, however, there is little explicit data on the environmental services that can be achieved, or lost, as a result of this restoration activity. While reinstatement of tidal flow has been successfully applied elsewhere to restore ecological function and improve water quality (Luke et al., 2017), this study appears to be the first of its kind targeting wetland weeds and specifically ponded pastures in the GBR region. The Mungalla wetland tidal bund removal presents an important case study for similar restoration efforts proposed in other locations in the GBR catchments, and inform government's coastal wetland restoration ambitions under the Reef 2050 Plan (GBRMPA, 2014).

Prior to bund wall removal, the Mungalla wetland was overgrown with invasive aquatic weeds, degraded with persistently low dissolved oxygen availability for fish (Butler et al., 2009), and deemed in poor condition by the local Indigenous group (Grice et al., 2012). In an attempt to repair the system, bund removal in 2012 drove large declines in freshwater weeds, improved dissolved oxygen and fish diversity. Although initially deemed a success, the continued monitoring under this project has found that improvements are more nuanced. It is evident that saltwater ingress alone is insufficient to always control weeds, with rainfall and freshwater hydrology being influential and cyclical factors. Although bund removal can be a highly successful and low cost restoration technique, it is not a panacea for all circumstances. Below are recommendations for the on-going management and monitoring of the Mungalla wetland complex:

1. Continued funding support for the Nywaigi people for training and equipment to ensure the wetland is managed and protected from invasive weeds and animals.
2. Consider spraying weeds in wet years when saltwater penetration is likely to be ineffectual. This will help keep weeds in check and allow native vegetation to maintain dominance.
3. Further investigate pumping saline groundwater into the wetland to increase salinity and kill freshwater weeds. Following the findings of a pilot study by Waltham et al (2019), further investigation of the potential risks associated with elevated heavy metals, nutrients and hydrogen sulphide production is required (see Appendix 4 for a summary of findings).
4. Implement scientific treatment trials on Aleman grass using herbicides, saltwater, and a combination of both as a means of controlling the further spread of this weed.
5. Survey nearby coastal habitats to understand the local fish assemblages and benchmark whether fish assemblages are comparable, enriched, or depauperate (Abrantes et al., 2019).
6. Develop and implement a grazing and feral pig management plan (e.g., including stock rotation or fencing) to reduce the risk of grazing sensitive areas and times (e.g., flowering months and locations for aquatic vegetation), as observations during surveys suggest cattle and feral pig damage is present (Appendix 5). Consider offsetting the associated costs through a carbon scheme, such as that currently under preparation by the Australian and Queensland State Government departments (e.g. Land Restoration Fund, Department of Environment and Science).

7. Continue monitoring the wetland to better understand the restoration trajectory and patterns. Monitoring should cover the multifunctional approach presented here, with wetland vegetation species and extent collected every 2-3 years, continuation of the depth loggers in the field to track tidal inundation, model predictions, and continued biodiversity surveys to build an inventory of species using the wetland over time.
8. Consider re-assessing the carbon and nitrogen processing rates to track and potentially credit carbon abatement and denitrification, or understand the potential for other similar restoration projects. Adame et al., (2015) and Adame et al., (2019) have previously assessed the site (Appendices 7 & 8), and a similar assessment could be done every 5-10 years.
9. Assess and monitor the health and extent of mangrove assemblages, as field observations suggest the assemblages may be stressed (Appendix 6: Observation of mangrove stress). This may involve measuring stem diameters to give an estimate of the age of trees and species occurrence across appropriate transects, and using both satellite imagery and GPS-tagged time-lapse cameras to monitor changes over time.

REFERENCES

Abbott, B. N., Wallace, J., Nicholas, D. M., Karim, F., & Waltham, N. J. (2020). Bund removal to re-establish tidal flow, remove aquatic weeds and restore coastal wetland services—North Queensland, Australia. *PLOS ONE*, *15*(1), e0217531.

Abrantes, K. G., Sheaves, M., & Fries, J. (2019). Estimating the value of tropical coastal wetland habitats to fisheries: Caveats and assumptions. *PloS One*, *14*(4).

Adame, M. F., Franklin, H., Waltham, N. J., Rodriguez, S., Kavehei, E., Turschwell, M. P., Balcombe, S. R., Kaniewska, P., Burford, M. A., & Ronan, M. (2019). Nitrogen removal by tropical floodplain wetlands through denitrification. *Marine and Freshwater Research*, *70*, 1513–1521.

Adame, M. F., Santini, N. S., Tovilla, C., Vázquez-Lule, A., Castro, L., & Guevara, M. (2015). Carbon stocks and soil sequestration rates of tropical riverine wetlands. *Biogeosciences*, *12*, 3805–3818.

Arthington, A. H., Godfrey, P. C., Pearson, R. G., Karim, F., & Wallace, J. (2015). Biodiversity values of remnant freshwater floodplain lagoons in agricultural catchments: evidence for fish of the Wet Tropics bioregion, northern Australia. *Aquatic Conservation: Marine and Freshwater Ecosystems, 25*, 336-352.

Alldred, M., & Baines, S. B. (2016). Effects of wetland plants on denitrification rates: a meta-analysis. *Ecological Applications*, *26*, 676–685.

Allen, G. R., Midgley, S., & Allen, M. (2002). *Field guide ot the freshwater fishes of Australia*. CSIRO Publishing, Australia.

ANZECC. (2000). Australian and New Zealand guidelines for fresh and marine water quality. *Australian and New Zealand Environment and Conservation Council and Agriculture and Resource Management Council of Australia and New Zealand, Canberra*, 1–103.

Bainbridge, Z. T., Brodie, J., Faithful, J., Sydes, D. A., & Lewis, S. E. (2009). Identifying the land-based sources of suspended sediments, nutrients and pesticides discharged to the Great Barrier Reef from the Tully–Murray Basin, Queensland, Australia. *Marine & Freshwater Research*, *60*, 1081–1090.

Barbier, E. B. (2013). Valuing ecosystem services for coastal wetland protection and restoration: Progress and challenges . In *Resources* (Vol. 2, Issue 3, pp. 213–230). MDPI AG.

Barbier, E. B., Hacker, S. D., Kennedy, C., Koch, E. W., Stier, A. C., & Silliman, B. R. (2011). The value of estuarine and coastal ecosystem services. *Ecological Monographs*, *81*, 169–193.

Bell-James, J., & Lovelock, C. E. (2019). Tidal boundaries and climate change mitigation–the curious case of ponded pastures. *Australian Property Law Journal*, *27*, 114–133.

Blackman, J. G., Perry, T. W., Ford, G. I., Craven, S. A., Gardiner, S. J., & De Lai, R. J. (1999). *Characteristics of important wetlands in Queensland*. Queensland Government, Australia.

Brodie, J., & Waterhouse, J. (2012). A critical review of environmental management of the 'not so Great' Barrier Reef. *Estuarine, Coastal and Shelf Science*, 104–105, 1–22.

Burrows, D., & Butler, B. (2012). *Priminary studies of temperature regimes and temperature tolerance of aquatic fauna in freshwater habitats of northern Australia*. Report 12/08, Australian Centre for Tropical Freshwater Research, James Cook University, Australia.

Burrows, D., & Perna, C. (2005). *Identification of fish habitat and wetland management issues in the Haughton River Catchment, north Queensland*. Report 05/18, Austraian Centre for Tropical Freshwater Research, James Cook University, Townsville, Australia.

Burrows, D., Sheaves, M., Johnston, R., Dowe, J. L., & Schaffer, J. (2012). *Impact of excess freshwater flow on the lower Barratta Creek and estuary*. Report 12/09, TropWATER, James Cook University, Townsville, Australia.

Butler, B., & Burrows, D. W. (2007). *Dissolved oxygen guidelines for freshwater habitats of northern Australia.* Report 07/31. Australian Centre for Tropical Freshwater Research, James Cook University, Townsville, Australia.

Butler, B., Loong, D., Burrows, D., & Morgan, G. (2009). Aquatic ecology assessment of Mungalla wetlands. Report 09/38. TropWATER, James Cook University, Australia.

Challen, S., & Long, P. (2004). Fisheries guidelines for managing ponded pastures. In *Fish Habitat Guidelines* (Vol. 005). Department of Primary Industries, Queensland, Australia.

Chow, V. T. (1959). *Open channel hydraulics* (M.-H. I. Edition (ed.)).

Coleman, J., Huh, O., & Braud, D. (2008). Wetland loss in world deltas. *Journal of Coastal Research*, *24*, 1–14.

Creighton, C., Boon, P. I., Brookes, J. D., & Sheaves, M. (2015). Repairing Australia's estuaries for improved fisheries production–what benefits, at what cost? *Marine and Freshwater Research*, *66*, 493–507.

Creighton, C., Hobday, A. J., Lockwood, M., & Pecl, G. T. (2016). Adapting management of marine environments to a changing climate: a checklist to guide reform and assess progress. *Ecosystems*, *19*, 187–219.

Csurhes, S., & Edwards, R. H. (1998). *Potential environmental weeds in Australia*. Biodiversity Group, Environment Australia.

Csurhes, S., Mackey, A. P., & Fitzsimmons, L. (1999). *Hymenachne (Hymenachne amplexicaulis) in Queensland*. Land Protection, Department of Natural Resources and Mines. Queensland Government, Australia.

Davidson, N. C. (2014). How much wetland has the world lost? Long-term and recent trends in global wetland area. *Marine and Freshwater Research*, *65*, 934–941.

Davis, A., & Dowe, J. (2005). *Ecological Assessment of the Freshwater Wetlands in the Nicholson-Gregory Catchment, North-Western Queensland* Report 04/10. Australian Centre for Tropical Freshwater Research, James Cook University, Australia.

DEHP (2016). *Wetlands in the Great Barrier Reef Catchment Management Strategy 2016-2021*. Department of Environment and Science, Queensland Government, Australia

DHI. (2012). *MIKE21 Flow model, Hydraulics Module, Scientific Documentation* (D. H. I. W. and E. P. Ltd (ed.)).

Elliott, M, & Whitfield, A. K. (2011). Challenging paradigms in estuarine ecology and management. *Estuarine, Coastal and Shelf Science*, *94*, 306–314.

Elliott, Michael, Mander, L., Mazik, K., Simenstad, C., Valesini, F., Whitfield, A., & Wolanski, E. (2016). Ecoengineering with Ecohydrology: Successes and failures in estuarine restoration. *Estuarine, Coastal and Shelf Science*, *176*, 12–35.

Gaspar, P., & Ponte, R. M. (1997). Relation between sea level and barometric pressure determined from altimeter data and model simulations. *Journal of Geophysical Research: Oceans*, *102*, 961–971.

GBRMPA. (2014). *Great Barrier Reef Outlook Report 2014*. Great Barrier Reef Marine Park Authority, Australia.

Gorski, K., De Leeuw, J. J., Winter, H. V, Vekhov, D. A., Minin, A. E., Buijse, A. D., & Nagelkerke, L. A. J. (2011). Fish recruitment in a large, temperate floodplain: the importance of annual flooding, temperature and habitat complexity. *Freshwater Biology*,

56, 2210–2225.

Grice, A. C., Cassady, J., & Nicholas, D. M. (2012). Indigenous and non-Indigenous knowledge and values combine to support management of Nywaigi lands in the Queensland coastal tropics. *Ecological Management & Restoration*, *13*, 93–97.

Houston, W. A., & Duivenvoorden, L. J. (2002). Replacement of littoral native vegetation with the ponded pasture grass Hymenachne amplexicaulis: effects on plant, macroinvertebrate and fish biodiversity of backwaters in the Fitzroy River, Central Queensland, Australia. *Marine and Freshwater Research*, *53*, 1235–1244.

Hyland, S. L. (2002). *An investigation of the impacts of ponded pastures on Barramundi and other finfish populations in tropical coastal wetlands.* (Department of Primary Industries (ed.)). Queensland Government, Australia.

Karim, F., Kinsey-Henderson, A., Wallace, J., Arthington, A. H., & Pearson, R. G. (2012). Modelling wetland connectivity during overbank flooding in a tropical floodplain in north Queensland, Australia. *Hydrological Processes*, *26*, 2710–2723.

Karim, F., Nicholas, M., Grice, T., Marvanek, S., & Wallace, J. (2014). Hydrodynamic modelling of seawater intrusion in a riverine wetland in north Queensland, Australia. *Hydrology and Water Resources Symposium*, 645.

Kelleway, J., Serrano, O., Baldock, J., Cannard, T., Lavery, P., Lovelock, C. E., Macreadie, P., Masqué, P., Saintilan, N., & Steven, A. D. L. (2017). Technical review of opportunities for including blue carbon in the Australian Government's Emissions Reduction Fund. CSIRO, Canberra, Australia.

Knight, J. F., Corcoran, J. M., Rampi, L. P., & Pelletier, K. C. (2015). Theory and applications of object-based image analysis and emerging methods in wetland mapping. *Remote Sensing of Wetlands: Applications and Advances*, 175–194.

Lee, S. Y., Hamilton, S., Barbier, E. B., Primavera, J., & Lewis, R. R. (2019). Better restoration policies are needed to conserve mangrove ecosystems. *Nature Ecology & Evolution*, *3*, 870.

Lovelock, C. E., & Duarte, C. M. (2019). Dimensions of Blue Carbon and emerging perspectives. *Biology Letters*, *15*, 20180781.

Luke, H., Martens, M. A., Moon, E. M., Smith, D., Ward, N. J., & Bush, R. T. (2017). Ecological restoration of a severely degraded coastal acid sulfate soil: A case study of the East Trinity wetland, Queensland. *Ecological Management & Restoration, 18*, 103-114.

Mackay, C., Suter, S., Albert, N., Morton, S., & Yamagata, K. (2015). Large scale flexible mesh 2D modelling of the Lower Namoi Valley. *Floodplain Management Australia National Conference*, 1–14.

Paschke, M. W., Perkins, L. B., & Veblen, K. E. (2019). Restoration for multiple use. *Restoration Ecology*, *27*, 701–704.

Perna, C. N., Cappo, M., Pusey, B. J., Burrows, D. W., & Pearson, R. G. (2012). Removal of Aquatic Weeds Greatly Enhances Fish Community Richness and Diversity: An Example from the Burdekin River Floodplain, Tropical Australia. *River Research and Applications*, *28*(8), 1093–1104.

Reid, B., Grice, T., Holtum, J., Nicholas, M., Wallace, J., & Waltham, N. (2018). Assessing the potential for controlling four invasive aquatic plant species (aleman grass, water hyacinth, olive hymenachne and para grass) using seawater in northern Australian coastal wetlands. Report 18/31, TropWATER, James Cook University, Townsville, Australia.

Rogers, K., Saintilan, N., Mazumder, D., & Kelleway, J. J. (2019). Mangrove dynamics and blue carbon sequestration. *Biology Letters*, *15*, 20180471.

Stewart, B. A., Close, P. G., Cook, P. A., & Davies, P. M. (2013). Upper thermal tolerances of key taxonomic groups of stream invertebrates. *Hydrobiologia*, *718*, 131–140.

United Nations General Assembly. (2015). Transforming our world: the 2030 Agenda for Sustainable Development. *Division for Sustainable Development Goals: New York, NY, USA*.

Van Coppenolle, R., & Temmerman, S. (2019). A global exploration of tidal wetland creation for nature-based flood risk mitigation in coastal cities. *Estuarine, Coastal and Shelf Science*, *226*, 106262.

Waltham, N. (2018). Acute thermal effects in an inland freshwater crab Austrothelphusa transversa (von Martens, 1868) occupying seasonal, tropical rivers. *Journal of Crustacean Biology*, *38*, 497–503.

Waltham, N., Buelow, C., & Burrows, D. (2019). *Restoring wetland values under Greening Australia's Reef Aide program - Crooked Waterhole and Mungalla wetland complex*. Report 18/33, TropWATER, James Cook University, Townsville, Australia.

Waltham, N., Burrows, D., Wegscheidl, C., Buelow, C., Ronan, M., Connolly, N., Groves, P., Audas, D., Creighton, C., & Sheaves, M. (2019). Lost floodplain wetland environments and efforts to restore connectivity, habitat and water quality settings on the Great Barrier Reef. *Frontiers in Marine Science*, *6*, 71.

Waltham, N., Elliott, M., Lee, S. Y., Lovelock, C., Duarte, C. M., Buelow, C., Simenstad, C., Nagelkerken, I., Classens, L., Wen, C. C. K., Barletta, M., Connolly, R. M., Gillies, C., Mitsch. W. J., Ogburn, M. B., Purandare, J., Possingham, H., & Sheaves, M. (2020). UN Decade on Ecosystem of Restoration 2021-2030 – what chance for success in restoring coastal ecosytems? *Frontiers in Marine Science*. 7, 71.

Waltham, N., & Fixler, S. (2017). Aerial herbicide spray to control invasive water hyacinth (Eichhornia crassipes): Water quality concerns fronting fish occupying a tropical floodplain wetland. *Tropical Conservation Science*, *10*, 1940082917741592. https://doi.org/10.1177/1940082917741592

Waltham, N., McCann, J., Power, T., Moore, M., & Buelow, C. (2020). Patterns of fish use in urban estuaries: Engineering maintenance schedules to protect broader seascape habitat. *Estuarine, Coastal and Shelf Science*, 106729.

Waterhouse, J., Brodie, J., Lewis, S., & Audas, D. (2016). Land-sea connectivity, ecohydrology and holistic management of the Great Barrier Reef and its catchments: time for a change. *Ecohydrology & Hydrobiology*, *16*, 45–57.

Wearne, L. J., Clarkson, J., Grice, A. C., van Klinken, R. D., & Vitelli, J. S. (2010). The Biology of Australian Weeds 56.'Hymenachne amplexicaulis'(Rudge) Nees. *Plant Protection Quarterly*, *25*, 146.

Weinstein, M. P., Hazen, R., & Litvin, S. Y. (2019). Response of nekton to tidal salt marsh restoration, a meta-analysis of restoration trajectories. *Wetlands*, *39*, 575–585.

Zedler, J. B., & Callaway, J. C. (2000). Evaluating the progress of engineered tidal wetlands. *Ecological Engineering*, *15*, 211–225.

APPENDIX 1: RAINFALL AND HYDROLOGY

A1.1 Rainfall

Rainfall has been recorded daily at the Victoria Point Sugar Mill (032045, Bureau of Meteorology, BOM) station since 1897 (about 10km from Mungalla wetland). Analysis of these data reveals that the highest accumulative wet season (November to March) rainfall occurred 2018/19 (3645 mm) while the lowest was 1901/02 (336mm) (Table 1). Annual summer rainfall totals recorded during the study were generally below the long-term average (Table 10), and in fact were below the 20 percentile for all records (Figure 18). The exception was the 2018/19 wet season, which was the largest on record (Table 9).

Table 9: Summary wet season (Nov – March) statistics of rainfall recorded at Victoria Point Sugar Mill station

Statistic	Wet season rainfall (mm)
Minimum	335.7 (1901/1902)
Maximum	3645.3 (2018/2019)
Overall mean	1593.0
95th percentile	2603
5th percentile	650.8
2016/17 wet season total	1004.2
2017/18 wet season total	1653.3
2018/19 wet season total	3645.3

Table 10: Summary dry season (April – October) statistics of rainfall recorded at Victoria Point Sugar Mill station

Statistic	Dry season rainfall (mm)
Minimum	77.1 (1945/46)
Maximum	1415 (1919/1920)
Overall mean	427.9
95th percentile	870.5
5th percentile	142.4
2016/17 dry season total	337.0
2017/18 dry season total	189.0
2018/19 dry season total	198.0

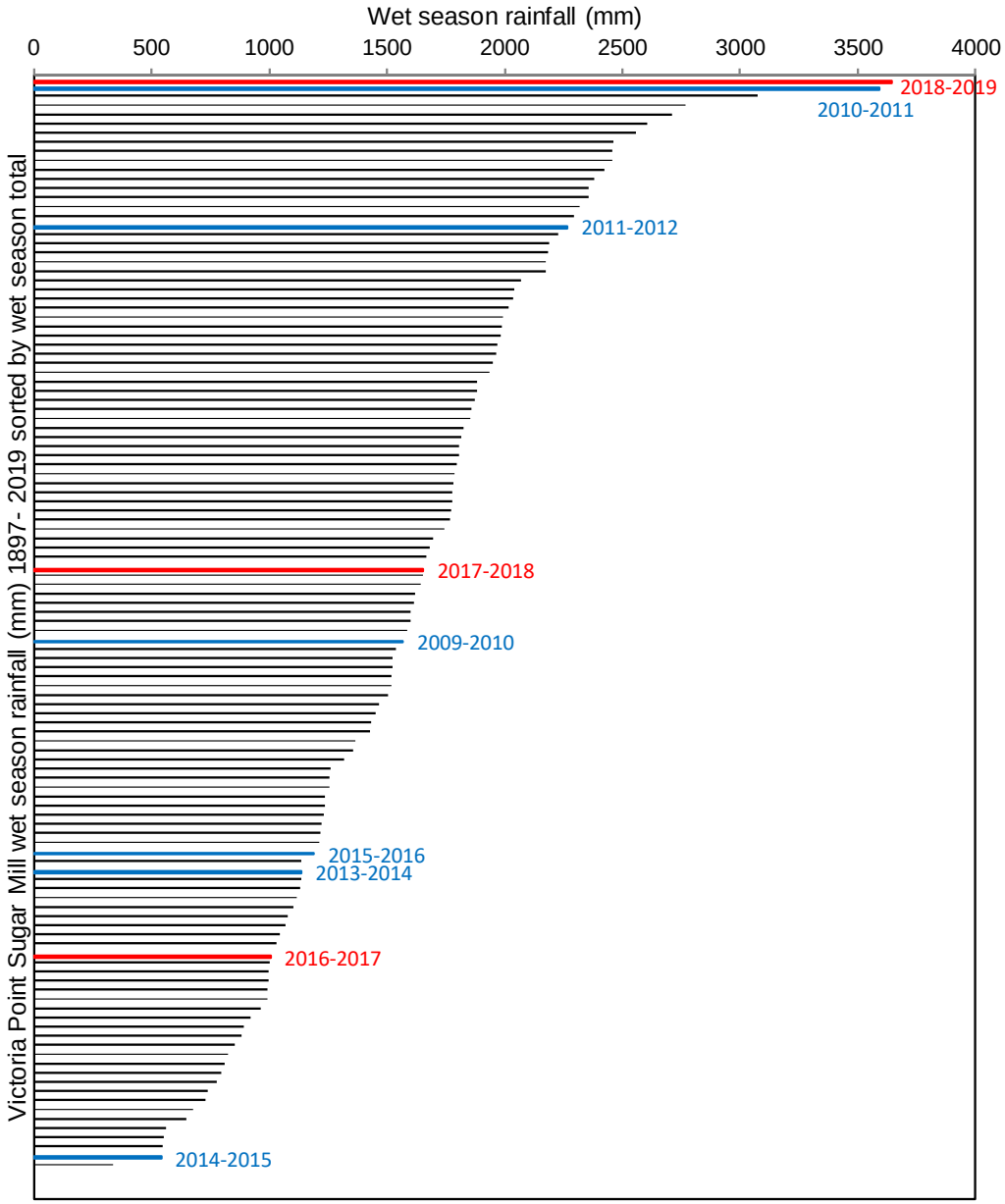


Figure 17: BOM wet-season (Nov - March) rainfall data recorded at Victoria Point Sugar Mill (station number 32045) ranked in order of decreasing total rainfall (mm). Blue bars show total rainfall over the past few years, red bars cover wet season during this survey

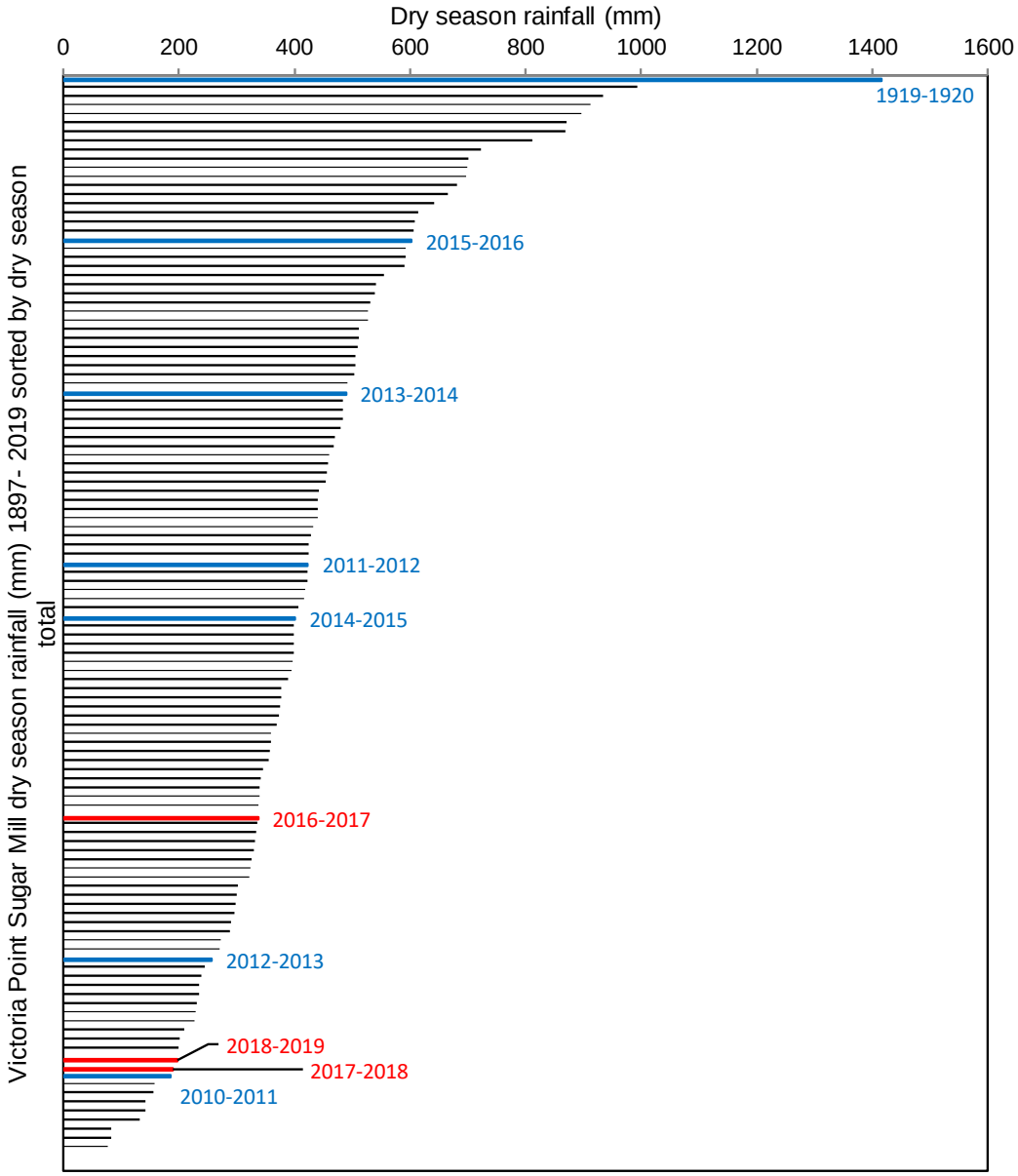


Figure 18: BOM dry-season (April - October) rainfall data recorded at Victoria Point Sugar Mill (station number 32045) ranked in order of decreasing total rainfall (mm). Blue bars show total rainfall over the past few years, red bars cover dry season during this survey

A1.2 Streamflow and catchment runoff

Mungalla wetland is in the Herbert River catchment along the GBR coast. The Herbert river drains the eastern side of the Great Dividing Range and flows south-east into the Coral Sea and the South Pacific Ocean. The mainstream length of the Herbert River is approximately 240 km. During high flow events, the wetland receives freshwater from the Herbert River through Palm Creek. The Stone River is one of the major tributaries of the Herbert River and it also supplies freshwater to the Mungalla wetland through Trebonne Creek. Streamflow in all tributaries and distributaries of the Herbert River are ephemeral. There is a large inter-annual variability in flow magnitude in the entire catchment including the Stone River. For example, a typical time series of mean annual flow at Running Creek on the Stone River between 1980 and 2014 is presented in Figure 19.

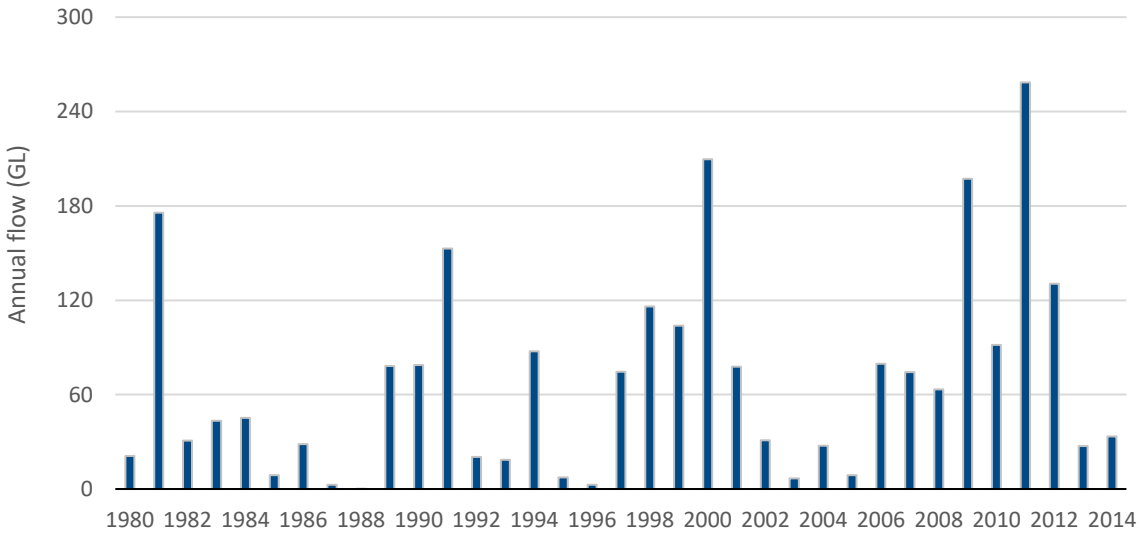


Figure 19: Annual flow in the Stone River at Running Creek upstream of the Mungalla wetland

There are also large seasonal variations in streamflow (Figure 20), with about 93% of flow occurring in the wet-season months of December to April with the highest flow in February (36%).

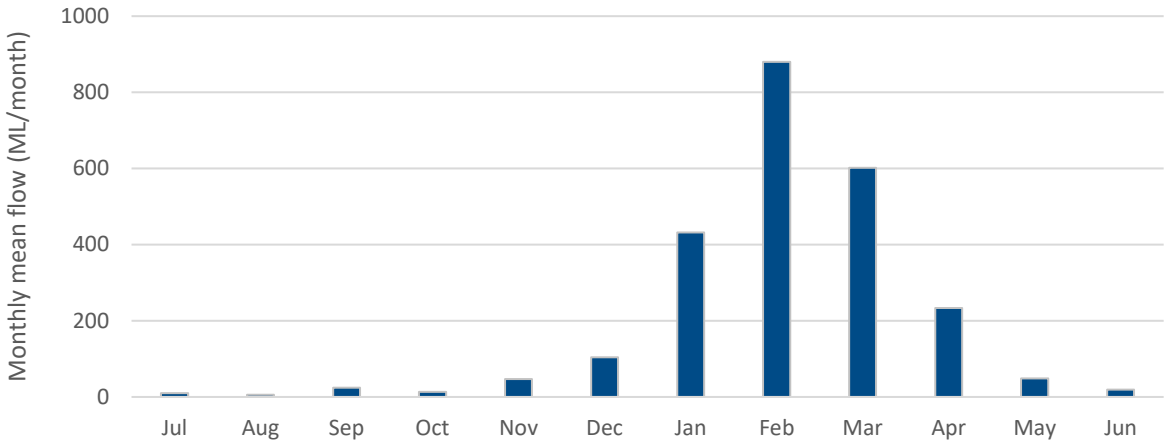


Figure 20: **Mean monthly flow distribution at Running Creek in the Stone River based on observed flow records for the period of 1980 to 2014.**

A1.3 Tide and wetland inundation

The nearest tide gauge to Mungalla wetland is located at Lucinda, which is about 20 km north-east of Mungalla. The Maritime Safety unit of the Department of Transport and Main Roads of Queensland Government is the main source of tide data for the study area. Another useful source is the Willey Weather (https://tides.willyweather.com.au/qld/northern/lucinda.html), that provide predicted tide level for short periods of time. Tides at the Mungalla coast are semidiurnal having one large and one small peak in a day. There is large variation in tidal range, for example, from 0.1 m to about 4.0 m from observations between 2001 and 2016. The typical tidal cycles at Forrest Beach (3 km from the Mungalla wetland) is presented in Figure 21. In any year there are two 'king' tides that are the highest, one of them occurs during summer (January/February) and the other during winter (July/August). The king tides occur because of the combined influence of a number of astronomical factors related to the Sun and the Moon (and their alignments) and the gravitational attraction they each have on the water surface of the Earth. During the king tides there is the potential for the Mungalla wetland to become inundated. Past records show that tides above around 3.7m with respect to the lowest astronomical tide (LAT) have the potential to reach to the Mungalla wetland. Across Australia, tides are measured with respect to the LAT datum. At Lucinda, Australian height datum (AHD) is 1.844 m above the LAT and mean sea level (MSL) is 1.897 m above the LAT.

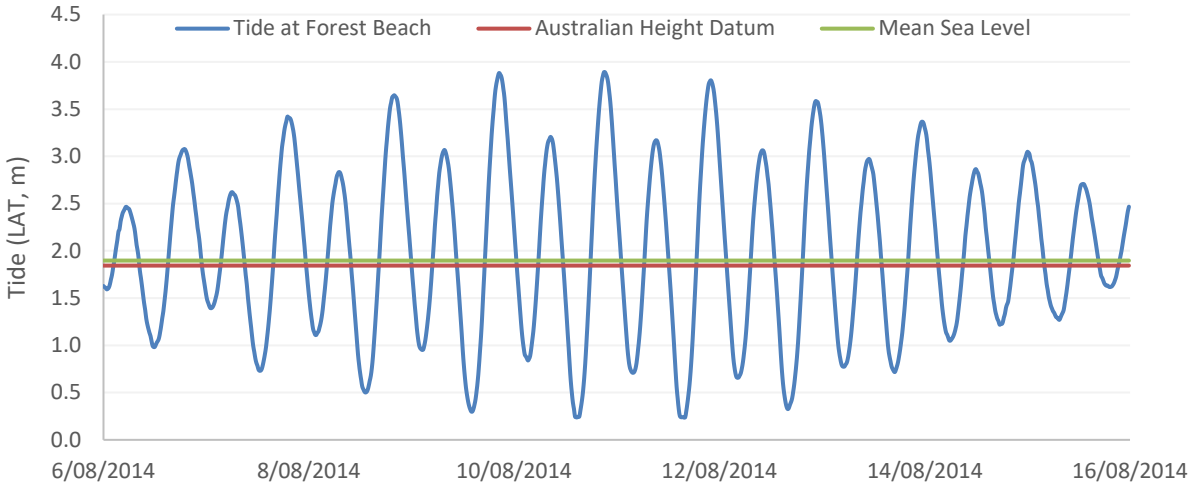


Figure 21: An example of typical tidal cycles at Forrest Beach. Data are presented with respect to lowest astronomical tide (LAT) datum.

A1.3.1 Frequency of high tides

Measured water quality data at 5 logger sites across the wetland show that tides of 3.7 m or greater (at nearby Forrest Beach) have the potential to reach the Mungalla wetland. To assess frequency of tidal inundation of the wetland a summary of all high tides > 3.7 m since 2012 are identified Figure 22.

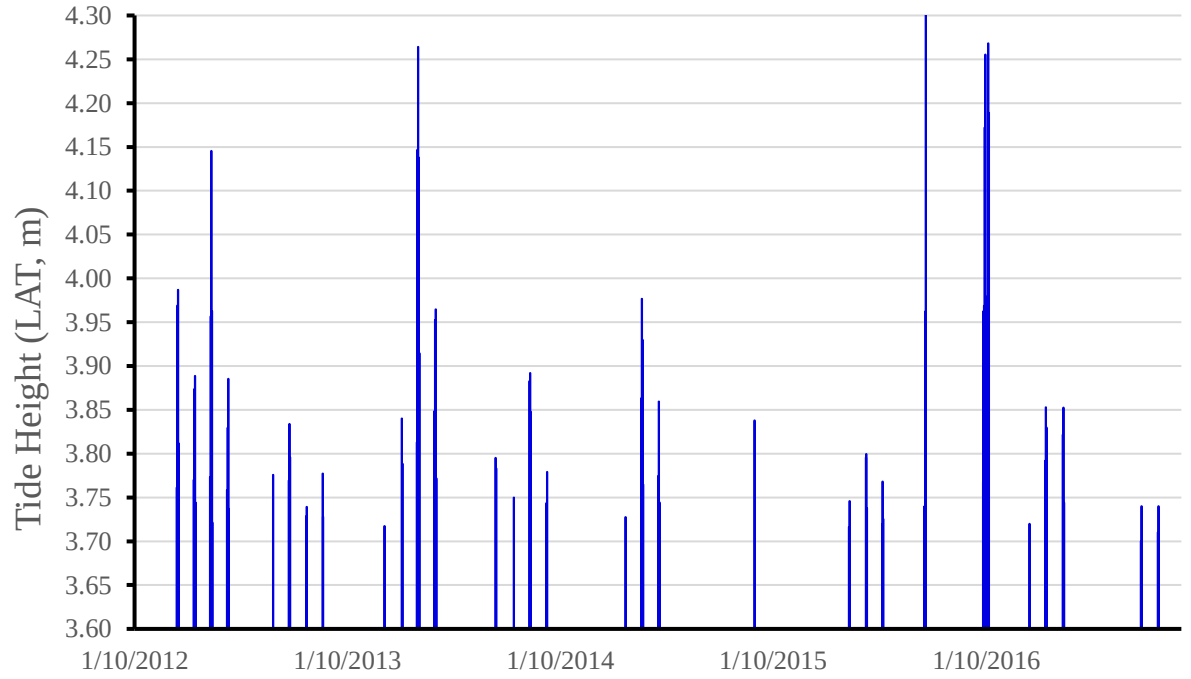


Figure 22: Observed tides at Forrest Beach since 2012 that are greater than 3.7 m. Data are presented with respect to lowest astronomical tide (LAT) datum (AHD is 1.844 m above LAT and 0.053 m below MSL)

Results show that there are about 19 days per year when tide height is greater than 3.7 m that have the potential to reach the Boolgooroo wetland (northern part of the Mungalla wetland). These tend to occur in events of 2 to 3 consecutive days, so the wetland inundation frequency per event is between 6 and 10 times a year. Inundation frequency is lower for the less common larger tides (Table 11). For example, only 0 to 5 tides > 4.1 m occurred each year (mean 2.3 per year), which would usually occur in a single annual event.

Table 11: Number of tides per year greater than 3.7 to 4.1 m at Forrest Beach (3 km from the Mungalla wetland).

Year	Tide > 3.7 m	Tide > 3.9 m	Tide > 4.0 m	Tide > 4.1 m
2012	11	6	2	0
2013	22	8	3	1
2014	19	11	6	3
2016	23	10	9	5

APPENDIX 2: HYDRODYNAMIC MODEL DEVELOPMENT

A2.1 Modelling tools

Hydrodynamic models have been in common use for inundation modelling for several decades worldwide. The main advantages of using a hydrodynamic model are that they produce floodplain hydraulics to estimate inundation extent, duration, depth and frequency of wetting and drying at desired spatial (e.g. 5 to 10 m grid) and temporal (e.g. hourly) scales (Horritt & Bates 2002). Technical considerations include the size of the hydrodynamic model domain, irregularity in land topography, availability of topography data, and complexity of the hydraulic regime. Based on the objectives and availability of input data one can select one-dimensional (1D) and two-dimensional (2D) or coupled one- and two-dimensional models (Horritt & Bates 2002, Teng et al. 2017). However, the correct schematisation of floodplain features in a 1D model is complex, especially at higher flow rates where there is a transverse gradient in water level across the cross-section. Two-dimensional (2D) modelling avoids much of the conceptualisation required to build an accurate 1D model. Nonetheless, the application of traditional fixed grid 2D models is not good enough to reproduce river conveyance because model grids are not aligned with the river banks and in many cases the lowest points of the rivers disappear in the model. The grid size has to be small enough to actually model the hydraulic effects producing the hydraulic gradients through the floodway, particularly for sharp bends and narrow channels. If the grids are solely chosen to make sure the floodway is adequately modelled, this will lead to a computationally slow model that produces unnecessarily detailed results for much of the floodplain. More recently flexible mesh (also called irregular grid) models have been found to be superior to regular grid models in terms of accuracy and computational time (Mackay et al. 2015). The use of a flexible mesh 2D model can overcome many of the limitations of other 2D models as they allow complex floodway geometries to be modelled with precision in 2D. They do not require the remainder of the floodplain be modelled at the same scale and they allow the computational mesh to be aligned and refined to suit the geometry of the problem (Syme 2001).

Among others, MIKE21 (DHI 2012), TUFLOW (Syme 2001), LISFLOOD-FP (Bates et al. 2013) are some of commonly used 2D hydrodynamic models in Australia. All models have the options to choose from regular grid or flexible mesh 2D model or a combination of 1D and 2D model. However, MIKE21 has the added advantage of simulating tidal inundation. For the first phase (2012-2014) of the Mungalla wetland study, a two-dimensional regular grid model was used. In the current phase of the study a two-dimensional flexible mesh model (MIKE21 FM) was used. The selection of the flexible mesh model is primarily based on availability of fine-scale laser altimetry (LiDAR) data and the availability of supercomputing facilities (e.g. multi-core GPU machine) at CSIRO. A brief description of the two models is presented in the following sections.

A2.1.2 Regular grid model

The two-dimensional hydrodynamic model, MIKE21, is the basic computational hydrodynamic module that simulates the water level variation and streamflow in response to a variety of forcing functions in floodplains, lakes, estuaries, bays and coastal areas. The model is based on two-dimensional Saint-Venant's equations of mass and momentum conservation (DHI 2012). Water depth and flux are resolved on rectangular grids and the model uses the

alternating direction implicit (ADI) technique to solve the mass and momentum matrix at each time step. The boundary conditions in MIKE21 can vary in both time and space. Point sources and sinks can also be incorporated in the model. The main strength of the MIKE21 model is its ability to simulate wetting and drying of a floodplain during a flood event, and the large number of computational grids that it can handle (in the range of millions). The main limitation is the poor representation of stream channels because it can be difficult to align the rectangular grids to the river banks. Therefore, the model is not suitable for simulating channelised flow or very small overbank events. Like other two-dimensional models, computational time is a significant consideration when using the MIKE21 model. In the first of the Mungalla wetland study (2012-2014), a regular grid model was used because flexible grid option was not available at that time.

A2.1.2 Flexible grid model

The hydrodynamic module of the MIKE21 Flow Model FM (hereafter referred to as MIKE21 FM) is based on the numerical solution of the two-dimensional incompressible Reynolds averaged Navier-Stokes equations, assuming hydrostatic pressure. Primitive variable equations are discretised using an element-centred finite volume method. The spatial domain is discretised into non-overlapping elements, which can be either triangular or quadrilateral (DHI 2016). The finite volume method sets up an Equivalent Riemann Problem (ERP) across each element interface and solves it to determine the variable fluxes between elements. The technique used in MIKE21 FM determines an exact solution to an approximate Riemann problem. The approach treats the problem as one-dimensional in the direction perpendicular to each element interface.

MIKE21 FM has two options for time integration accuracy, with these being a first order explicit Euler method (referred to as the lower temporal order scheme), and a second order Runge Kutta method (referred to as the higher temporal order scheme). There are also two options for spatial integration, with the second order (higher order) accuracy being achieved through a variable gradient reconstruction technique prior to the ERP formulation (DHI 2016). The flexible mesh model is preferable over the classic MIKE21 regular grid model when highly detailed elevation data (e.g. LiDAR) are available because the model allows selection of a very small gird at the area of interest and the alignment of model grids to the river banks. A flexible mesh hydrodynamic model of the Mungalla wetland was configured and calibrated for this project.

A2.2 Model inputs

Hydrodynamic models are data intensive. A large amount of temporal and spatial data is required for the configuration and calibration of a hydrodynamic model for inundation simulation. While some input data (e.g. stream network, tide, water level, discharge) can be extracted from secondary sources, most input data are case specific and need to be prepared before running the model. Data needed for model configuration and calibration are briefly described in the following sections.

A2.2.1 Topography

The topography data for the study area were obtained from a 30 m resolution hydrologically corrected SRTM (Shuttle Radar Topography Mission) dataset for the entire catchment and a

Laser altimetry (LiDAR) derived fine resolution (1 m) data set covering the Mungalla wetlands and surrounding areas. The bathymetry data for the ocean part of the study area were obtained from the Geoscience Australia's 250m resolution Bathymetric Grid of Australia. By re-sampling the above data sets, a 10 m resolution digital elevation model (DEM) was produced for the hydrodynamic modelling domain covering an area of 66 km^2. In the re-sampling procedures, an algorithm was used to ensure stream topography as seen in the 1m DEM was maintained in the re-sampled grids. The DEM was further corrected using surveyed cross-sections for streams that were deemed to have contained water during the LiDAR survey. Elevations of stream grids were manually checked and adjusted at some locations where necessary, to ensure a continuous stream until it met with another stream or open sea. A minimum of 3 grid cell streams were enforced to maintain the numerical stability of hydrodynamic modelling. A field survey was conducted in November 2018 to measure the bathymetry of the two main wetlands, Annabone and Boolgooroo (Figure 23). The DEM was updated using the surveyed elevation data. The DEM was subsequently processed using MIKE21 FM tools and a bathymetry file was produced for the modelling domain by specifying elevation data at the vertices of model mesh.

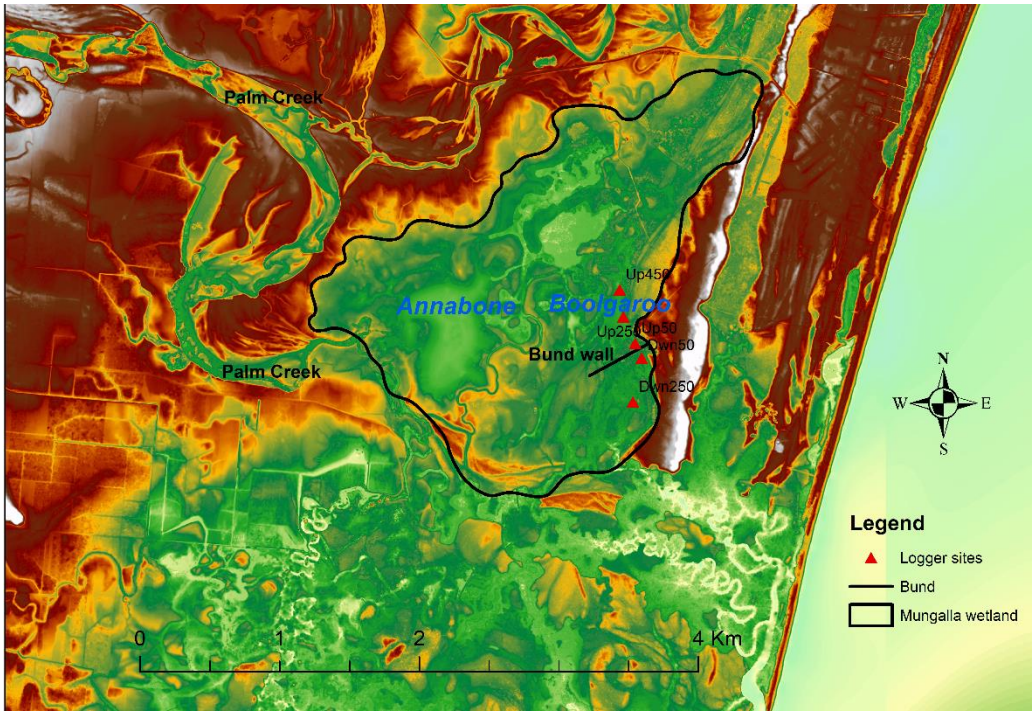


Figure 23: Mungalla topography model showing Annabone and Boolgooroo lagoons, logger sites and bund wall

A2.2.2 Surface roughness

Hydraulic roughness of the land surface was derived using Geoscience Australia's dynamic land cover map and was represented in the hydrodynamic model using Manning's roughness coefficient (n). The land use was categorised into ocean water, mangroves, salt pans, streams, riparian vegetation, wetlands, pasture, agriculture and trees. The land use was converted to a roughness map by substituting the land use code with a corresponding roughness coefficient. Initial roughness coefficients were estimated based on published literature (e.g. Chow, 1959) and a similar study for the neighbouring Tully catchment by Karim et al. (2012). These coefficients were refined as a part of the calibration process.

A2.2.3 Inflow

The hydrodynamic modelling domain was confined by two inflow boundaries at the upstream and an open boundary in the downstream. The Mungalla wetland receives freshwater through Palm and Lucy creeks during summer months (Nov-Apr). Both are ephemeral streams and carry a large volume of water during wet season floods. Palm Creek is relatively large (~100 m wide and ~6 m deep) compared with Lucy Creek (~20 m wide and 2 m deep). Palm Creek acts as a distributary of the Herbert River during summer months (Nov-Apr) and remains dry during winter months (May-Sep). A simple rainfall-runoff model (NAM; DHI, 2009) was calibrated to estimate inflow through the Palm and Lucy Creeks. Initial model parameters were obtained from Karim et al. (2012) and the parameters were recalibrated for the Stone River catchment which is a sub-catchment of the Herbert River.

A2.2.4 Seaside boundary

The nearest tide gauge to Mungalla wetland is located at Lucinda, which is about 20 km north-east of Mungalla. Tide data for the Lucinda gauge were obtained from Maritime Safety Queensland for the period of 2001 to 2015. Observed tide data for the period of September 2011 to August 2012 were used to estimate 60 tidal constituents at Lucinda which were then used to simulate tide levels at the Mungalla coast (Forrest Beach) using the inbuilt tide analysis package in MIKE 21 (DHI 2012). The constituents were estimated using the ISO (Institute of Ocean Science, CANADA) method based on Rayleigh criterion. Once the constituents (that include 45 astronomical main constituents and 24 shallow water constituents) were estimated, high and low waters were estimated and compared with the observed tides at Lucinda. Tide levels at Mungalla were then predicted using the estimated constituents. The time lag between tides at Lucinda and Mungalla was estimated using a separate set of tide data recorded at Mungalla, by the Hinchinbrook Shire Council of Queensland, using two temporary gauging stations just below the bund.

A2.3 Model configuration

Two hydrodynamic models were configured, one using regular grid option and the second a flexible grid option of the MIKE 21 model. A brief description of each model configuration is described in the following sections.

A2.3.1 Regular grid model [MIKE 21]

The MIKE 21 HD model (DHI, 2012) was used to simulate tidal ingress to the wetland and flow connection between the coast, rivers and wetlands. The model was configured for the lower part of the Herbert River that comprises Mungalla wetlands, major streams and a small part of ocean. The computational domain was 66.7 km^2 (8.33 × 8 km) covering the entire Mungalla area. Inputs to the model were land topography, surface roughness coefficients and boundary information. Model boundaries include inflows through the Palm and Lucy Creeks and water levels at the seaside boundary. The hydrodynamic model domain was divided into approximately 667,000 computational grids each 10×10 m. Computational time increment was derived after satisfying numerical stability criteria. A time step of 1 sec was used as this produced a stable solution for a king tide and large inflow conditions. Simulation of each model setup was carried out for 4 to 5 days covering several high and low waters. Computed time-varying water depths across the computational domain were recorded hourly and at some

selected locations half-hourly. These data were then used to estimate the tidal influences in and around the Mungalla wetland.

A2.3.2 Flexible grid model [MIKE 21 FM]

The flexible mesh hydrodynamic modelling domain covered the same area as rectangular grid model except that the seaward boundary was aligned along the coastline. The DEM was processed using the MIKE21 FM mesh generator tool to create a model mesh of variable sizes. The process of creating the model mesh is briefly described here. At first, a network of triangular mesh elements of variable size was produced for the hydrodynamic model domain using a finer mesh for rivers and creeks followed by slightly larger grids as river buffers. A third category mesh of medium size was used for the floodplains that are subject to inundation. A much larger mesh size was used for the rest of the hydrodynamic model domain (Figure 24). The final mesh consisted of 604,200 triangular mesh elements with the minimum element size of 1.86 m^2 and the maximum element size of 6200 m^2. A smooth transition between the mesh zones was maintained by enforcing a minimum angle of 30 degrees for every mesh element.

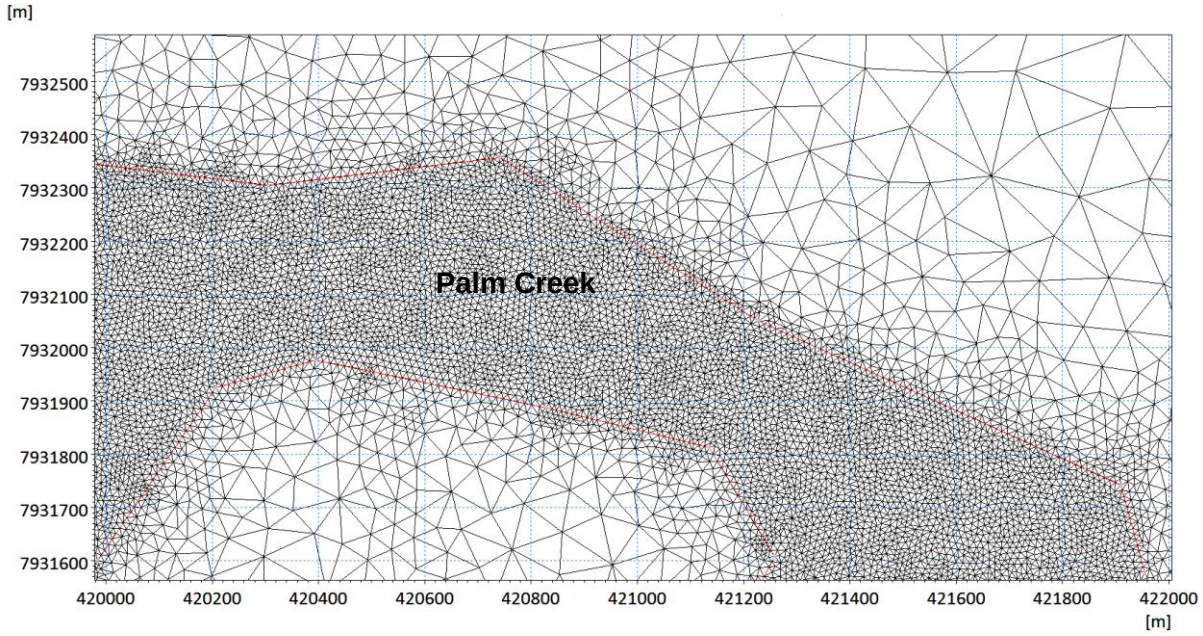


Figure 24: An example of flexible mesh hydrodynamic modelling grids with different mesh zones for rivers, riparian zones and the adjacent land subject to inundation.

A2.4 Model calibration

Model calibration is an important part of hydrodynamic modelling as it provides not only the realistic representation of the physical systems but also the reliability and confidence on predicted results. At first the model was calibrated for the tidal constituents and then for simulations of tide intrusion in and around the Mungalla wetland. The model was calibrated for two high tides in 2013 (before the bund removal), using tide levels at several locations in the Mungalla wetland and on the creeks that connect the wetland with open sea. Observed tide levels from the five automatic loggers that gave continuous water elevation data for different

tide levels were used to constrain the hydrodynamic model in calibration. The main calibration parameter was the surface roughness coefficient, Manning's n, and the eddy viscosity.

Before the hydrodynamic model is calibrated it is important to simulate the timing and size of the tides at Forrest Beach, as this is the key driver of inundation in the wetland. Firstly, the astronomical model ISO (Institute of Ocean Science, Canada) was calibrated using observed tidal data at Lucinda (Figure 25). The model gives a good prediction of tide levels with median absolute error of about 6 cm.

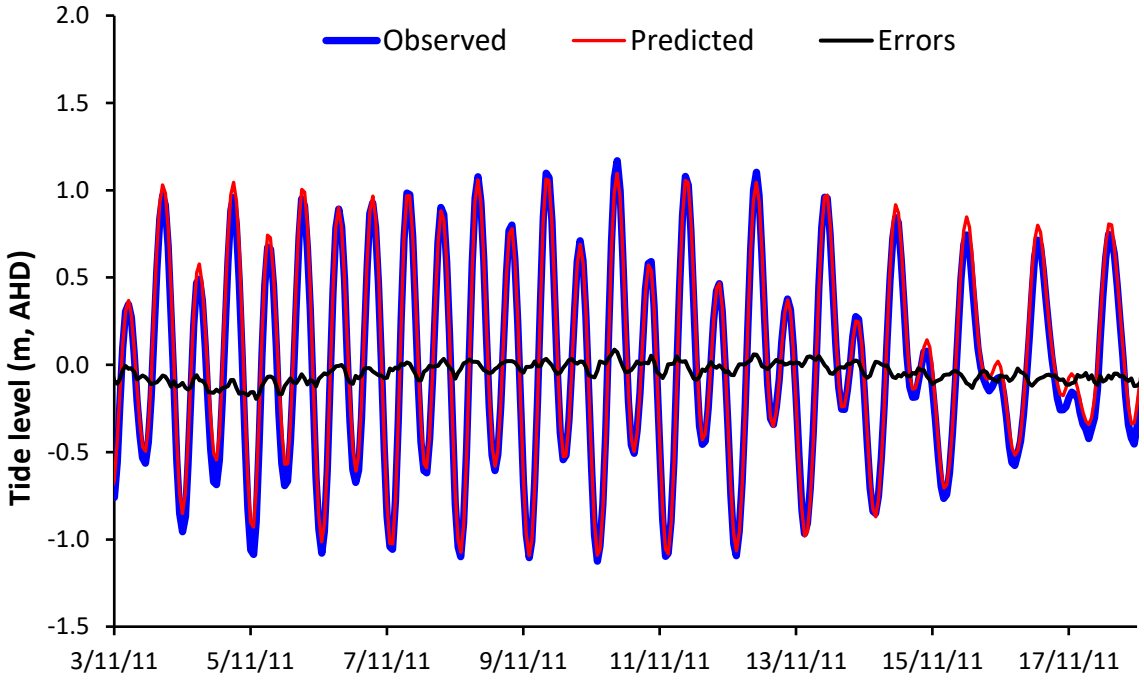


Figure 25: Comparison between observed (blue) and predicted (red) tide level at Lucinda. The black line shows the prediction error (Note: MSL at Lucinda is 0.053 m above AHD)

In the above ISO model calibration a total of 60 tidal constituents were found significant, however, only seven of them are major constituents having 10% or more contribution on amplitude (
Table 12). Tide at Lucinda is semi-diurnal because the periods of the top four constituents are close to 12 hours.

Table 12: Major tide constituents at Lucinda (based on 1 year of tide data)

Name	Symbol	Period (hours)	Amplitude	Phase
Principal Lunar	M_2	12.42	0.72	283.36
Principal Solar	S_2	12.00	0.41	254.71
Larger Elliptical Lunar	N_2	12.66	0.33	257.67
Luni-Solar Declinational	K_2	11.97	0.23	253.49
Luni-Solar	K_1	23.93	0.16	191.48

Declinational				
Principal Lunar	O_1	25.82	0.11	154.62
Principal Solar	P_1	24.07	0.10	187.14

The calibrated ISO model was then used to simulate the tide height at Forrest Beach adjacent to the Mungalla wetland. The comparison between simulated tide at Forrest Beach and the observed tide in Lucinda is presented in Figure 26. These results show that the timing of the tidal pulse is accurately captured and that the difference between tide heights at Lucinda and Forrest Beach is relatively small (<5 cm).

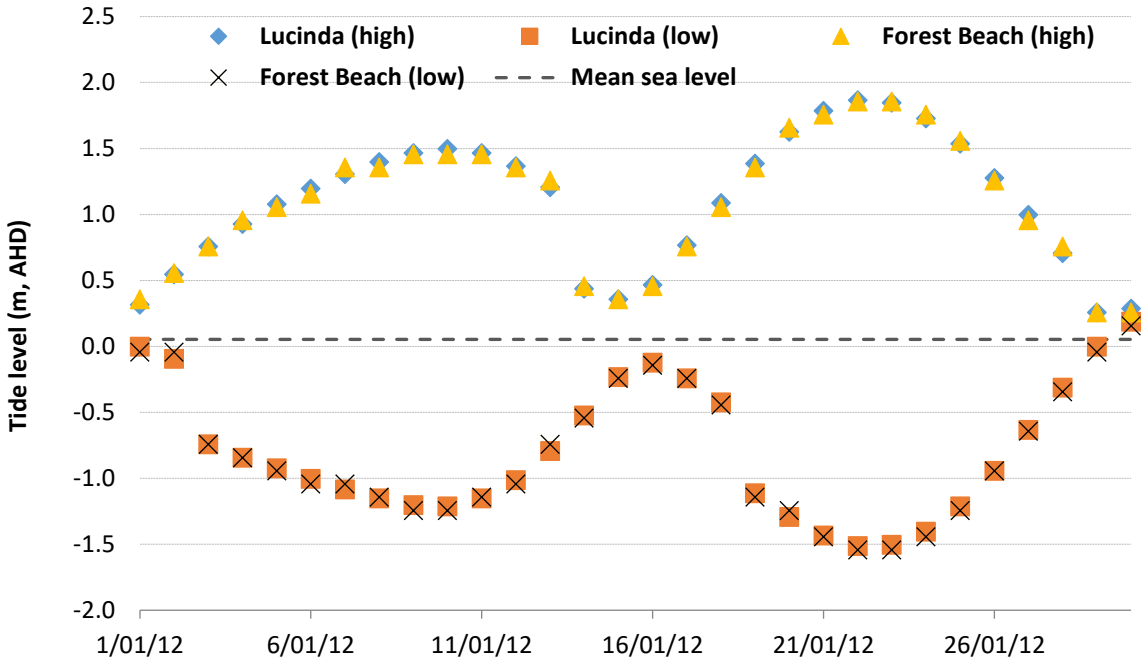


Figure 26: Comparison between high and low tides at Lucinda (observed) and Forrest Beach (simulated) for January 2012

The MIKE 21 FM model parameters were calibrated against a large tide (4.2 m) in January 2014 and verified against two others tides of 3.9m (August 2014) and 4.0 m (February 2015). In the January 2014 calibration run model performance in simulating tide intrusion was evaluated using a time series comparison at four logger locations, 50 and 250 m below the bund and 250 and 450 m above the bund (Figure 27). The model has produced good agreement with logger data at all four measuring sites. The magnitude and timing of peak depths is very well reproduced, although the rate at which the model depth declines after the peaks is more rapid than observed, especially at the upstream loggers. The latter difference should have little effect on the simulation of the timing and maximum volume of seawater intrusion within the wetland. These are the key outputs of model simulations for other tides that can include the impact of on shore wind and sea level rise.

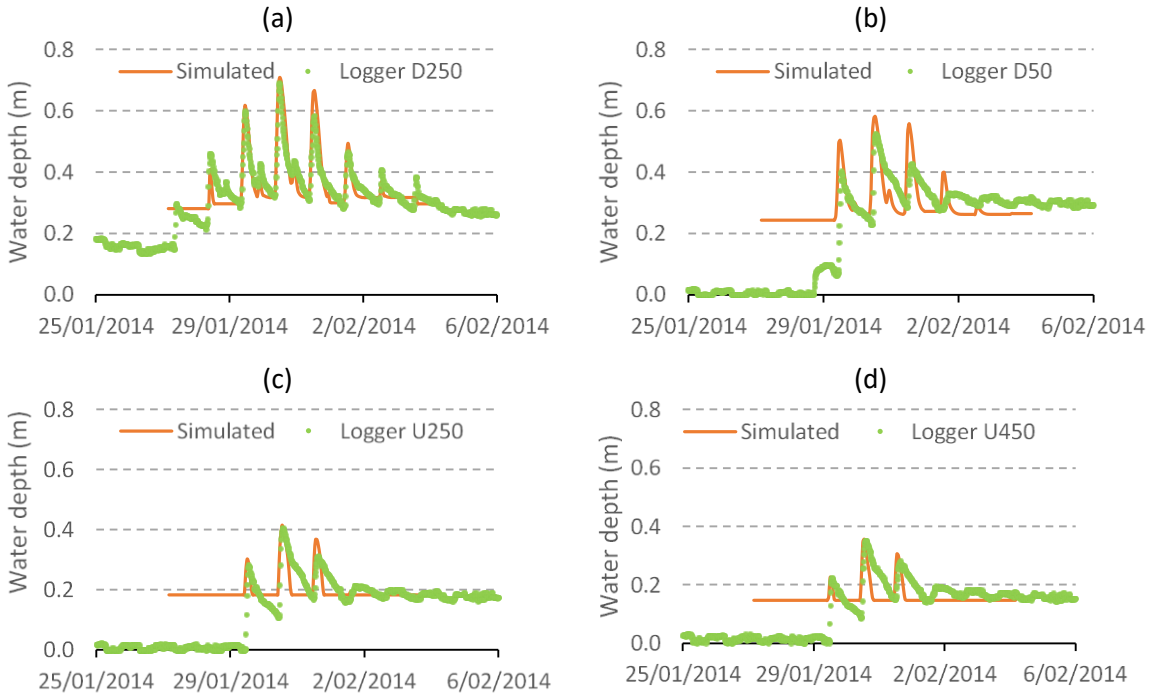


Figure 27: Comparison between observed (green dots) and simulated (orange line) water depths in the Mungalla wetland at (a) 250 m and (b) 50 m below the bund, and (c) 250 m and (d) 450 m above the bund for the tide in January 2014 (calibration).

The model verification simulations for the high tides in August 2014 (3.9 m) and February 2015 (4.0 m) are shown in (Figure 28). In these runs the model parameters were left as determined in the calibration runs and no further adjustments were made. Again, the model reproduces the number, timing and size of the water depth peaks very well. This gives confidence in the ability of the model with calibration parameters to predict the timing and size of peak seawater depth and its maximum volume for a range of tide heights associated with a number of future scenarios (see section 2.6).

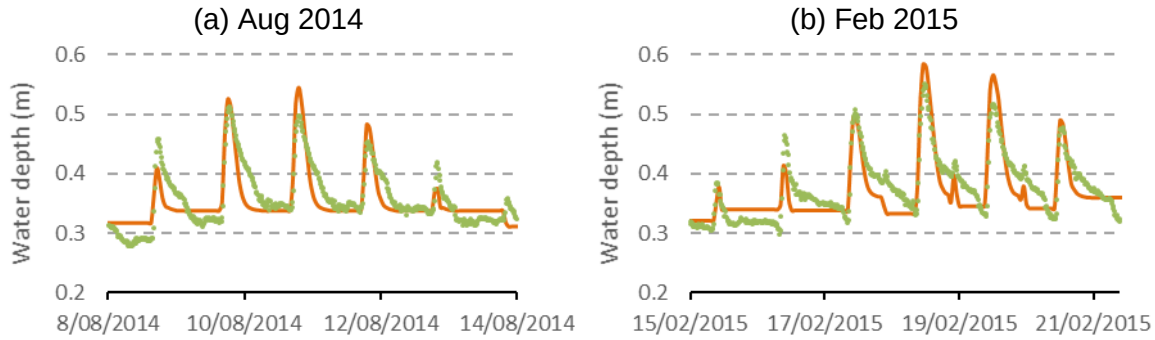


Figure 28: Comparison between observed (green dots) and simulated (orange line) water depths at 250 m below the bund for the tides of 3.9 m in August 2014 and 4.0 m in February 2015 (verification).

APPENDIX 3: VEGETATION COMPOSITION CHANGE

Table 13: Area inhabited by vegetation groups (%): pre- (2012/13) and post (2014 - 2017) bund removal - tidal inundation

Satellite Classification (% of Boolgooroo lagoon)	Survey Year						
	2012	2013	2014	2015	2016	2017	2018
Exotic aquatic plants							
Aleman grass† (*Echinochloa polystachya*)	1.85	3.12	1.18	10.26	4.87	18.93	37.11
Olive hymenachne*† (*Hymenachne amplexicaulis*)	48.94	43.04	12.61	5.11	10.51	5.23	7.36
Para grass† (*Urochloa mutica*)	13.26	6.45	4.24	15.16	6.83	10.42	9.80
Salvinia* (*Salvinia molesta*)	2.41	2.61	0.04	0.00	40.53	10.12	11.59
Water hyacinth* (*Eichhornia crassipes*)	2.68	16.72	0.55	0.03	0.00	0.00	0.00
Native aquatic plants							
Bulkuru (*Eleocharis dulcis*)	0.00	0.00	0.00	11.46	0.26	2.59	1.75
Club rush (*Schoenoplectus litoralis*)	0.00	0.00	0.00	0.00	0.00	0.10	0.26
Duck weed (*Spirodela punctata)*	0.00	0.00	0.31	3.57	0.00	0.00	0.00
Water lily (*Nymphaea gigantea*)	2.66	10.16	3.31	14.07	12.91	17.54	9.31
Other							
Open Water	24.56	13.38	73.71	36.38	20.56	31.70	17.93

*Weeds of national significance, †Ponded pasture grasses.

Table 14: Area inhabited by vegetation groups (%): pre- (2012/13) and post (2014 - 2017) bund removal - no tidal intrusion.

Satellite Classification (% of Annabone and north Boolgooroo)	Survey Year						
	2012	2013	2014	2015	2016	2017	2018
Exotic aquatic plants							
Aleman grass† (*Echinochloa polystachya*)	0.96	0.00	0.00	0.00	0.00	0.00	0.03
Olive hymenachne*† (*Hymenachne amplexicaulis*)	40.84	41.15	64.29	66.20	71.86	73.45	74.19
Para grass† (*Urochloa mutica*)	18.90	21.25	9.04	32.92	24.77	21.72	20.32
Salvinia* (*Salvinia molesta*)	0.00	0.00	0.00	0.00	0.00	0.1	0.00
Other exotic grasses	0.00	0.00	0.00	0.00	0.00	1.40	0.48
Native aquatic plants							
Water lily (*Nymphaea gigantea*)	0.00	7.27	0.00	0.00	0.02	0.04	0.54
Other							
Open Water	39.30	30.33	26.67	0.88	3.34	3.30	4.46

*Weeds of national significance, †Ponded pasture grasses.

APPENDIX 4: SALINE GROUNDWATER TRIAL

The option of accessing saline groundwater to be used in Annabone (as an approach to supplement tidal ingress from the breached bund wall at least during above average rainfall years or until inundation increases under anticipated sea level rise), to control invasive aquatic plants has been trialled by installing bores into the salt groundwater aquifer and pumping salty groundwater into small trial wetland areas (Waltham et al., 2019). While these trials had some level of success for the objective of destroying invasive freshwater vegetation, the groundwater sample results suggest some important level of risk that require consideration. The main issues identified in a first round of sampling were: 1) ammonia concentrations in the groundwater are extremely high and would become highly toxic to aquatic fauna (especially juvenile fish) if pH levels were to become alkaline. (Note that because ammonia is a highly available nutrient it would likely stimulate algal growth which could in turn cause pH levels in the water to become alkaline – and the ammonia to therefore become toxic); 2) the groundwater is highly enriched with uranium. There were insufficient uranium toxicity data available for ANZECC (2000) to be able to derive a high reliability trigger value for the protection of aquatic ecosystems but the authors recommended adopting a low reliability working level of 0.5 µg/L. On that basis the ambient uranium concentrations in bores 1 to 3 are between 178 and 268 times higher than would be deemed safe for the aquatic ecosystem; 3) the concentrations of iron, manganese, zinc and cobalt in each bore were also high enough to be potentially toxic to aquatic fauna, as were the concentrations of arsenic and copper; 4) the groundwater iron and manganese almost certainly occur in reduced chemical form, and would tend to oxidise if released into aerated surface waters. Ammonia also oxidises (to form nitrite and nitrate) if there is adequate oxygen present. The combined load of ammonia, iron and manganese in these waters therefore represents a substantial oxygen demand and would likely exacerbate the wetlands' pre-existing hypoxia problems; and 5) the elevated sulphate concentrations in the bore water are a natural characteristic of seawater and would not present a potential hazard if the water was being introduced to a well-oxygenated wetland environment. However, available evidence suggests that these wetlands are naturally prone to hypoxia, and due to the combined effects of chemical oxygen demand from the bore water and decomposition of weeds killed by the saline water, it is very likely that the introduction of bore water would lead to the development of severe hypoxia and ideal conditions for the proliferation of sulphate-reducing bacteria. In the absence of adequate free oxygen these bacteria obtain oxygen from sulphate, in the process producing hydrogen sulphide (rotten egg gas) as a by-product. Hydrogen sulphide is extremely toxic to both aquatic and terrestrial animals, including humans. Personnel working in environments where hydrogen sulphide production is possible should be aware that the human nose is extremely sensitive to the gas when it is present in very low (sub-lethal) concentrations, but it cannot detect the gas when it is present in very high (potentially lethal) concentrations. Overall, the use of salty groundwater as a means to suppress aquatic weeds might be problematic, though further sampling is underway and investigation into the potential implications of this strategy, and whether timing of its use, immediate before the wet season are be considered.

APPENDIX 5: GRAZING DAMAGE OBSERVATIONS

Allowing cattle to access coastal wetlands as a late season supplement seems a common practice in coastal areas along the GBR catchments (Waltham et al. 2020). This practice has been in place for many years at Mungalla Station and appears to impact heavily on marine vegetation. Although not explicitly examined here, from our observations cattle access to the wetland saltmarsh areas presumably has secondary implications to the wetland condition, including exposure of soils to oxidation and sulphate soil generation, increased erosion, compaction of soils that provide habitat for many intertidal in-fauna such crabs, and is a direct source of nutrients via cattle excrement. There is a case that cattle consuming saltmarsh is an effective means of transferring stored carbon in this plant into cattle production (usually for human food consumption, acknowledging however, that humans expire CO_2). While this is plausible, and is the case elsewhere (e.g., sheep graze saltmarsh; Laffaille et al. 2000), there are important secondary consequences of cattle in wetlands. Grazing in saltmarsh areas has been linked to increased soil temperature as a result of reduced shading or reduced vegetation extent (Persico et al. 2017), also compacting soils limiting anaerobic respiration – a consequence of increased soil temperature is higher rates of evaporation and thereby higher soil salinity (which was shown here) (Davidson et al. 2017).

Grazing also alters saltmarsh patch heterogeneity through direct consumption or trampling on vegetation. This process results in fewer arthropods (Puzin & Pétillon 2019), and invertebrates (Kneib 1984), all of which decreases both available plant and food resources for juvenile fish and crustaceans accessing saltmarsh areas (Minello & Zimmerman 1983, Hollingsworth & Connolly 2006, Mazumder et al. 2006), but also water birds (Gu et al. 2018).

Feral pig damage to the wetland was evident (Figure 29) and probably contributed to the measured reduction in Bulkuru (*E. dulcis*) between 2015 and 2016 in Boolgooroo lagoon (see Figure 32). These introduced animals have caused untold, severe and extreme damage amongst wetland marginal vegetation attempting to adapt and respond to the transitioning described above. The pigs root extensively along the sensitive high tide margin across the Mungalla area and further afield, given the many field observations of pig rooting grounds along the high tide margin. This damage is characterised by the severe upheaval of native vegetation bordering saline areas including the sedge Bulkuru, the herb saline plant (*Sesuvium portulacastrum*). Control of feral pig numbers in coastal wetlands is important, and this may be achieved with targeted fencing and selected shooting, but it needs to be completed before the damage is irreversible. It is suggested that such control measures be undertaken in conjunction with: 1) mapping to properly describe the affected areas; and 2) photo-point sampling to show change with recovery and on-going transition processes. Additionally, cattle that access the tidal saltmarsh areas need to be controlled as they can trample (Figure 30) protected marine plants.



Figure 29: Example of the feral pig damage to Mungalla tidal wetland region across saltmarsh meadow



Figure 30: Example of the cattle access and trampling of important marine aquatic plants. Fencing cattle from accessing coastal wetland areas is necessary in order to prevent further damage and further loss of the ecosystem services provided

APPENDIX 6: OBSERVATION OF MANGROVE STRESS

In the region of the second bund wall, transitions in the vegetation were observed at a number of locations along the interface between freshwater and saltwater communities (Figure 31). This transition can mostly be attributed to interventions like the removal of old bund walls installed earlier to expand areas of freshwater influence and grazing pasture lands. However, there are also likely to be further influences of regional rising sea levels (~8 mm/yr). Perhaps the clearest example of the transition was the encroachment of mangroves into low-lying terrestrial vegetation upstream of the breached wall. This was shown by the presence of seedlings of Milky mangrove (*Excoecaria agallocha*) in stands of mature but stressed and dying supra-tidal *Melaleuca* trees (Figure 32). It would be useful to measure stem diameters to give an estimate of the age of trees and species occurrence across appropriate transects. Examination of satellite imagery would also be useful to measure vegetation change over time. This requires a few things, starting with labelled permanent field post markers both for identifying the camera position and locating the camera field of view. These photographs could be taken using a standard hand-held camera with GPS tagging – or with an installed time-lapse camera.

Downstream of the breached bund wall, there was notable stagnation and pooling within upper tidal mangrove wetlands. Stagnant pools were surrounded by unusually long breathing roots of Grey mangroves (*Avicennia marina*). Note that at low tide – healthy tidal mangrove habitats are drained, forming more stagnating pool that can provide little habitat for fish. As a further consequence, the lesser flows probably have resulted in the silting-up of estuarine tributaries and their choking of mangrove plants growing in the newly deposited sediments. It will take a number of years for the re-opened waterway to become fully re-established, with possible downstream impacts on existing mangrove vegetation. It is imperative to have accurate study site maps of the tidal wetlands downstream, and to monitor the ongoing changes to vegetation, bathymetry and sediment condition of mangrove areas.

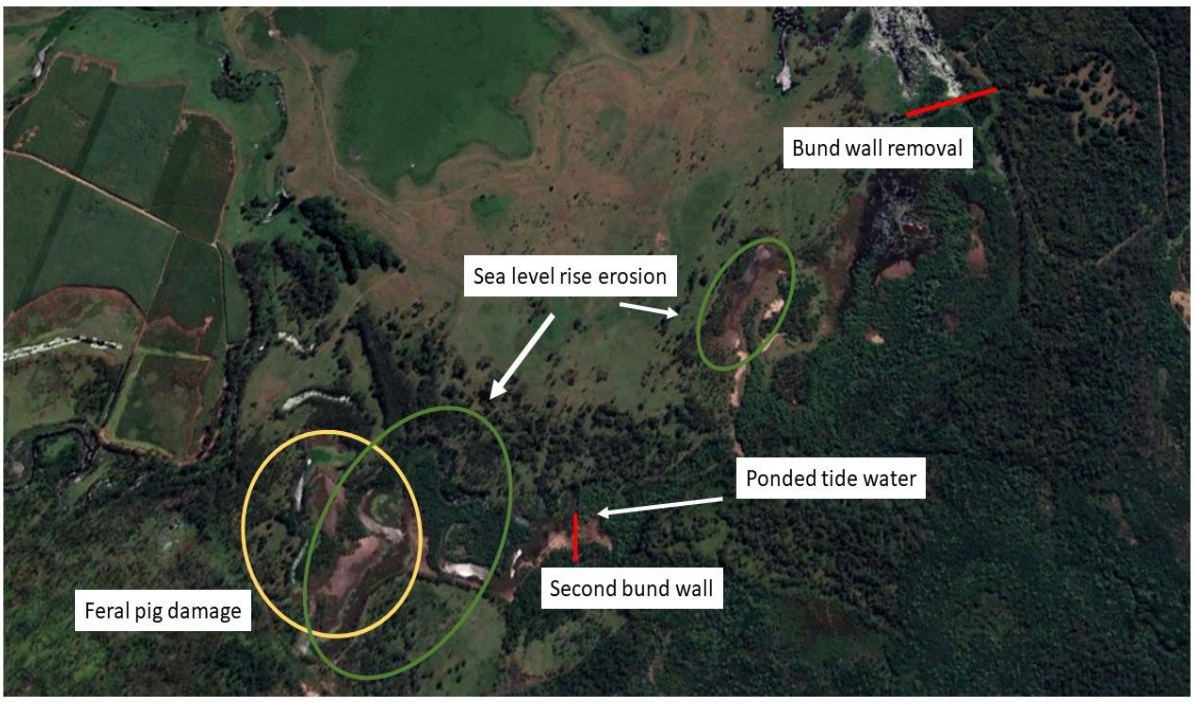


Figure 31: Second bund wall site located in Mungalla. Yellow polygon shows where feral pig impact was greatest, green polygons show where erosion of saltmarsh vegetation greatest because of increased sea level rise, and ponded tidal water downstream of the second bund wall illustrating altered hydrology following construction of the bund wall, and its breach some years ago



Figure 32: Example of a mangrove in Mungalla wetland under stress from changing local conditions

APPENDIX 7: NITROGEN REMOVAL BY TROPICAL FLOODPLAIN WETLANDS THROUGH DENITRIFICATION

CSIRO PUBLISHING

Marine and Freshwater Research, 2019, **70**, 1513–1521
https://doi.org/10.1071/MF18490

Nitrogen removal by tropical floodplain wetlands through denitrification

M. F. Adame[A,E], *H. Franklin*[A], *N. J. Waltham*[B], *S. Rodriguez*[A], *E. Kavehei*[A,C], *M. P. Turschwell*[A], *S. R. Balcombe*[A], *P. Kaniewska*[D], *M. A. Burford*[A] and *M. Ronan*[D]

[A]Australian Rivers Institute, Griffith University, 170 Kessels Road, Nathan, Qld 4111, Australia.
[B]TropWATER (Centre for Tropical Water and Aquatic Ecosystem Research), James Cook University, 373 Flinders Street, Qld 4810, Australia.
[C]School of Engineering and Built Environment, Griffith University, 170 Kessels Road, Nathan, Qld 4111, Australia.
[D]Department of the Environment and Science, Queensland Government, 400 George Street, Brisbane, Qld 4000, Australia.
[E]Corresponding author: f.adame@griffith.edu.au

Abstract. Excess nitrogen (N) leading to the eutrophication of water and impacts on ecosystems is a serious environmental challenge. Wetlands can remove significant amounts of N from the water, primarily through the process of denitrification. Most of our knowledge on wetland denitrification is from temperate climates; studies in natural tropical wetlands are very scarce. We measured denitrification rates during a dry and a wet season in five floodplain forests dominated by *Melaleuca* spp., a coastal freshwater wetland of tropical Australia. We hypothesised that the denitrification potential of these wetlands would be high throughout the year and would be limited by N and carbon (C) availability. Mean potential denitrification rates (D_t) were 5.0 ± 1.7 mg m^{-2} h^{-1}, and were within the reported ranges for other tropical and temperate wetlands. The rates of D_t were similar between the dry and the wet seasons. From the total unamended denitrification rates (D_w, 3.1 ± 1.7 mg m^{-2} h^{-1}), 64% was derived from NO_3^- of the water column and the rest from coupled nitrification–denitrification. The factor most closely associated with denitrification was background water NO_3^--N concentrations. Improved management and protection of wetlands could play an important role in improving water quality in tropical catchments.

Additional keywords: Australia, Great Barrier Reef, isotope pairing, *Melaleuca*, palustrine, water quality.

Received 21 December 2018, accepted 8 April 2019, published online 15 July 2019

Introduction

Excess nitrogen (N) pollution is one of the most significant environmental challenges of our times (Kulkarni *et al.* 2008). In the past century, humans have increased the amount of reactive N in our planet by a factor of nine (Galloway and Cowling 2002). The discovery of artificial N fixation (Haber-Bosch process) has allowed for large-scale food production, which has sustained an increasing human population (Galloway *et al.* 2003). However, more than 90% of the reactive N created is never consumed by humans, and almost half of it ends up in the environment where it can cause land and water degradation (Galloway and Cowling 2002; Galloway *et al.* 2003).

Wetlands are one of the most productive and valuable ecosystems on Earth (Costanza *et al.* 1997) and have long been recognised as ecosystems with the capacity to improve water quality by removing N (Land *et al.* 2016). In some regions, wetlands can be five times more efficient at reducing N loads than are the most-effective land management strategies, including land retirement (Hansen *et al.* 2018). For instance, restoring 3–7% of wetland cover in the Mississippi basin has the potential to remove 20–50% of the catchment N inputs (Mitsch *et al.* 2001). The protection and restoration of wetlands may be an effective and cheaper option, when combined with on-site management techniques and treatment systems, than solely relying on traditional engineered solutions (Jones *et al.* 2012). Thus, wetlands will play an essential role in meeting the water needs of the future.

The potential of floodplain wetlands to remove N could have significant implications for tropical regions. In the Great Barrier Reef catchments in Australia, wetlands comprise a small proportion of the land (<6%, Wetland*Info*, see https://wetlandinfo.des.qld.gov.au/wetlands/, accessed September 2018), but may contribute disproportionally to N processing at the catchment scale. Wetlands could contribute to improving the water quality

Journal compilation © CSIRO 2019



Fig. 1. (*a*) Location of five sampling sites in tropical Queensland, Australia: Halifax Bay Wetlands National Park (HX), Insulator Creek (IC), Mungalla Station (MG), Girramay National Park (GI), and Hull Heads National Park (HH). (*b*) Forested wetland dominated by *Melaleuca quinquenervia*. Photo M. F. Adame.

within the Great Barrier Reef catchments (Reef 2050 Water Quality Improvement Plan 2017–2022, Department of Environment and Heritage Protection 2017*a*) for recovering the health and resilience of the Reef. However, so as to support the inclusion of wetland restoration and conservation as a means of achieving water-quality targets (Department of Environment and Heritage Protection 2016), the potential of natural wetlands to remove N needs to be assessed. The role of wetlands in N cycling within the Great Barrier Reef catchments, as well for most tropical wetlands, is poorly understood (Piña-Ochoa and Álvarez-Cobelas 2006; Waterhouse *et al.* 2017).

The removal of N by wetlands is mainly the result of respiratory denitrification. Denitrification is the process from which nitrate (NO_3^-) is reduced to nitrite (NO_2^-), nitric oxide (NO), nitrous oxide (N_2O) and, finally, to gaseous N_2, which is released to the atmosphere (Matheson *et al.* 2002; Kulkarni *et al.* 2008). There are some other potential pathways for the removal of N in wetlands, such as anaerobic ammonium oxidation and chemoautotrophic denitrification (Burgin and Hamilton 2007). However, respiratory denitrification is likely to be the most important (Kulkarni *et al.* 2008; Zhou *et al.* 2014). Denitrification can occur naturally in soils and water and is highest in places where oxygen is low and organic carbon (OC) is high, conditions that are prevalent in most wetlands (Mitsch and Gosselink 2015). Denitrification rates can be highly variable among wetlands and are associated with multiple factors, including ambient temperature, inundation frequency, vegetation cover, available N and C content (Mulholland *et al.* 2008; Song *et al.* 2014; Yao *et al.* 2016). However, most of our knowledge on denitrification in wetlands comes from studies on artificial wetlands in temperate climates (e.g. Mulholland *et al.* 2008; Bruesewitz *et al.* 2011; Land *et al.* 2016); similar studies in natural tropical wetlands are very scarce (Piña-Ochoa and Álvarez-Cobelas 2006).

In this study, we measured denitrification rates in floodplain forested (*Melaleuca* spp.) wetlands, a dominant coastal ecosystem of tropical and subtropical Australia. Our goal was to determine the potential of floodplain wetlands to remove N in a region where N loads from agricultural practices are a serious threat to the health of freshwater, estuarine and marine ecosystems (Brodie and Waterhouse 2012). We compared denitrification rates in the dry and wet seasons in five floodplain wetlands and investigated environmental factors associated with denitrification. We hypothesised that these tropical wetlands would have high denitrification rates that would be limited by C and N. We also hypothesised that because of the relatively minor annual temperature oscillations in tropical relative to temperate climates, denitrification potential would not vary significantly throughout the year.

Materials and methods

Study sites

Sampling was conducted in forested wetlands dominated by the tree species *Melaleuca quinqueflora* or *M. viridiflora*, which typically occur in Australia's floodplains (Finlayson 2005; Fig. 1, Table 1). The sites were located within the catchments of the Great Barrier Reef in the Wet Tropics of north-eastern Queensland in the Herbert and the Tully–Murray Rivers. We sampled five sites located in Halifax Bay Wetlands National Park (HX), Insulator Creek (IC), Mungalla Station (MG), Girramay National Park (GI), and Hull Heads National Park (HH; Fig. 1). The climate is tropical with monthly mean temperatures ranging from 22 to 34°C (Australian Bureau of Meteorology, 1907–2018, see http://www.bom.gov.au/climate/data/). Mean total annual rainfall is >2000 mm, mostly falling between January and May. Annual mean rainfall is lower in the southern Herbert catchment (2087 mm, Australian Bureau of Meteorology, 1960–2017, see http://www.bom.gov.au/climate/data/) than in the northern Tully River catchment (2700 mm, Australian Bureau of Meteorology, 1871–2017, see http://www.bom.gov.au/climate/data/). Sampling was conducted during the

Table 1. Location and forest structure of *Melaleuca* floodplain wetlands in the Wet Tropics, Queensland, Australia
DBH, diameter at breast height

Site	Location	DBH (cm)	Tree density (trees ha^{-1})	Biomass (kg ha^{-1})	Dominant species
Halifax (HX)	−18.7945°N, 146.2485°E	15 ± 2.3	732 ± 135	119 ± 28.7	*M. quinquenervia*
Insulator Creek (IC)	−18.8957°N, 146.2594°E	30 ± 3.3	507 ± 127	898 ± 290	*M. quinquenervia*
Mungalla (MG)	−18.7187°N, 146.2808°E	9.3 ± 1.0	6677 ± 2498	328 ± 58.6	*M. quinquenervia*
Girramay (GI)	−18.2213°N, 146.0034°E	15 ± 1.4	2088 ± 303	494 ± 69.8	*M. quinquenervia*
Hull Heads (HH)	−18.0007°N, 146.0445°E	11 ± 1.0	4474 ± 833	412 ± 25.2	*M. viridiflora*

dry (August 2016, October 2017) and wet (February 2017) seasons. Denitrification has been associated with vegetation cover, as well as physicochemical characteristics of the wetland (Mulholland *et al.* 2008; Song *et al.* 2014; Yao *et al.* 2016). Thus, at each site, we measured forest structure, background soil and water characteristics, and denitrification rates. The detailed methodology is explained below.

Forest structure

All sites were located within areas comprising a mosaic of rainforest, mangroves, marshes and *Melaleuca* forest. Sampling sites were located within the *Melaleuca* forests (areas between 6 to 26 ha). At each site, we measured five plots of 5-m radius separated by 20 m over a linear transect from the water edge (Adame *et al.* 2015). In plots where forest density was >3000 trees ha^{-1}, a 3-m radius was used instead. In each plot, we counted and measured the diameter at breast height (DBH) of every tree with a DBH of >2 cm; we did not include tree saplings because they were not a significant component of the forest structure. Aboveground biomass was estimated from the allometric equations derived for *Melaleuca viridiflora* (Eqn 1) and *Melaleuca* sp. (Eqn 2) in northern Australia (Finlayson *et al.* 1993), as follows:

$$\log(\text{biomass}) = 2.338\,(\log \text{DBH}) - 0.561 \quad (1)$$

$$\log(\text{biomass}) = 2.266\,(\log \text{DBH}) - 0.502 \quad (2)$$

where biomass is in kilograms and DBH in centimetres.

Background conditions of water and soil

To establish background conditions, we measured physicochemical characteristics of water and soil at each site. Water samples were either obtained from standing water in the forest (10–20 cm deep; wet season), or the closest source if the forest was not inundated at the time of sampling (dry season). We measured water temperature, electrical conductivity, dissolved oxygen and pH in the field with a calibrated water-quality meter (ProPlus, YSI meter, Yellow Springs, OH, USA). Surface-water samples (~20 cm deep) were collected in triplicate, filtered through a 0.45-µm membrane filter, and stored frozen before being analysed for nutrients within the next week (colorimetric analyses; Chemistry Centre, Department of Science Information Technology and Innovation, Brisbane, Australia). Detection limits (mg L^{-1}) were 0.002 for NH_4^+-N, and 0.001 for NO_x^--N and PO_4^--P.

Surface-soil samples (top 10 cm) were collected during the dry season (2016, 2017) at each site in triplicate with a stainless-steel corer of 4-cm diameter. The samples were oven-dried at 60°C for 48 h. Bulk density was estimated from the dry weight of the sample, which had a known volume. All soil samples were analysed for %N, and organic %C with an elemental analyser (EA-IRMS, Serco System, ThermoFischer Scientific, Waltham, MA, USA). A separate set of soils was analysed for particle size. These samples were pre-treated with 30% H_2O_2 to remove organic matter, dispersed with 10% $Na(PO_3)_6$ and analysed by laser granulometry (Particle Size Analyser LP 13320, Beckman Coulter, Brea, CA, USA). Soil particles were classified as sand (62.5–2000 µm), silt (39–62.5 µm) or clay (<39 µm).

Denitrification

We used the isotope-pairing technique (Nielsen 1992; Steingruber *et al.* 2001) to measure denitrification in the sediment at the five sites. We measured each site during at least one dry and one wet season to account for differences in temperature and flooding (wet and hot in the summer; drier and cooler in the winter). The isotope-pairing technique consists of adding enriched ^{15}N-NO_3 to water overlying sediments at a saturating concentration and estimating denitrification rates from ^{15}N-N_2 gas production.

At each site, we collected intact sediment cores of approximately 8-cm depth inside Perspex tubes (4.8-cm internal diameter × 30 cm long). The sediment cores were selected to be representative of the natural conditions of each site and included small roots and litter. To assess within-site variability, we compared denitrification rates in one site (IC) with contrasting sediment conditions (sand *v.* organic sediment). The sediment cores were capped at the bottom with a rubber bung, filled with water collected from each site, and left to equilibrate overnight. Experiments for HX in the dry season ran with water from IC, because we could not find water over the wetland or nearby it. For each experiment, we collected 12 sediment cores to allow three cores to be sampled at time 0, 2, 6 and 12 h. Preliminary results showed that ^{15}N-N_2 concentrations plateaued at ~5 h; thus, subsequent sampling included time intervals only from 0 to 6 h. In total, we conducted 11 experiments, consisting of 154 cores, and a total of 462 samples for ^{15}N-N_2 gas analyses (Fig. S1, available as Supplementary material to this paper).

The day after collection, the experiments were run at a nearby town (Ingham, Queensland), with similar ambient light and air temperature as in the field. The sediment cores were set in large plastic rectangular containers (1030 × 510 × 495 mm) filled with water maintained at a constant temperature, which was recorded

throughout the experiment (YSI meter, ProPlus; 24–28°C in the dry season, and 29–31°C in the wet season). For each experiment, we ran a blank sample of distilled water (Fig. S1).

At the beginning of the experiment, $^{15}N\text{-}NO_3$ was added to each core. Nutrient samples were taken from three cores per experiment, before and after $^{15}N\text{-}NO_3$ additions. The experiments were run with final concentrations between 0.01 and 0.17 mg $N\text{-}NO_3$ L^{-1}, all within the range of natural background conditions (Water Monitoring Information Portal, Queensland Government, see https://water-monitoring.information.qld.gov.au/, accessed September 2018; Fig. S2, available as Supplementary material to this paper). Cores were topped up with water and capped to minimise headspace. Natural water movement was simulated by a stirrer bar suspended ~3 cm above the sediment at each core driven by a rotating magnet that moved at ~60–70 rpm (Cook *et al.* 2004). After ~20 min, one core from each batch was sacrificed as a time zero measurement by adding 1 mL of 50% w/v zinc chloride ($ZnCl_2$), which was mixed throughout the sediment and overlying water to halt bacterial activity. Triplicate 10-mL water samples from each core were collected using a syringe and placed in a 12.5-mL Exetainer vial (Labco, High Wycombe, UK) with 250 µL of 50% w/v $ZnCl_2$. At each time interval, a new set of cores was sacrificed (Fig. S1). The headspace gas was analysed by continuous-flow mass spectrometry for $^{28}N_2$, $^{29}N_2$ and $^{30}N_2$-gas (EA-IRMS, Serco System, ThermoFischer Scientific). The detection limit for denitrification rates was 0.01 mg N m^{-2} h^{-1}. Denitrification rates are reported for ambient light conditions in milligrams of nitrogen per square metre per hour.

The isotope pairing technique is one of the most precise techniques for measuring denitrification because it includes denitrification from the overlying water and coupled sediment nitrification–denitrification (Steingruber *et al.* 2001). The calculations for estimating the different rates of denitrification with this method are as follows:

(1) D_{15}: denitrification from labelled $^{15}NO_3^-$ measured from the production rate of the $^{29}N_2$ and $^{30}N_2$

$$D_{15} = r_{29} + 2r_{30} \quad (3)$$

where r_{29} and r_{30} are the production rates of $^{29}N_2$ and $^{30}N_2$ respectively

(2) D_{14}: denitrification from unlabelled $^{14}NO_3$

$$D_{14} = D_{15} \cdot \frac{r_{29}}{2r_{30}} \quad (4)$$

(3) D_t: total denitrification or potential denitrification

$$D_t = D_{15} + D_{14} \quad (5)$$

(4) D_w^{tot}: total denitrification of NO_3^- from the water column

$$D_w^{tot} = \frac{D_{15}}{\varepsilon} \quad (6)$$

where ε is NO_3^-enrichment during incubation as a result of $^{15}NO_3^-$ additions

$$\varepsilon = \frac{[NO_3^-]_a - [NO_3^-]_b}{[NO_3^-]_a}$$

where a and b refer to concentrations after and before $^{15}NO_3^-$ addition.

(5) D_w: denitrification from the water column corrected for tracer addition

$$D_w = D_w^{tot}(1 - \varepsilon) \quad (7)$$

(6) D_n: coupled nitrification–denitrification

$$D_n = D^{tot} - D_w^{tot} \quad (8)$$

Data analyses

We used a combination of correlation analyses and linear regression to identify significant relationships between total denitrification (D_t) and environmental data, which included water nutrient concentrations (NH_4^+-N, NO_x^--N, and PO_4^--P), the temperature during the experiment, pH and electrical conductivity (EC) of the water. To maximise any subsequent analyses, we first tested for differences for D_t and nutrient concentrations between the two seasons (dry and wet) to see whether data could be combined (paired Student's *t*-tests). Differences were not significant ($P > 0.05$) for D_t or environmental predictors; hence, data were combined, resulting in a total of 10 observations. We checked collinearity among our predictor variables using Spearman's rank correlation and removed variables with a correlation coefficient of >0.6. The variables that were retained were correlated against D_t; any significant ($P < 0.05$) correlations were further tested as predictor variables in linear regression. If was not possible to use multiple regression because of a restricted number of data points ($n = 10$ denitrification rates, averaged from three replicates for each experiment); hence, we included only one predictor variable per model to avoid overfitting. Soil characteristics (%C, %N, BD, grain size) were also tested separately against D_t for samples during the dry season when soil was simultaneously sampled. Data for regression analyses were log-transformed before analyses. Model residuals were checked for normality. Data were analysed with R statistical software (ver. 3.4.3, R Foundation for Statistical Computing, Vienna, Austria, see http://www.R-project.org/, accessed September 2018).

Results

Forest structure

The structure of the forests greatly varied among sites, with tree density ranging from 732 to 6677 trees ha^{-1}, mean DBH ranging from 9.3 to 30 cm, and plant biomass from 119 to 898 kg ha^{-1} (Table 1).

Background conditions of water and soil

Nutrient concentrations in the standing water or in the closest source to the *Melaleuca* floodplain wetlands had mean values of 0.04 ± 0.01 mg L^{-1} for NH_4^+-N, 0.02 ± 0.007 mg L^{-1} for NO_x^--N, and 0.006 ± 0.002 mg L^{-1} for PO_4^--P (Table 2), with there being no significant difference between the wet and dry

Table 2. Physicochemical characteristics of standing water or closest source of water of *Melaleuca* floodplain wetlands in the Wet Tropics, Queensland, Australia

Values are means ± s.e. EC, electrical conductivity. The HX site was dry during sampling and water was obtained from IC. See Table 1 for explanation of site abbreviations

Site	pH	EC ($mS\ cm^{-1}$)	NH_4^+-N ($mg\ L^{-1}$)	NO_x^--N ($mg\ L^{-1}$)	PO_4^--P ($mg\ L^{-1}$)
Wet season					
HX	4	2.5	0.02 ± 0.004	0.002 ± 0.001	<0.001
IC	7	0.11	0.02 ± 0.003	0.03 ± 0.01	0.004 ± 0.001
MG	7	0.23	0.08 ± 0.002	0.01 ± 0.002	0.02 ± 0.002
GI	4	2	0.05 ± 0.01	0.004 ± 0.002	<0.001
HH	6	5.4	0.05 ± 0.04	0.01 ± 0.004	<0.001
Dry season					
HX	7	0.06	0.02 ± 0.004	0.08 ± 0.02	0.004 ± 0.001
IC	7	0.14	0.02 ± 0.002	0.02 ± 0.007	0.003 ± 0.007
MG	7	0.56	0.08 ± 0.004	0.01 ± 0.001	0.003 ± 0.009
GI	3	5.5	0.04 ± 0.007	0.01 ± 0.005	<0.0001
HH	–	–	0.03 ± 0.02	0.007 ± 0.001	0.001 ± 0.002

Table 3. Physicochemical characteristics of surface soil (0–10 cm deep) of *Melaleuca* floodplain wetlands in the Wet Tropics, Queensland, Australia during the dry season

Values are means ± s.e. for triplicate plots within each forest. BD, bulk density; OC, organic carbon; N, nitrogen. See Table 1 for explanation of site abbreviations

Site	BD ($g\ cm^{-3}$)	%OC	%N	C : N
HX	0.85 ± 0.13	1.0 ± 0.20	0.059 ± 0.0082	21 ± 0.29
IC	0.66 ± 0.10	7.8 ± 2.2	0.54 ± 0.14	19 ± 1.2
MG	0.62 ± 0.075	7.6 ± 2.8	0.44 ± 0.15	22 ± 0.70
GI	0.60 ± 0.023	4.1 ± 0.44	0.34 ± 0.018	24 ± 0.42
HH	0.43 ± 0.050	14 ± 1.4	0.78 ± 0.044	22 ± 2.2

seasons ($t(8) = -0.716$, $P = 0.494$; $t(7) = -0.232$, $P = 0.823$; and $t(5) = -1.20$, $P = 0.286$, for NH_4^+-N, NO_x^--N, and PO_4^--P respectively). Highest NH_4^+-N and PO_4^--P concentrations were measured in MG, and they were 0.08 mg L^{-1} and 0.02 mg L^{-1} respectively, and highest NO_x^--N concentrations were measured at IC, being 0.08 mg L^{-1}. All the water sampled within or near the wetlands was within the lower ranges of concentrations of the main river channels of the Herbert and Tully rivers (Fig. S2). The water was acidic, with pH values of 5.7 ± 0.6, and conductivity was <5.5 mS cm^{-1}, with the lowest values (<0.2 mS cm^{-1}) at IC (Table 2).

The particle size of the surface sediment ranged from 39 to 56% sand, 34 to 39% silt and 8.9 to 18% clay. The surface soil of all the sites sampled had mean values of 6.9 ± 2.2% OC, 0.43 ± 0.12% N, and molar C : N of 21 ± 0.86. The mean bulk density of the soil was 0.63 ± 0.067 g cm^{-3}. Sites IC, MG and HH had the highest %OC (7.8, 7.6 and 14% respectively), and highest %N (0.54, 0.44, and 0.78%). Site HX had the lowest OC (1.0%), lowest N (0.059%) and the highest bulk density (0.85 g cm^{-3}) among the sampled sites (Table 3).

Denitrification rates

Mean D_t rate for all sites and seasons (mean ± propagated error) was 5.0 ± 1.7 mg N m^{-2} h^{-1} (1.1 – 9.7 mg N m^{-2} h^{-1}, Table 4). There were no significant differences in denitrification rates between seasons ($t(4) = 0.390$, $P = 0.716$), with mean values of 4.6 ± 1.6 mg N m^{-2} h^{-1} in the wet *v.* 5.3 ± 0.57 mg N m^{-2} h^{-1} in the dry season. The variation in denitrification was greatest among replicate cores within each site, with site variability ranging from 11 to 88% in IC. When comparing denitrification rates within one site (IC), we measured higher rates in the organic soil (6.1 ± 2.9 mg m^{-2} h^{-1}) than in sand (2.0 ± 1.0 mg m^{-2} h^{-1}), highlighting the differences at small spatial scales.

Of the total NO_x^--N that underwent denitrification, 64% originated from the water column (background plus added N during incubation), with D_w^{tot} of 2.3 ± 0.61 mg N m^{-2} h^{-1} in the wet season and 3.8 ± 1.0 mg N m^{-2} h^{-1} in the dry season. The remaining denitrification was derived from NO_3^--N from coupled nitrification–denitrification in the sediment, with mean values of 2.3 ± 1.1 mg N m^{-2} h^{-1} in the wet season and 1.5 ± 1.0 mg N m^{-2} h^{-1} in the dry season (Table 4). Finally, unamended denitrification, i.e. D_w or denitrification corrected for N additions during the experiment, was estimated at 1.1 ± 0.32 mg N m^{-2} h^{-1} in the wet season and 0.39 ± 0.15 mg N m^{-2} h^{-1} during the dry season.

We found that water EC was highly correlated with both pH and PO_4^--P concentrations, and experimental NO_x^--N concentration was also correlated with NO_x^--N concentrations of water

Table 4. Denitrification rates (mg N m^{-2} h^{-1}) of soils in *Melaleuca* floodplain wetlands during a dry and a wet season in the Wet Tropics, Australia
Values are means ± s.e. D_t, total or potential denitrification during experiment; D_w^{tot}, total denitrification of labelled plus unlabelled NO_3^- from water column; D_w, natural denitrification rate without tracer addition; D_n, coupled nitrification–denitrification; ε, nitrate enrichment factor during experiment; and time (h), duration of the incubation. See Table 1 for explanation of site abbreviations

Site	D_t	D_w^{tot}	D_w	D_n	ε	Time (h)
Wet season						
HX	1.6 ± 1.0	1.0 ± 0.9	0.34 ± 0.30	0.52 ± 0.45	0.67	12.2
IC	9.7 ± 5.1	3.3 ± 1.7	2.2 ± 1.2	6.4 ± 3.4	0.34	5.5
MG	1.1 ± 1.0	0.67 ± 0.57	0.45 ± 0.38	0.27 ± 0.23	0.60	12.4
GI	4.8 ± 1.0	3.2 ± 0.6	1.1 ± 0.21	1.6 ± 0.32	0.67	8.1
HH	5.8 ± 0.7	3.5 ± 0.39	1.4 ± 0.16	2.3 ± 0.26	0.60	5.5
Dry season						
HX	6.2 ± 1.8	0.69 ± 0.20	0.61 ± 0.18	5.5 ± 1.6	0.10	6.1
IC	6.1 ± 2.9	5.7 ± 2.7	0.30 ± 0.14	0.32 ± 0.15	0.95	6.8
MG	6.4 ± 1.0	6.2 ± 1.0	0.18 ± 0.03	0.18 ± 0.03	0.97	6.3
GI	4.0 ± 2.0	4.0 ± 2.0	0.03 ± 0.02	0.03 ± 0.02	0.99	6.6
HH	3.8 ± 0.34	2.6 ± 0.23	0.85 ± 0.08	1.3 ± 0.11	0.67	6.2

Table 5. Correlation and significance (*P*-value in parentheses) between total denitrification (D_t) and selected variables using Spearman's correlation coefficient (r_s)
Significant correlations are shown in bold. Temp, temperature

	D_t	NO_x^--N	NH_4^+-N	PO_4^--P	Temp
NO_x^--N	0.67 **(0.03)**				
NH_4^+-N	−0.24 (0.51)	−0.27 (0.44)			
PO_4^--P	−0.18 (0.62)	0.15 (0.69)	−0.22 (0.55)		
Temp	−0.07 (0.85)	0.24 (0.50)	−0.27 (0.46)	0.24 (0.51)	
Water pH	0.59 (0.10)	0.55 (0.13)	−0.29 (0.44)	0.59 (0.10)	−0.15 (0.70)

(Table S1, available as Supplementary material to this paper). Hence, both water EC and experimental NO_x^--N concentration were removed from subsequent analyses The Spearman's correlation coefficient for the remaining variables showed that D_t was significantly correlated only with NO_x^--N ($r_s = 0.67$, $P = 0.03$; Table 5). It appeared that water pH was also associated with D_t, but the correlation was not significant ($r_s = 0.59$, $P = 0.10$; Table 5). A linear regression showed a positive influence of (ln), NO_x^--N (ln) although this was not statistically significant (adjusted $r^2 = 0.25$, $F_{1,8} = 3.94$, $P = 0.082$; Table S2 (available as Supplementary material to this paper, Fig. 2), probably because of very low denitrification rate in MG during the wet season. No other parameter studied (including BD, soil OC, N, C : N or gran size) was better at explaining denitrification than was background NO_x^--N during the time of sampling.

Discussion

Denitrification potential in floodplain wetlands of tropical Australia did not differ among seasons and was not associated with ambient temperature during the experiments. This result could be explained because the temperature coefficient of denitrification is low at high temperatures ($\theta = 1.07$), meaning that changes in temperature between 20 and 35°C result in small changes in denitrification rates (Kadlec and Reddy 2001). In contrast to temperate wetlands, tropical wetlands are likely to maintain similar potential denitrification rates throughout the year.

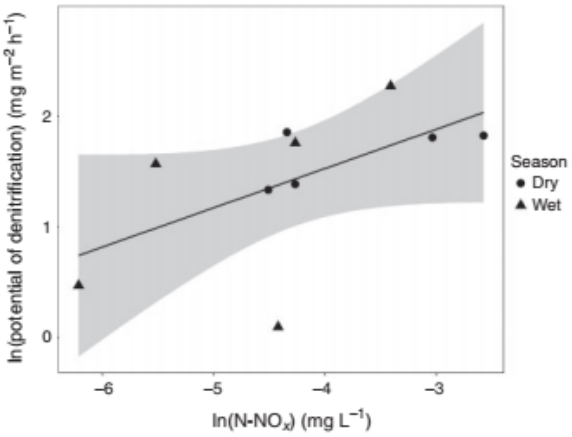


Fig. 2. Total potential (ln) denitrification rates (D_t, mg m^{-2} h^{-1}) across five forested wetlands in the Wet Tropics, Australia, as a function of background (ln) NO_x^--N (mg L^{-1}) concentrations in the water. Experiments in the dry season (closed circles), and those in the wet season (closed triangles) are shown.

Denitrification rates in these tropical wetlands were most closely associated with the background water NO_3^--N concentration of each site at the time of sampling. Studies in temperate

systems have also found a similar association between denitrification and NO_3 availability (Peterson *et al.* 2001; Piña-Ochoa and Álvarez-Cobelas 2006; Mulholland *et al.* 2008). The present study supports the idea that NO_3 could be one of the most important factors driving global wetland denitrification. The NO_3 concentrations in our study sites were low compared with those in other locations and were always lower than the K_m values (concentration at which denitrification reaches half of its potential) reported in other studies (0.2–20 mg L^{-1}; García-Ruiz *et al.* 1998; Zhou *et al.* 2014). Thus, NO_3 concentrations at these sites were always below those required to reach full denitrification potential.

Although NO_3^--N concentration appears to be the over-riding factor associated with denitrification in this and other studies, other factors were not measured and are also likely to be important. For instance, denitrification would occur only if soils are waterlogged and maintain adequate redox conditions because denitrification decreases when redox is below −200 or above 400 mV (Seo and DeLaune 2010). Additionally, the soil microbial composition will influence the long-term denitrification potential for each site (Wallenstein *et al.* 2006), with higher denitrification rates for fungi when soil redox is low, and higher for bacteria when soil redox is high (Seo and DeLaune 2010).

The plant composition within a wetland will also influence the microbial community and, in turn, their denitrification potential. For example, in a wetland treatment, the bacterial community of *Elodea canadensis* had a three times higher denitrification potential than did the community of other plants species (Bastviken *et al.* 2005). Vegetation abundance will also affect coupled nitrification–denitrification, which is favoured in wetlands with dense vegetation where it can reach values of up to 5 mg m^{-2} h^{-1} (Reddy *et al.* 1989). The understorey shrub vegetation at our sites was usually dense, although highly variable throughout the year. Coupled nitrification–denitrification at our sites ranged from 0.05 to 6.5 mg m m^{-2} h^{-1} and accounted for 36% of total denitrification.

The *Melaleuca* floodplain wetlands in this study had potential denitrification rates (D_t) of 5.0 ± 1.6 mg m^{-2} h^{-1} (1.1–9.7 mg N m^{-2} h^{-1}), which are values within the range of those in other aquatic systems (0.16–4.7 mg m^{-2} h^{-1}; reviewed by Piña-Ochoa and Álvarez-Cobelas 2006). Compared with other tropical wetlands, our results are similar to those of mangroves in Malaysia (0.23–6.6 mg m^{-2} h^{-1}, Alongi *et al.* 2004), and tropical streams of Puerto Rico (0.30–9.6 mg m^{-2} h^{-1}, Potter *et al.* 2010), but higher than those in subtropical lakes in China (0.033–0.65 mg m^{-2} h^{-1}, Yao *et al.* 2016) and mangroves in Mexico (0.03–0.13 mg m^{-2} h^{-1}, Rivera-Monroy *et al.* 1995; Table S3, available as Supplementary material to this paper). Denitrification rates are highly variable, mostly owing to methodological differences and limited replication, with values ranging between 0.020 and 34 mg m^{-2} h^{-1} (Wetzel 2001). However, despite variability, we found that potential denitrification rates in these tropical wetlands are within the reported values of other studies including temperate and artificial wetlands.

The potential of forested wetlands to remove N could have significant implications at the catchment level in tropical regions. For example, in the Great Barrier Reef region, losses of N to waterways from fertilisers on sugarcane farms are ~16 kg N ha^{-1} $year^{-1}$ (Smart *et al.* 2016), resulting in high NO_3^--N concentrations (up to 0.40 mg L^{-1}; Water Monitoring Information Portal, see https://water-monitoring.information.qld.gov.au/; Fig. S2). However, the potential for denitrification at the catchment scale will not only depend on NO_3^--N concentrations, but on the size of the wetland relative to catchment area, position in the landscape, water residence time, and connectivity of the wetland with the waterway, i.e. whether this NO_3^--N flows through the wetland or bypasses it (Karim *et al.* 2012; Waterhouse *et al.* 2017; Hansen *et al.* 2018).

Connectivity of wetlands to waterways in tropical regions is strongly dependent on the duration, timing and intensity of seasonal rainfall (e.g. Davis *et al.* 2016). Intermittent flooding favours denitrification in floodplain areas for days or even weeks after flooding (Tomasek *et al.* 2019). In the Great Barrier Reef catchments, during the wet season, big floods can transport large amounts of NO_3^--N into the waterways. During this time of the year, a large volume of water can overflow river banks and inundate adjacent wetlands (Karim *et al.* 2012), with the implication for high potential denitrification (Tomasek *et al.* 2019). However, the volume of water may be too large, and the area of wetland inundated too small to allow detection of significant changes of NO_3^--N in the water column. During the dry season, water flows and nutrients will be low, but as the season progresses, NO_3^--N will increase (Davis *et al.* 2016). Throughout the dry season, groundwater flows will continue to deliver NO_3^--N to some wetlands (Rasiah *et al.* 2003). At this time, denitrification potential might be lower, but its effects at the landscape level may be higher (Bruesewitz *et al.* 2011; Waterhouse *et al.* 2017).

The potential for wetlands to reduce N loads has implications for water-quality offset schemes. Simulated results for the region have shown that catchment N-load limits in a nutrient market could make it profitable for landowners to convert marginal sugarcane land to constructed wetlands (Smart *et al.* 2016; Waltham *et al.* 2017). Results from the present study support the concept that restoration of wetlands or constructed wetlands could complement strategies for achieving water-quality targets. In Queensland, Australia, a voluntary policy instrument allows for offsetting point-source N loads by actions, such as wetland restoration or creation (Department of Environment and Heritage Protection 2014, 2017*b*; Waltham *et al.* 2017). The denitrification potential of wetlands shown in the present study may provide an opportunity for point-source operators to consider wetlands as a viable investment option for offsetting point-source N loads.

Although wetlands are important for reducing N, excess N can have deleterious effects of wetlands, such as changes in species communities, eutrophication and greenhouse emissions, such as N_2O (Verhoeven *et al.* 2006; Hernández *et al.* 2018). Emissions of N_2O are mostly derived from denitrification and account for 0.1–0.5% of the N that is denitrified. Emissions of N_2O in some *Melaleuca* wetlands could be significant (Livesley and Andrusiak 2012), especially during the wet season (Kiese *et al.* 2008). However, in other freshwater wetlands, N_2O emissions are small (Audet *et al.* 2014). Future studies are needed to determine interactions among nitrogen loads, denitrification, and N_2O emissions in tropical wetlands. The N loads to wetlands need to be carefully monitored to avoid reaching

thresholds of change (estimated at 25 kg N ha^{-1} $year^{-1}$ in temperate wetlands, Verhoeven *et al.* 2006) and to use a combination of wetland protection, management and improvement of agricultural practices to reduce N pollution in tropical waterways.

Conclusions

Melaleuca floodplain wetlands have potential denitrification rates (D_t) of 5.0 ± 1.7 mg m^{-2} h^{-1}, with similar values between the dry and wet seasons. The denitrification rates measured in this study are within the values reported for natural wetlands and complement global literature, which suggests that the main driver of denitrification is NO_3 concentrations. The results of this study support the inclusion of wetland protection, restoration and creation as a complementary solution for removing excess N in tropical catchments.

Conflicts of interest

The authors declare that they have no conflict of interest.

Declaration of funding

This work was supported by funding from the Queensland Government through the Advance Queensland Fellowship granted to M. F. Adame, and the Australian Government National Environmental Sciences Programme (Tropical Water Quality Hub, Project 3.3.2) granted to N. J. Waltham and M. F. Adame. We thank the Wetland Team and Reef Water Quality Program from the Queensland Government for financial and logistic support.

Acknowledgements

We acknowledge the Traditional Owners of the land from which this project was conducted, especially the Nywaigi people of Mungalla Station and Girringun Corporation. We also thank Sam and Santo Lamari for allowing us to work in their property and sharing with us their knowledge on wetlands. Fieldwork was conducted under permit WITK17503016 (Department of Environment and Science, Queensland Government). We thank Vanessa Wong and Diego Rodriguez for providing information on the particle size of sediments within our sites.

References

Adame, M. F., Santini, N. S., Tovilla, C., Vázquez-Lule, A., Castro, L., and Guevara, M. (2015). Carbon stocks and soil sequestration rates of tropical riverine wetlands. *Biogeosciences* **12**, 3805–3818. doi:10.5194/BG-12-3805-2015

Alongi, D., Sasekumar, A., Chong, V., Pfitzner, J., Trott, L., Tirendi, F., Dixon, P., and Brunskill, G. (2004). Sediment accumulation and organic material flux in a managed mangrove ecosystem: estimates of land–ocean–atmosphere exchange in peninsular Malaysia. *Marine Geology* **208**, 383–402. doi:10.1016/J.MARGEO.2004.04.016

Audet, J., Hoffmann, C. C., Andersen, P. M., Baattrup-Pedersen, A., Johansen, J. R., Larsen, S. E., Kjaergaard, C., and Elsgaard, L. (2014). Nitrous oxide fluxes in undisturbed riparian wetlands located in agricultural catchments: emission, uptake and controlling factors. *Soil Biology & Biochemistry* **68**, 291–299. doi:10.1016/J.SOILBIO.2013.10.011

Bastviken, S. K., Eriksson, P. G., Premrov, A., and Tonderski, K. (2005). Potential denitrification in wetland sediments with different plant species detritus. *Ecological Engineering* **25**, 183–190. doi:10.1016/J.ECOLENG.2005.04.013

Brodie, J., and Waterhouse, J. (2012). A critical review of environmental management of the 'not so Great' Barrier Reef. *Estuarine, Coastal and Shelf Science* **104–105**, 1–22. doi:10.1016/J.ECSS.2012.03.012

Bruesewitz, D. A., Hamilton, D. P., and Schipper, L. A. (2011). Denitrification potential in lake sediment increases across a gradient of catchment agriculture. *Ecosystems* **14**, 341–352. doi:10.1007/S10021-011-9413-2

Burgin, A. J., and Hamilton, S. K. (2007). Have we overemphasized the role of denitrification in aquatic ecosystems? A review of nitrate removal pathways. *Frontiers in Ecology and the Environment* **5**, 89–96. doi:10.1890/1540-9295(2007)5[89:HWOTRO]2.0.CO;2

Cook, P., Revill, A., Butler, C., and Eyre, B. (2004). Benthic carbon and nitrogen cycling on intertidal mudflats of a temperate Australian estuary II. Nitrogen cycling. *Marine Ecology Progress Series* **280**, 39–54. doi:10.3354/MEPS280039

Costanza, R., D'Arge, R., de Groot, R., Farber, S., Grasso, M., Hannon, B., Limburg, K., Naeem, S., O'Neill, R. C., Paruelo, J., Gaskin, R. G., Sutton, P., and van den Belt, M. (1997). The value of the world's ecosystem services and natural capital. *Nature* **387**, 253–260. doi:10.1038/387253A0

Davis, A. M., Pearson, R. G., Brodie, J. E., and Barry, B. (2016). Review and conceptual models of agricultural impacts and water quality in waterways of the Great Barrier Reef catchment area. *Marine and Freshwater Research* **69**, 1–19.

Department of Environment and Heritage Protection (2014). Flexible options for managing point source water emissions: a voluntary market-based mechanism for nutrient management. (Queensland Government: Brisbane, Qld, Australia.) Available at https://www.ehp.qld.gov.au/water/monitoring/documents/market-based-nutrient-managment-pilot.pdf [Verified 20 May 2019].

Department of Environment and Heritage Protection (2016). Wetlands in the Great Barrier Reef Catchments. Management strategy 2014–21. (Queensland Government: Brisbane, Qld, Australia.) Available at https://wetlandinfo.ehp.qld.gov.au/resources/static/pdf/management/policy/wetlands-gbr-strategy2016-21v13.pdf [Verified 20 May 2019].

Department of Environment and Heritage Protection (2017*a*). Reef 2050 water quality improvement plan 2017–2022. (Queensland Government: Brisbane, Qld, Australia.) Available at https://www.reefplan.qld.gov.au/__data/assets/pdf_file/0017/46115/reef-2050-water-quality-improvement-plan-2017-22.pdf [Verified 20 May 2019].

Department of Environment and Heritage Protection (2017*b*). Draft point source water quality offsets policy. (Queensland Government: Brisbane, Qld, Australia.) Available at https://www.ehp.qld.gov.au/water/monitoring/documents/draft-point-source-water-quality-offsets-policy.pdf [Verified 20 May 2019].

Finlayson, C. M. (2005). Plant ecology of Australia's tropical floodplain wetlands: a review. *Annals of Botany* **96**, 541–555. doi:10.1093/AOB/MCI209

Finlayson, C. M., Cowie, I. D., and Bailey, B. J. (1993). Biomass and litter dynamics in a *Melaleuca* forest on a seasonally inundated floodplain in tropical, northern Australia. *Wetlands Ecology and Management* **2**, 177–188. doi:10.1007/BF00188152

Galloway, J. N., and Cowling, E. B. (2002). Reactive nitrogen and the world: 200 years of change. *Ambio* **31**, 64–71. doi:10.1579/0044-7447-31.2.64

Galloway, J., Aber, J., Erisman, J., Seitzinger, S., Howarth, R., Cowlilng, E., and Cosby, B. (2003). The nitrogen cascade. *Bioscience* **53**, 341–356. doi:10.1641/0006-3568(2003)053[0341:TNC]2.0.CO;2

García-Ruiz, R., Pattinson, S. N., and Whitton, B. A. (1998). Kinetic parameters of denitrification in a river continuum. *Applied and Environmental Microbiology* **64**, 2533–2538.

Hansen, A. T., Dolph, C. L., Foufoula-Georgiou, E., and Finlay, J. C. (2018). Contribution of wetlands to nitrate removal at the watershed scale. *Nature Geoscience* **11**, 127–132. doi:10.1038/S41561-017-0056-6

Hernández, M., Galindo-Zetina, M., and Hernández-Hernández, J. (2018). Greenhouse gas emissions and pollutant removal in treatment wetlands

with ornamental plants under subtropical conditions. *Ecological Engineering* **114**, 88–95. doi:10.1016/J.ECOLENG.2017.06.001

Jones, H. P., Hole, D. G., and Zavaleta, E. S. (2012). Harnessing nature to help people adapt to climate change. *Nature Climate Change* **2**, 504–509. doi:10.1038/NCLIMATE1463

Kadlec, R. H., and Reddy, K. R. (2001). Temperature effects in treatment wetlands. *Water Environment Research* **73**, 543–557. doi:10.2175/106143001X139614

Karim, F., Kinsey-Henderson, A., Wallace, J., Arthington, A. H., and Pearson, R. G. (2012). Modelling wetland connectivity during overbank flooding in a tropical floodplain in north Queensland, Australia. *Hydrological Processes* **26**, 2710–2723. doi:10.1002/HYP.8364

Kiese, R., Hewett, B., and Butterbach-Bahl, K. (2008). Seasonal dynamic of gross nitrification and N_2O emission at two tropical rainforest sites in Queensland, Australia. *Plant and Soil* **309**, 105–117. doi:10.1007/S11104-007-9468-1

Kulkarni, M. V., Groffman, P. M., and Yavitt, J. B. (2008). Solving the global nitrogen problem: it's a gas! *Frontiers in Ecology and the Environment* **6**, 199–206. doi:10.1890/060163

Land, M., Granéli, W., Grimvall, A., Hoffmann, C. C., Mitsch, W. J., Tonderski, K. S., and Verhoeven, J. T. A. (2016). How effective are created or restored freshwater wetlands for nitrogen and phosphorus removal? A systematic review. *Environmental Evidence* **5**, 9. doi:10.1186/S13750-016-0060-0

Livesley, S. J., and Andrusiak, S. M. (2012). Temperate mangrove and salt marsh sediments are a small methane and nitrous oxide source but important carbon store. *Estuarine, Coastal and Shelf Science* **97**, 19–27. doi:10.1016/J.ECSS.2011.11.002

Matheson, F. E., Nguyen, M. L., Cooper, A. B., Burt, T. P., and Bull, D. C. (2002). Fate of N-nitrate in unplanted, planted and harvested riparian wetland soil microcosms. *Ecological Engineering* **19**, 249–264. doi:10.1016/S0925-8574(02)00093-9

Mitsch, W. J., and Gosselink, J. (2015). 'Wetlands', 5th edn. (Wiley: Hoboken, NJ, USA.)

Mitsch, W. J., Day, J. J. W., Gillam, J. W., Groffman, P., Hey, D. L., Randall, G. W., and Wang, N. (2001). Reducing nitrogen loading to the Gulf of Mexico from the Mississippi River Basin: strategies to counter a persistent ecological problem. *Bioscience* **51**, 373–388. doi:10.1641/0006-3568(2001)051[0373:RNLTTG]2.0.CO;2

Mulholland, P. J., Helton, A. M., Poole, G. C. Jr, Hamilton, R. O. H., Peterson, S. K., Tank, B. J., Ashkenas, J. L., Cooper, L. R., Dahm, L. W., Dodds, C. N., Findlay, W. K., Gregory, S. E. G., Grimm, S. V., Johnson, N. B., Mcdowell, S. L., Meyer, W. H., Valett, J. L., Webster, H. M. Jr, Arango, C. P., Beaulieu, J. J., Bernot, M. J., Burgin, A. J., Crenshaw, C. L., Johnson, L. T., Niederlehner, B. R., Brien, J. M. O., Potter, J. D., Sheibley, R. W., Sobota, D. J., and Thomas, S. M. (2008). Stream denitrification across biomes and its response to anthropogenic nitrate loading. *Nature Letters* **452**, 202–205. doi:10.1038/NATURE06686

Nielsen, L. (1992). Denitrification in sediment determined from nitrogen isotope pairing. *FEMS Microbiology Ecology* **86**, 357–362. doi:10.1111/J.1574-6968.1992.TB04828.X

Peterson, B. J., Wollheim, W. M., Mulholland, P. J., Webster, J. R., Meyer, J. L., Tank, J. L., Marti, E., Bowden, W. B., Vallett, H. M., Hershey, A. E., McDowell, W. H., Dodds, W. K., Hamilton, S. K., Gregory, S., and Morrall, D. D. (2001). Control of nitrogen export from headwaters by headwater streams. *Science* **292**, 86–90. doi:10.1126/SCIENCE.1056874

Piña-Ochoa, E., and Álvarez-Cobelas, M. (2006). Denitrification in aquatic environments: a cross-system analysis. *Biogeochemstry* **81**, 111–130. doi:10.1007/S10533-006-9033-7

Potter, J. D., McDowell, W. H., Merriam, J. L., Peterson, B. J., and Thomas, S. M. (2010). Denitrification and total nitrate uptake in streams of a tropical landscape. *Ecological Applications* **20**, 2104–2115. doi:10.1890/09-1110.1

Rasiah, V., Armour, J. D., Yamamoto, T., Mahendrarajah, S., and Heiner, D. H. (2003). Nitrate dynamics in shallow groundwater and the potential for transport to off-site water bodies. *Water, Air, and Soil Pollution* **147**, 183–202. doi:10.1023/A:1024529017142

Reddy, K. R., Patrick, W. H. Jr, and Lindau, C. W. (1989). Nitrification-denitrification at the plant root–sediment interface in wetlands. *Limnology and Oceanography* **34**, 1004–1013. doi:10.4319/LO.1989.34.6.1004

Rivera-Monroy, A. V. H., Twilley, R. R., Boustany, R. G., Day, J. W., Vera-Herrera, F., Ramirez, C., Rivera-Monroy, V. H., Twilley, R. R., Boustany, R. G., Day, J. W., Vera-Herrera, F., and Ramirez, C. (1995). Direct denitrification in mangrove sediments in Terminos Lagoon, Mexico. *Marine Ecology Progress Series* **126**, 97–109. doi:10.3354/MEPS126097

Seo, D. C., and DeLaune, R. D. (2010). Fungal and bacterial mediated denitrification in wetlands: Influence of sediment redox condition. *Water Research* **44**, 2441–2450. doi:10.1016/J.WATRES.2010.01.006

Smart, J., Syezlin, H., Volders, A., Curwen, G., Fleming, C., and Burford, M. (2016). A tradable permit scheme for cost-effective reduction of nitrogen runoff in the sugarcane catchments of the Great Barrier Reef. Report to the National Environmental Science Programme, Cairns, Qld, Australia.

Song, K., Hernandez, M. E., Batson, J. A., and Mitsch, W. J. (2014). Long-term denitrification rates in created riverine wetlands and their relationship with environmental factors. *Ecological Engineering* **72**, 40–46. doi:10.1016/J.ECOLENG.2013.06.041

Steingruber, S., Friedrich, J., Gachter, R., and Wehrli, B. (2001). Measurement of denitrification in sediments with the ^{15}N isotope pairing technique. *Applied and Environmental Microbiology* **67**, 3771–3778. doi:10.1128/AEM.67.9.3771-3778.2001

Tomasek, A. A., Hondzo, M., Kozarek, J. L., Staley, C., Wang, P., Lurndahl, N., and Sadowsky, M. J. (2019). Intermittent flooding or organic-rich soil promotes the formation of denitrification hot moments and hot spots. *Ecosphere* **10**, e02549. doi:10.1002/ECS2.2549

Verhoeven, J. T. A., Arheimer, B., Yin, C., and Hefting, M. M. (2006). Regional and global concerns over wetlands and water quality. *Trends in Ecology & Evolution* **21**, 96–103. doi:10.1016/J.TREE.2005.11.015

Wallenstein, M. D., Myrold, D. D., Firestone, M., and Voytek, M. (2006). Environmental controls on denitrifying communities and denitrification rates: insights from molecular methods. *Ecological Applications* **16**, 2143–2152. doi:10.1890/1051-0761(2006)016[2143:ECODCA]2.0.CO;2

Waltham, N. J., Wegscheidl, C. J., Smart, J. C. R., Volders, A., Hasan, S., and Waterhouse, J. (2017). Scoping land conversion options for high DIN risk, low-lying sugarcane, to alternative use for water quality improvement in Wet Tropics catchments. Report to the National Environmental Science Programme. Reef and Rainforest Research Centre Limited, Cairns, Qld, Australia.

Waterhouse, J., Schaffelke, B., Bartley, R., Eberhard, R., Brodie, J., Star, M., Thorburn, P., Rolfe, J., Ronan, M., Taylor, B., and Kroon, F. (2017). 'Scientific Consensus Statement. Land Use Impacts on Great Barrier Reef Water Quality and Ecosystem Condition.' (The State of Queensland: Brisbane, Qld, Australia.)

Wetzel, R. G. (2001). 'Limnology. Lake and River Ecosystems', 3rd edn. (Academic Press: London, UK.)

Yao, L., Jiang, X., Chen, C., Liu, G., and Liu, W. (2016). Within-lake variability and environmental controls of sediment denitrification and associated N_2O production in a shallow eutrophic lake. *Ecological Engineering* **97**, 251–257. doi:10.1016/J.ECOLENG.2016.10.023

Zhou, S., Borjigin, S., Riya, S., Terada, A., and Hosomi, M. (2014). The relationship between anammox and denitrification in the sediment of an inland river. *The Science of the Total Environment* **490**, 1029–1036. doi:10.1016/J.SCITOTENV.2014.05.096

Handling Editor: Richard McDowell

APPENDIX 8: CARBON AND NITROGEN SEQUESTRATION OF MELALEUCA FLOODPLAIN WETLANDS IN TROPICAL AUSTRALIA

Ecosystems (2020) 23: 454–466
https://doi.org/10.1007/s10021-019-00414-5

© 2019 Springer Science+Business Media, LLC, part of Springer Nature

ECOSYSTEMS

Carbon and Nitrogen Sequestration of *Melaleuca* Floodplain Wetlands in Tropical Australia

M. F. Adame,[1]* R. Reef,[2] V. N. L. Wong,[2] S. R. Balcombe,[1] M. P. Turschwell,[1] E. Kavehei,[1] D. C. Rodríguez,[2] J. J. Kelleway,[3,4] P. Masque,[5,6,7] and M. Ronan[8]

[1]*Australian Rivers Institute, Grifith University, Nathan, Queensland 4111, Australia;* [2]*School of Earth, Atmosphere and Environment, Monash University, Clayton, Victory 3800, Australia;* [3]*Department of Environmental Sciences, Macquarie University, North Ryde, New South Wales 2109, Australia;* [4]*School of Earth, Atmospheric and Life Sciences, University of Wollongong, Wollongong, New South Wales 2522, Australia;* [5]*School of Science, Centre for Marine Ecosystems Research, Edith Cowan University, Joondalup, Western Australia 6027, Australia;* [6]*Institut de Ciència i Tecnologia Ambientals, Departament de Física, Universitat Autònoma de Barcelona, Barcelona, Spain;* [7]*Oceans Institute, School of Physics, The University of Western Australia, Crawley, Western Australia 6009, Australia;* [8]*Wetlands Team, Environment Policy and Planning, Department of Environment and Science, Queensland Government, Brisbane, Queensland 4000, Australia*

Abstract

Wetlands of *Melaleuca* spp. in Australia form large forests that are highly threatened by deforestation and degradation. In America, *Melaleuca* has invaded large areas of native wetlands causing extensive damage. Despite their status as an endangered native ecosystem and as a highly invasive one, little is known about their C and N dynamics. In this study, we sampled five *Melaleuc*a wetlands and measured their C and N ecosystem stocks (aboveground biomass and soil), tree accumulation rates, sedimentation rates, and soil stability. *Melaleuca* wetlands were highly heterogeneous, but most have large ecosystem C [mean ± SE (range); 360 ± 100 (80–670) Mg C ha^{-1}] and N [8100 ± 1900 (1600–13,000) kg N ha^{-1}] stocks. Tree accumulation rates were 5.0 ± 2.1 Mg C y^{-1} and 26 ± 14 kg N y^{-1}, and surface soil accumulation rates were 0.6 ± 0.2 Mg C ha^{-1} y^{-1} and 39 ± 1 kg N y^{-1}. We found evidence of long-term C and N accumulation in the soil, but also of some level of organic decomposition. Overall, we found that *Melaleuca* wetlands store and accumulate large amounts of C, especially in their trees, and large amounts of N in their soils, suggesting an important role in coastal biogeochemical cycles.

Key words: Aboveground biomass; Decomposition; Queensland; Soil; Sedimentation; Stable isotopes.

Highlights

- Most *Melaleuca* wetlands have large ecosystem C and N stocks.
- Some organic compounds in *Melaleuca* wetlands are stable in the soil for long periods.
- In *Melaleuc*a wetlands, most C is stored and accumulated in the trees, most N in the soil.

Received 26 March 2019; accepted 12 June 2019;
published online 19 July 2019

Electronic supplementary material: The online version of this article (https://doi.org/10.1007/s10021-019-00414-5) contains supplementary material, which is available to authorized users.

Authors' contributions MFA and MR designed the study; MFA, RR, VNLW, SRB, MT, EK, and SR conducted field work; VNLW, EK, SR, DCR, and PM conducted laboratory work, MFA, RR, VNLW, MT, JJ, and PM analysed the data; MFA, RR, SRB, JJK, PM, and MR wrote the manuscript.

*Corresponding author; e-mail: f.adame@griffith.edu.au

- *Melaleuca* wetlands have an important role in coastal biogeochemical cycles.

Introduction

Melaleuca spp., commonly known as paperbark or tea trees, is a genus of the Myrtaceae family which has approximately 300 species (Barlow 1988). *Melaleuca* trees can form dense stands in waterlogged soils and withstand long periods of inundation and sporadic tidal flooding (Figure 1B). They can be found in near-coastal or coastal floodplains of tropical and subtropical Australia (Finlayson 2005) with an estimated area of 6.4 million ha, (ABARES 2016, Figure 1A). Although this estimate includes some non-wetland forest, it greatly exceeds the distribution of both mangroves (1.1 million ha) and tidal marsh (1.5 million ha) in Australia (Geoscience Australia 2005; Giri and others 2011). *Melaleuca* distributions outside Australia are also notable, with some species found in Southeast Asia (Tran and others 2013a, b). Some species of *Melaleuca*, such as *M. quinquenervia*, have become highly invasive in Hawaii, Mainland, USA, the Caribbean, and South America. In Florida alone, dense forests of *M. quinquenervia* cover an area larger than those of native mangroves (> 200,000 ha) and have had serious effects on native wetlands by displacing native species and drastically modifying the landscape (Turner and others 1998). Despite their large area in Australia and their importance as an invasive ecosystem, *Melaleuca* ecosystems are poorly studied. There is little information apart from physiological studies as a cultivated species and the antimicrobial properties of the oil produced by their leaves (e.g. Carsib and others 2006).

Melaleuca wetlands occur in a range of geomorphic settings with varying degrees of connection to coastal water bodies. Some low-lying coastal *Melaleuca* wetlands could be considered ''tidal freshwater forested wetlands'' (Krauss and others 2018) as they mainly live in freshwater conditions, but they can be sporadically flooded by tides, which makes their soils moderately saline (Boland and others 2006; Mensforth and Walker 1996). Similar to other tidal forested wetlands, *Melaleuca* forests could be a globally significant C stock (Tran and Dargusch 2016; Krauss and others 2018) due to their high productivity (≥ 1 g C m^2 d^{-1}, Finlayson and others 1993; Greenway 1994), high aboveground biomass (> 100 Mg ha^{-1}), and organic-rich soils (> 100 Mg C $ha^{-1,}$ to soil depth of 30 cm, Tran and Dargusch 2016). In Australia, a large portion of *Melaleuca* wetlands (> 1 million ha) are located in private land and have limited protection (ABARES 2016). Due to their high potential to store and sequester C and their high risks of deforestation, *Melaleuca* wetlands have the potential to be incorporated in greenhouse mitigation strategies as blue carbon ecosystems (Lovelock and Duarte 2019). However, little is known on the processes that govern the C cycling in *Melaleuca* wetlands (Lovelock and Duarte 2019).

Melaleuca wetlands are also likely to be important for improving water quality by transforming nitrogen through denitrification, by accumulating nutrients in the sediment, and through tree uptake (Greenway and Jenkins 2004; Kulkarni and others 2008; Adame and others 2019). The role of storing and sequestering N is partly associated with the capacity of these forests to retain sediment deposited during flooding (Adame and others 2015) and the capacity of the trees to grow and store N in their trunks for long periods. However, similar to C dynamics, there are only a handful of published studies on the role of *Melaleuca* wetlands for storing and sequestering N (Adame and others 2019; Greenway and Jenkins 2004).

In this study, we investigated C and N ecosystem stocks (aboveground biomass and soil), tree growth, soil accumulation, and soil C and N stability of five *Melaleuca* wetlands in tropical Queensland, Australia. For comparison, we also sampled a nearby sugar cane plantation, a saltmarsh, and a mangrove forest. We hypothesised that *Melaleuca* wetlands would have relatively large C and N stocks, with high tree and soil accumulation rates, and stable C and N in deep soils, conditions that would make them suitable for consideration in C and N mitigation strategies.

Methods

Study Sites

Sampling was conducted in five natural floodplain wetlands dominated by *Melaleuca quinquenervia* or *Melaleuca viridiflora* in Queensland, Northeast Australia: Halifax Bay Wetlands National Park (HX), Insulator Creek (IC), Mungalla Station (MG), Girramay National Park (GI), and Hull Heads National Park (HH; Figure 1C). For comparison, we sampled at IC a sugar cane plantation, which is a common land use of the area, a mangrove forest dominated by *Bruguiera gymnorrhiza*, and a saltmarsh dominated by *Schoenoplectus subulatus*. The sites were located in the Wet Tropics, within the catchments of the Herbert and the Tully–Murray Rivers. The

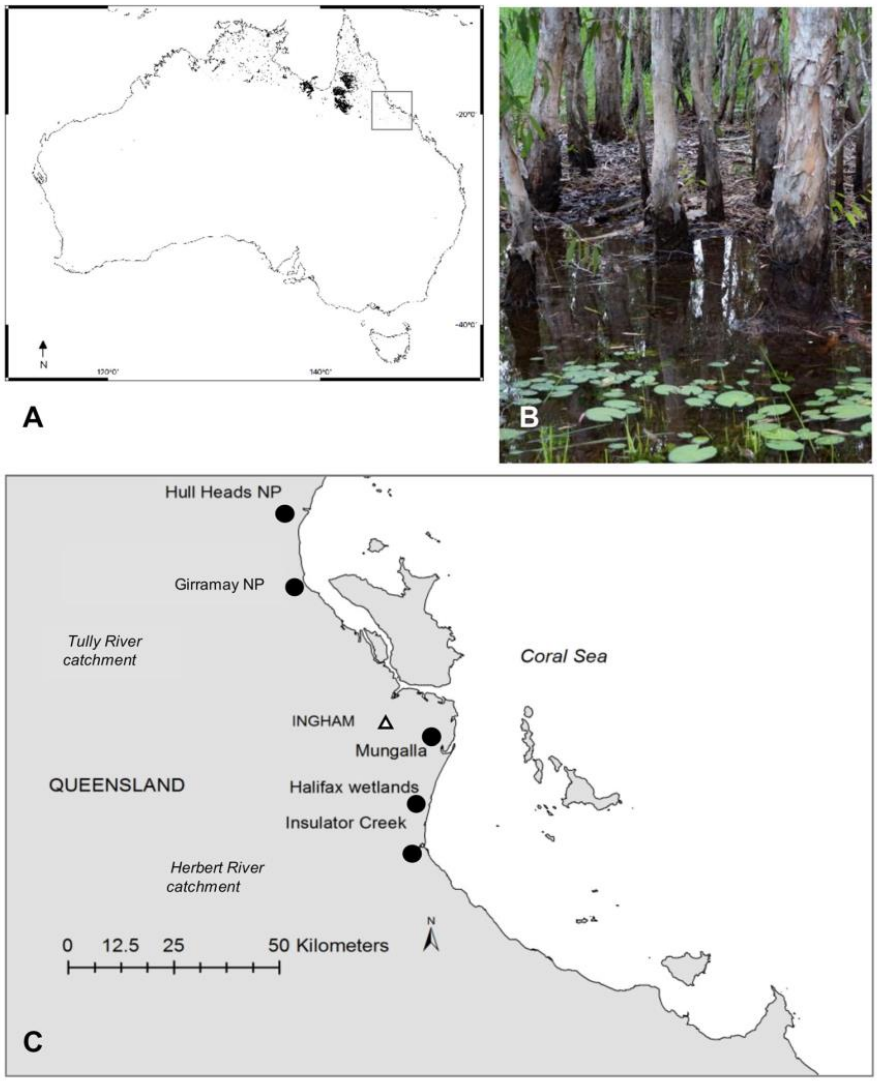


Figure 1. (**A**) Distribution of *Melaleuca* sp. in Australia (ABARES, 2016); (**B**) floodplain wetland dominated by *Melaleuca quinquenervia* (photograph by MF Adame). Location of five sampling sites in tropical Queensland, Australia: Halifax Bay Wetlands National Park (HX), Insulator Creek (IC), Mungalla Station (MG), Girramay National Park (GI), and Hull Heads National Park (HH).

climate is tropical with monthly mean temperatures ranging from 22 to 34°C (Australian Bureau of Meteorology, ABM 2018: 1907–2018) and a mean total annual rainfall above 2,000 mm, mostly falling between January and May (ABM 2018: 1871–2018).

The Herbert and Tully Rivers drain a catchment of about 10,000 and about 1600 km^2, respectively, and discharge into the Coral Sea and into the Great Barrier Reef. The rivers are characterised by dry periods during the winter months and sporadic overbank floods in the summer that inundate the adjacent wetlands from 1 to 12 days at a time (Karim and others 2012). Groundwater flows are also important, mainly after rainfall events, but also as lateral flows during the dry season (Rasiah and others 2010). From our sites, HX, IC, and MG (Herbert catchment) are primarily influenced by saline groundwater flow and GI and HH (Tully–Murray catchment) by low-salinity groundwater flow (State of Queensland, 2014). From our observations, the site at HX is sporadically flooded

by tides, IC, MG, and GI are flooded by rain and overbank flows in the wet season, and HH is permanently flooded. Tides in the region are mesotidal with amplitudes between 3 and 5 m (ABM 2018).

Both catchments are characterised by alluvial fans in the lower slopes and an alluvial plain with swamps in wet areas close to the coast (Wilson and Baker 1990; Murtha and Smith 1994). The soils types are typically Rudosol, Kandosol, and Sodosol on the alluvial fans, Dermosol, Kurosol, Vertosol, and Sodosol on the alluvial plain, Tenosol on the beach ridges, and Organosol in swamp areas (Isbell 2002).

Sampling was conducted in the dry seasons (May–October) of 2016 and 2017. At each site, aboveground C and N stocks, tree accumulation rates, soil characteristics, soil C and N stocks, surface soil accumulation rates, and soil stability were examined. The detailed methodology is explained below.

Aboveground C and N Stocks

At each site, we measured five plots of 5 m radius separated by 20 m over a linear transect from the water edge (Adame and others 2015). At each plot, we counted and measured the diameter at breast height of every tree larger than 2 cm to obtain forest density and biomass. When forest density was greater than 3000 trees per ha, plots of 3 m radius were used instead. Sampling sites were located within *Melaleuca* forests with an area of 6 to 26 ha; thus, our sampling intensity for aboveground biomass per forest was relatively low ($< 2\%$ of the total area), but it was compensated by a large number of sites ($n = 5$) within a large geographical location (over 200 km) to account for the high variability of *Melaleuca* forests structures observed in the region. Aboveground biomass was estimated from the allometric equations derived for *Melaleuca viridiflora* (Equation 1) and *Melaleuca* spp. (Equation 2) in Northern Australia by Finlayson and others (1993).

$$\log\left[\text{tree biomass (kg)}\right] = 2.338\left[\log \text{ DBH (cm)}\right] - 0.561 \quad (1)$$

$$\log\left[\text{tree biomass (kg)}\right] = 2.666\left[\log \text{ DBH (cm)}\right] - 0.502 \quad (2)$$

Information on tree biomass and forest density has been previously published in Adame and others (2019). The C and N stocks of *Melaleuca* trees were obtained by multiplying biomass of the forest by the C and N content of the wood, which was estimated from ten pieces of wood obtained with a tree corer (see below Methods for tree coring) and analysed in an elemental analyser (EA-IRMS, Serco System, Griffith University). On average, *Melaleuca* wood was $48 \pm 2\%$ C and $0.09 \pm 0.03\%$ N.

The biomass of the saltmarsh was obtained from five plots within a 50-m transect; at each plot, two quadrants of 30 cm^2 were set, from which all the plant material above the root was clipped. The plant material was weighed dry to obtain dry biomass per area, which was multiplied by the C and N content of stems to obtain aboveground stocks. The C and N content of marsh was $44 \pm 1\%$ C and $0.89 \pm 0.11\%$ N (EA-IRMS, Serco System, Griffith University). The aboveground biomass of sugar cane and mangroves was obtained from Robertson and others (1996) and Clough (1998), respectively. The C and N content for sugar cane was obtained from leaves collected at IC; the C and N content of mangrove wood was obtained from Gong and Ong (1990).

Tree Accumulation Rates

Tree C and N accumulation rates were estimated through dendrochronology by analysing three to five cores at each site (for example, Fortier and others 2015). Wood cores of 10–25 cm were obtained at breast height from the trunks with a tree increment borer (Haglöf, Sweden). The cores were selected from trees of different sizes that were representative of the forest. Usually, *Melaleuca* trees have annual rings as their growth is associated with annual rainfall (Finlayson and others 1993; Greenway 1994). Tree cores were sanded, and the incremental tree ring widths were measured using a dissection microscope to obtain annual increments in diameter at breast height. Biomass accumulation over time was estimated from the allometric equation of Finlayson and others (1993, Eqs. 1 and 2). Tree C and N accumulation rates were obtained by multiplying biomass increments by wood C and N content. The annual rate of N uptake is underestimated as *Melaleuca* trees are likely to reabsorb N from old wood during growth (Meerts 2002).

Soil C and N Stocks

Soil C and N stocks were estimated by obtaining a 50-cm soil core at three plots at each site with a stainless steel gouge auger of 4 cm diameter (GA, Dormer Soil Samplers, NSW Australia). Samples were collected from cores in either 10 cm increments (i.e. 0–10, 10–20, 20–30, 30–40, and 40–50 cm) or at distinct facies change. The organic

matter layer in all the cores sampled was always 55 cm or less. Soil samples were oven-dried at 60°C for 48 h to measure C. A subset of samples was oven-dried at 105°C for 48 h to correct for the total water content of the samples that was not removed at 60°C. Bulk density (BD) was estimated from the dry weight of the sample, which had a known volume. Soil samples were analysed for N and C with an elemental analyser (EA-IRMS, Serco System, Griffith University). Organic carbon (herein ''carbon'') was estimated by subtracting the inorganic C, which was measured from the difference from samples analysed with and without HCl (10%). In all sites, inorganic C concentration was below 2% of the total C. Soil C and N stocks were estimated by multiplying BD by %N and %C by the depth of the soil layer (Adame and others 2015). Stocks were estimated to 50 cm deep, which was the depth at which a distinct organic layer was usually found above mineral-dominated strata.

Three additional cores were taken at each plot as described above to measure pH and electrical conductivity (EC). Samples were dried at 105°C for 24 h, lightly crushed, and passed through a 2-mm sieve. The pH and EC were measured in duplicate in 1: 5 soil/water extracts (Rayment and Lyons 2001; TPS 90-FLMV Field Laboratory Analyser). Soils that were analysed for particle size were pretreated with 30% H_2O_2 to remove organic matter, dispersed with 10% Na $(PO_3)_6$, and analysed by laser granulometry (Beckman Coulter LP 13320 Particle Size Analyser). Soil particles were classified as sand (62.5–2000 μm), silt (39–62.5 μm), or clay (< 39 μm).

Sedimentation, and Soil C and N Accumulation Rates

Sediment cores were analysed for ^{210}Pb to determine accumulation rates during the last century for three sites: IC, MG, and HH. Samples were obtained by extracting an undisturbed sediment core with an open auger (GA, Dormer Soil Samplers, NSW, Australia) and sampling every two cm from the top 20 cm of soil. Samples were oven-dried at 60°C. The concentrations of ^{210}Pb were determined by alpha spectrometry through the determination of ^{210}Po in equilibrium with ^{210}Pb after addition of ^{209}Po as an internal tracer and digestion in acid media using an analytical microwave (Sanchez-Cabeza and others 1998). Excess ^{210}Pb concentrations were determined as the difference between total ^{210}Pb and ^{226}Ra (supported ^{210}Pb), which was analysed by gamma spectrometry at various depths along each core. The concentrations of ^{226}Ra were quantified via the emission peaks of its two decay products ^{214}Pb (295 and 352 keV) and ^{214}Bi (609 keV) using a high-purity germanium detector (CANBERRA, mod. GCW3523) in calibrated geometries. Samples were sealed for at least 21 days to reach secular equilibrium with ^{214}Pb and ^{214}Bi, that is, when the quantity of radioactive isotope remains constant because its production rate is equal to its decay rate.

Sediment accumulation rates were calculated applying the CSR (constant rate of supply) and the CF/CS models (constant flux/constant sedimentation; Krishnaswami and others 1971; Appleby and Oldfield 1978; Arias-Ortiz and others 2018). Soil C and N accumulation rates were estimated from soil accumulation rates and C and N content along the cores and down to the depth at which the excess ^{210}Pb horizon was met.

Soil Stability and Decomposition

The stability of soil C and N was determined from the variation of δ^{13}C and δ^{15}N values with depth (Adame and Fry 2016). The δ^{13}C and δ^{15}N values tend to increase with decomposition due to the preferential metabolic uptake of δ^{12}C and δ^{14}N over δ^{13}C and δ^{15}N (Nadelhoffer and Fry 1988). Thus, we expected that isotopic values would remain constant with depth if C and N were stable through time and decomposition was low; on the contrary, if decomposition were high, isotopic values would increase with depth (Nadelhoffer and Fry 1988; Adame and Fry 2016). We collected three soil cores at each site and took samples with depths (see cores for C and N above). Samples were oven-dried at 60°C and analysed for δ^{13}C and δ^{15}N in a mass spectrometer coupled to an isotopic ratio mass spectrometer (EA-IRMS, Serco System, Griffith University) with an analytical standard deviation below 0.1‰ for δ^{13}C and below 0.2‰ for δ^{15}N.

Data Analyses

Differences among sites and soil depths were tested with a linear model where the site was the random factor and depth the fixed factor of the model. Linearity, normality, and homogeneity of variance were assessed from residual plot analyses and Shapiro–Wilk and Kolmogorov–Smirnov tests. When data were not normal (%C, %N, C:N), they were transformed (log, 1/x). Data were analysed with SPSS statistical program (v24, IBM, New York, USA) and shown as mean ± standard errors (range). Stocks are shown in units of Mg (= metric tonne). Data were rounded to significant figures as appropriate.

Results

Aboveground C and N Stocks

Mean *Melaleuca* aboveground C and N stocks were 210 ± 60 Mg C ha^{-1} and 450 ± 130 kg N ha^{-1}, respectively (Table 1, Figure 2). In comparison, nearby mangroves, sugar cane, and saltmarsh had lower C stocks with 140 ± 20 Mg C ha^{-1}, 24 ± 12 Mg C ha^{-1}, and 2.8 ± 0.2 Mg C ha^{-1}, respectively. *Melaleuca* wetlands had higher N stocks than those of marsh with 51 ± 4 kg N ha^{-1}, but lower than both mangroves and sugar cane, which had values of 1480 ± 170 and 1780 ± 80 kg N ha^{-1}, respectively.

Soil Characteristics

The soils at all sites and all depths were acidic with a pH mean of 4.9 (4.1–5.5; Table 2). The EC of the sites ranged from no more than 0.2 mS cm^{-1} (MG and GI) to greater than 1 mS cm^{-1} (HX, HH and IC). Highest EC values were measured at HH with 3.1 mS cm^{-1}. All sites showed a general decrease in EC with depth. The soil of MG and IC was dominated by sand (47 ± 1%), whereas the soil at the rest of the sites was dominated by silt (52 ± 2%; Table 2).

Soil C and N Stocks

Considering all sites, BD mean was 1.1 ± 0.08 g cm^{-3} (0.92–1.2 g cm^{-3}), mean soil C content was 3.7 ± 1.2% (0.5–8.0%), and mean N content was 0.23 ± 0.06% (0.03–0.41%). Soil BD was similar throughout sites, but C and N contents were more variable, with HX having the lowest C and N. In all sites, BD increased, while C and N concentrations decreased with depth (BD $F_{3,12}$ = 22.53, $P < 0.001$; logC% $F_{3,71}$ = 15.33, $P < 0.001$; logN% $F_{3,71}$ = 12.94, $P < 0.001$). Mean C/N was 22 ± 2 (19–32), with HH having the lowest values (Table 3).

The mean C stock in the upper 50 cm was 140 ± 40 (20–230) Mg C ha^{-1}, and the mean N stock was 8.0 ± 1.9 (1.6–13) Mg N ha^{-1}. The soil C stocks were at least 130 Mg C ha^{-1} for all sites, except in HX, where the C stocks were much lower at 23 Mg C ha^{-1} (Table 3). The highest C density was found in the upper 30 cm, although at IC, GI, and MG, the C concentrations were high down to 50 cm in depth. Below 50 cm deep, a distinct change from organic to mineral strata was usually found. If we only consider the first 30 cm of soil, stocks were 26% lower with 104 ± 28 (19–200) Mg C ha^{-1}.

Ecosystem C and N Stocks

The mean ecosystem stocks of *Melaleuca* wetlands were 350 ± 100 (80–663) Mg C ha^{-1} and 9 ± 2 (2–14) Mg N ha^{-1}. Lowest stocks were measured at HX and highest at IC. In comparison with the other ecosystems in IC, the mean C stock of *Melaleuca* wetlands was similar to that of the mangrove site (310 Mg C ha^{-1}), twofold larger than that of the saltmarsh site (140 Mg C ha^{-1}), and about six times larger than that of the sugar cane plantation (55 Mg C ha^{-1}). N stocks of *Melaleuca* wetlands were similar than those of saltmarsh (9 Mg N ha^{-1}), sugar cane (9 Mg N ha^{-1}), and mangroves (10 Mg N ha^{-1}). Soil contributed between 28 and 57% of the total C stock and between 93 and 96% of the total N stock (Figure 2).

Tree C and N Accumulation Rates

Mean tree accumulation rate was 5 ± 2 Mg C y^{-1} ha^{-1} and 26 ± 14 kg N y^{-1} ha^{-1}. Highest C and N sequestration values were measured at IC and MG, respectively; lowest C and N sequestration values were measured at HH (Table 1).

Soil C and N Accumulation Rates

The concentration profiles of excess ^{210}Pb in cores MG and IC suggested sediment mixing in the upper

Table 1. Tree C and N Stocks and Accumulation Rates of *Melaleuca* Wetlands in Tropical Australia

Site	Dominant sp	C stock (Mg C ha^{-1})	N stock (kg N ha^{-1})	C accumulation (Mg C y^{-1} ha^{-1})	N accumulation (kg N y^{-1} ha^{-1})
HX	*M. quinquenervia*	57 ± 14	120 ± 30	9.3 ± 1.8	5.4 ± 1.0
IC	*M. quinquenervia*	430 ± 140	900 ± 300	12.2 ± 1.1	20 ± 4
MG	*M. quinquenervia*	110 ± 30	330 ± 60	3.3 ± 1.0	85 ± 30
GI	*M. quinquenervia*	240 ± 30	490 ± 70	2.4 ± 0.3	33 ± 4
HH	*M. viridiflora*	198 ± 12	410 ± 30	1.7 ± 0.1	3.2 ± 0.2

C = carbon, N = nitrogen.

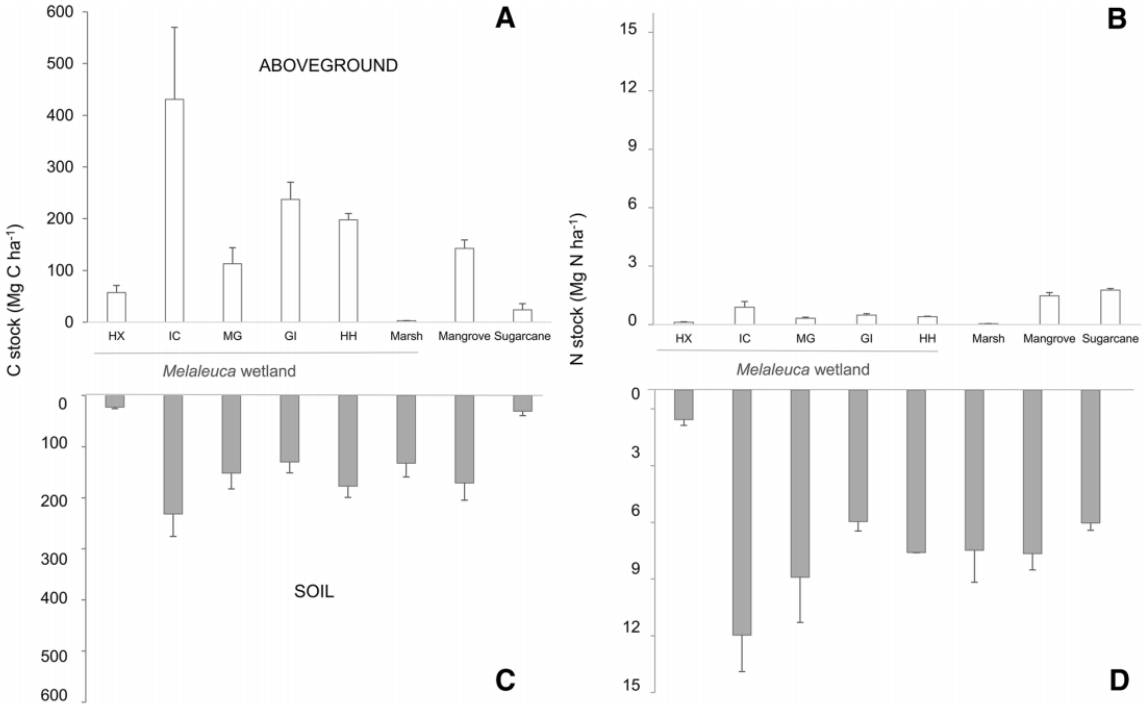


Figure 2. Ecosystem C (**A**, **C**) and N (**B**, **D**; Mg ha^{-1} y^{-1}) stocks (aboveground biomass and soil) in five *Melaleuca* wetlands in tropical Australia: Halifax Bay Wetlands National Park (HX), Insulator Creek (IC), Mungalla Station (MG), Girramay National Park (GI), and Hull Heads National Park (HH), a saltmarsh, a mangrove, and sugar cane plantation at IC. Values are mean and standard errors of five plots for aboveground stocks and three plots for soil stocks. Aboveground C and N stocks were estimated from biomass values of sugar cane and mangroves from Clough (1998) and Robertson and others (1996).

4 cm, while strong mixing through at least the upper 20 cm was observed at HH. Therefore, sedimentation and C accumulation rates could only be estimated for IC and MG.

The concentration profiles of total ^{210}Pb in cores from IC and MG showed similar patterns, with relatively constant concentrations in the upper 4 cm (average 133 ± 7 Bq kg^{-1}), suggesting mixing, and a steady decrease with depth down to 47 ± 4 Bq kg^{-1} at 12 cm and 42 ± 3 Bq kg^{-1} at 16 cm, respectively (Figure 3). Average sedimentation rates during the last approximately 100 years calculated using the excess ^{210}Pb concentration profiles below the mixing layers were 1.13 ± 0.09 mm y^{-1} (0.079 ± 0.006 g cm^{-2} y^{-1}) for IC and 0.87 ± 0.12 mm y^{-1} (0.082 ± 0.011 g cm^{-2} y^{-1}) for MG.

Both models, CSR and CF/CS, gave similar results. For IC, the average C accumulation rate in the past 75 years was estimated with the CSR model as 0.55 ± 0.08 Mg C ha y^{-1} and 38 ± 6 kg N ha y^{-1} and with the CF/CS model as 0.55 ± 0.04 Mg C ha y^{-1} and 45 ± 4 kg N ha y^{-1}. For MG, for the past 90 years, the CSR model estimated 0.69 ± 0.13 Mg C ha y^{-1} and 40 ± 8 kg N ha y^{-1} and the CF/ CS model estimated 0.40 ± 0.05 Mg C ha y^{-1} and 42 ± 6 kg N ha y^{-1}. The oldest sample in the profile was dated back to the end of the nineteenth century (the year 1881 for MG, Figure 3).

Soil C and N Stability

Soil $\delta^{13}C$ and $\delta^{15}N$ mean values were − 25.9 ± 1.3‰ and 1.5 ± 0.6‰, respectively. These $\delta^{13}C$ values were higher than those for *Melaleuca* leaves (− 32.0 ± 0.6‰) and wood (− 28.0 ± 0.3‰). There were significant differences among sites; notably $\delta^{13}C$ and $\delta^{15}N$ values in HH were lower than the rest. The $\delta^{13}C$ values increased slightly with depth (1–5‰), but $\delta^{15}N$ and C/N remained constant ($P = 0.60$ and $P = 0.93$, respectively; Figure 4).

Table 2. Soil Characteristics of *Melaleuca* Wetlands in Tropical Australia

	Depth (cm)	pH	EC (mS/cm)	Sand (%)	Silt (%)	Clay (%)
HX	0–10	5.5	2.0	39	49	12
	10–20	5.3	0.6	37	50	12
	20–30	5.0	0.7	28	59	13
	30–35	4.8	0.9	31	56	14
IC	0–10	5.3	3.0	52	39	9
	10–20	4.8	1.9	37	48	15
	20–30	4.8	1.4	35	44	21
	30–40	4.7	1.4	69	26	5
MG	0–10	4.9	0.5	56	34	10
	10–20	4.9	0.7	33	47	21
	30–40	4.9	0.4	46	38	16
	40–50	4.6	0.4	49	35	16
GI	0–10	4.1	0.5	44	40	16
	10–20	4.3	0.3	31	50	19
	20–30	4.6	0.3	22	58	20
	30–40	4.4	0.2	31	46	23
HH	0–10	5.2	2.5	43	45	18
	10–20	5.4	3.1	44	50	19
	20–30	5.5	1.8	18	58	20
	30–40	5.2	1.2	31	46	23
	40–50	4.8	1.1	28	56	16

EC = electrical conductivity.

Discussion

Melaleuca wetlands of tropical Australia store large amounts of C (360 ± 100 Mg C ha^{-1}, including soil up to 50 cm deep), with similar values as other coastal C-rich wetlands. For example, mangroves around the world have ecosystem C stocks (trees and soil to 1 m deep) ranging from 70 to greater than 1,100 Mg C ha^{-1} (Hutchison and others 2014; Atwood and others 2017). Seagrass meadows have 140 (9–830) Mg C ha^{-1} (Fourqurean and others 2012), saltmarshes have 390 Mg C ha^{-1} (100–800; Chmura and others 2003), and other tidal freshwater wetlands have between 320 and 1300 Mg C ha^{-1} (Krauss and others 2018). Other studies in *Melaleuca* wetlands reported C stocks of 280 ± 40 Mg C ha^{-1} (subtropical Australia, Tran and Dargusch 2016) and 400 ± 110 Mg C ha^{-1} (Vietnam, Tran and others 2015), though these previous studies only included the surface 30 cm of soil in their estimates. However, different to other coastal C-rich ecosystems (Fourqurean and others 2012; Adame and others 2013) the organic layer of all the *Melaleuca* wetlands in this study was less than 1 m deep, and most of their C stock was stored in the trees, not in the soil.

The distribution of organic horizons within coastal wetland soil profiles is spatially variable, in part due to the eco-geomorphic development of a location relative to sea-level change (Rogers and others 2019). For instance, Australian tidal marshes have sub-surface horizons that correspond to lower elevation mangroves below contemporary upper intertidal surfaces. This horizon reflects sea levels that were about 1–2 m higher during the mid-Holocene compared to present (Hayes and others 2017; Kelleway and others 2017a). In some coastal *Melaleuca* wetlands, we might expect to find similar organic ''blue carbon'' deposits (potentially below our sampling depth of 50 cm), though this currently remains untested.

Unlike C, most of the N stock of *Melaleuca* wetlands (≥ 93%) was stored in the soil. *Melaleuca* wetlands are periodically flooded during high rainfall events when overbank flows cover them for days or even weeks at a time (Karim and others 2012). During these flooding events, fast flowing water carrying sediments and particulate nutrients could be deposited in the wetland as water velocity decreases. Some of the nutrients deposited could be decomposed and denitrified, consumed by trees, or sequestered for long periods in the soil. As a result, the soil of *Melaleuca* wetlands is a combination of in-situ production and other terrestrial material transported and compacted during floods. This would explain relatively high density of the soil

Table 3. Bulk Density (BD, g cm^{-3}), Organic Carbon (%C), Nitrogen (%N), and C and N Stocks (Mg ha^{-1}) of *Melaleuca* Wetlands in Tropical Australia

Depth (cm)	BD (g cm^{-3})	%C	%N	C stock (Mg ha^{-1})	N stock (Mg ha^{-1})
Halifax wetlands bay NP (HX)					
0–10	0.84 ± 0.12	1.0 ± 0.20	0.059 ± 0.008	8.2 ± 0.3	0.477 ± 0.014
10–20	1.21 ± 0.08	0.45 ± 0.13	0.030 ± 0.008	5.3 ± 1.0	0.36 ± 0.06
20–30	1.39 ± 0.02	0.26 ± 0.06	0.020 ± 0.005	3.6 ± 0.9	0.28 ± 0.07
30–50	1.44 ± 0.14	0.22 ± 0.04	0.019 ± 0.004	5.5 ± 1.5	0.47 ± 0.17
Total				23 ± 3	1.6 ± 0.3
Insulator creek (IC)					
0–10	0.65 ± 0.10	8 ± 2	0.54 ± 0.14	74 ± 19	2.8 ± 0.6
10–20	0.99 ± 0.13	5.3 ± 1.5	0.38 ± 0.11	78 ± 20	3.0 ± 0.7
20–30	1.36 ± 0.06	2.2 ± 0.4	0.14 ± 0.05	52 ± 10	1.9 ± 0.5
30–50	1.52 ± 0.16	1.30 ± 0.14	0.14 ± 0.04	26 ± 5	3.1 ± 1.6
Total				230 ± 40	13.0 ± 1.9
Mungalla station (MG)					
0–10	0.61 ± 0.07	8 ± 3	0.44 ± 0.2	43 ± 11	2.5 ± 0.5
10–20	0.85 ± 0.12	4.8 ± 1.2	0.27 ± 0.03	40 ± 12	2.28 ± 0.19
20–30	1.24 ± 0.08	3.1 ± 0.7	0.16 ± 0.03	38 ± 7	2.0 ± 0.30
30–50	1.75 ± 0.09	0.9 ± 0.5	0.06 ± 0.04	31 ± 18	2.1 ± 1.4
Total				150 ± 30	10 ± 3
Girramay NP (GI)					
0–10	0.59 ± 0.02	4.1 ± 0.4	0.34 ± 0.02	32.1 ± 1.3	2.01 ± 0.03
10–20	0.78 ± 0.09	2.6 ± 1.5	0.19 ± 0.09	24 ± 10	1.3 ± 0.57
20–30	0.95 ± 0.03	2.1 ± 0.4	0.20 ± 0.03	26 ± 3	1.8 ± 0.26
30–50	1.38 ± 0.12	1.2 ± 0.9	0.06 ± 0.02	48 ± 30	1.8 ± 0.79
Total				130 ± 20	7.0 ± 0.5
Hull heads NP (HH)					
0–10	0.34 ± 0.05	14.3 ± 1.4	0.78 ± 0.04	48 ± 5	2.6 ± 0.2
10–20	0.53 ± 0.08	11 ± 3.4	0.56 ± 0.13	56 ± 7	2.7 ± 0.18
20–30	0.87 ± 0.14	5 ± 2	0.28 ± 0.17	37 ± 12	2.0 ± 0.9
30–50	1.56 ± 0.081	1.2 ± 0.4	0.03 ± 0.01	36 ± 8	0.8 ± 0.2
Total				180 ± 20	8.6 ± 0.9

Data are for the top 50 cm of soil, and values are mean and standard errors from three (HX, MG, GI, HH) to five plots (IC) per site.

(> 1 g cm^{-3}), the dominance of coarse sediment in some sites, and the fact that the soil is not only composed of *Melaleuca* material (wood or leaves).

The soil accumulation in *Melaleuca* wetlands in this study was similar to other coastal wetlands with rates between 40 ± 6 kg N ha y^{-1} and 0.55 ± 0.05 Mg C ha y^{-1}, which are similar to the global mean for saltmarshes and mangroves (0.60 Mg C ha y^{-1}; Chmura and others 2003; Macreadie and others 2017). The rates of N accumulated in the soil were within the same order of magnitude than the rates of N accumulated in the trees (26 ± 14 kg N y^{-1} ha^{-1}). However, the rates of C accumulated in the soil were two orders of magnitude lower of the trees. Thus, *Melaleuca* wetlands accumulate much faster and larger amounts of C in their trees than in their soil and accumulate N at a similar rate in the soils and their trees. Overall, *Melaleuca* wetlands provide long-term C and N storage in their soils and trees.

Despite the relatively large N and C stocks accumulated in the soil of *Melaleuca* wetlands, we found evidence of soil decomposition with depth. Specifically, $\delta^{13}C$ significantly decreased with depth, which is a typical pattern of decomposition in terrestrial soils (Nadelhoffer and Fry 1988), but also coastal wetlands (Saintilan and others 2013; Kelleway and others 2016). The decrease in $\delta^{13}C$ values is consistent with loss of accumulated C through pore water exchange (Maher and others 2017). This result contrasts with other coastal wetlands, such as mangroves, which have shown remarkably similar $\delta^{13}C$ values with depth suggesting long-term stability (Adame and Fry 2016). Unlike $\delta^{13}C$, in *Melaleuca* wetlands, C/N and $\delta^{15}N$ values, which are also indicators of stability

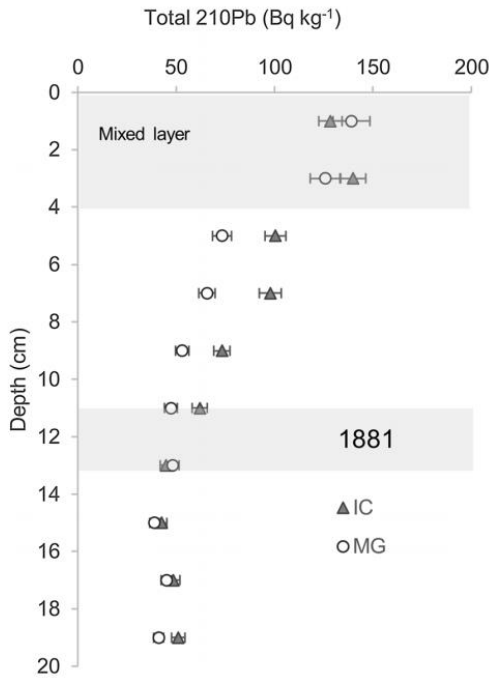


Figure 3. Total ^{210}Pb concentration (Bq kg^{-1}) profiles in two sediment cores (Insulator Creek, IC, and Mungalla Station, MG) from *Melaleuca* wetlands in tropical Australia. The top shaded area represents the mixed layer, and the bottom shaded area represents the oldest sample dated (the year 1881, 11–13 cm, CF/CS model) in the MG core.

(Nadelhoffer and Fry 1988), remained constant with depth. Our data show the some organic C and N compounds in the soil are relatively stable, and if undisturbed, may persist for over a century.

We found that variability in C and N stocks among sites was considerable. For example, HX had the lowest soil C content (≤ 1%) and ecosystem stocks (80 Mg C ha^{-1}), with values slightly higher than sugar cane plantation (55 Mg C ha^{-1}). The site HX was very close to mangroves and marshes and could have been at its salinity tolerance limit. Another example is the HH site, which had a very different isotopic profile compared to the rest of the sites, with significantly lower δ^{13}C and δ^{15}N, and higher C/N values in deep soils. This site differed from the rest as it was permanently flooded, conditions which have favoured methanogenesis, which could explain the low δ^{13}C values across the soil profile (Fry 2006). The high variability of the C and N dynamics among *Melaleuca* wetlands is probably related to the ability of this species to withstand a range of conditions of flooding and salinity (Tran and others 2015), which allows them to form forests in both terrestrial, sporadically flooded or permanently flooded conditions. The high adaptability and resilience of *Melaleuca* trees have allowed them to spread across terrestrial, freshwater, and saline wetlands as a native ecosystem in Australia and as a highly invasive

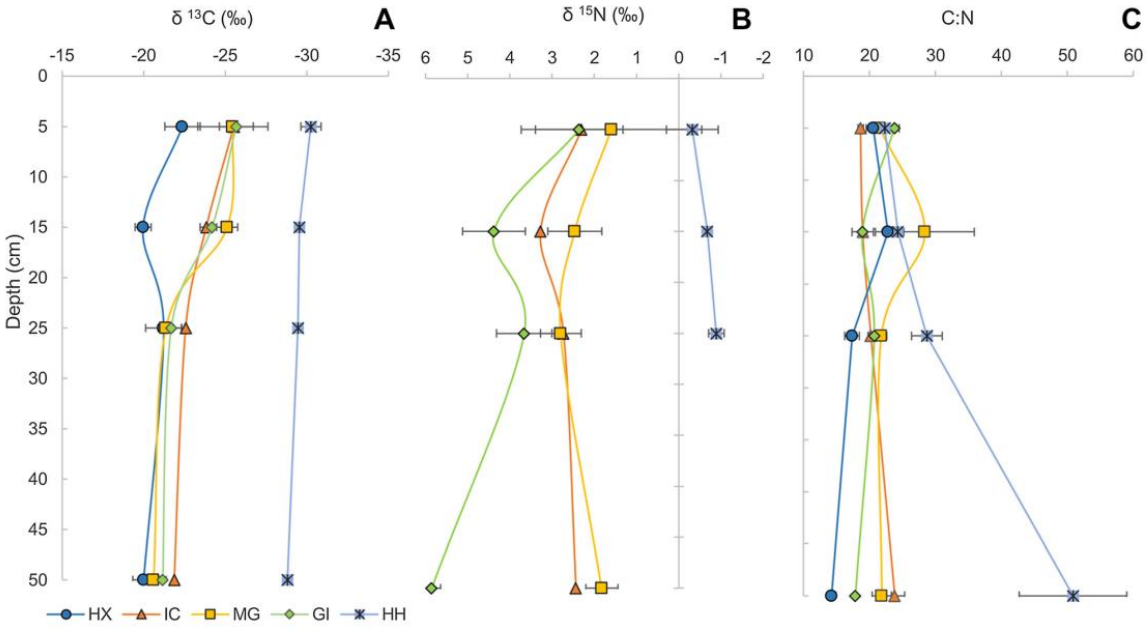


Figure 4. Soil C/N, δ^{13}C, and δ^{15}N (‰) of *Melaleuca* wetlands in tropical Australia. Values are mean ± standard errors of three cores per site. HX and deep soils of HH had N concentrations that were too low for δ^{15}N to be detected.

ecosystem across the American continent (Turner and others 1998).

Management Implications

In Australia, *Melaleuca* wetlands are considered to have an ecosystem C stock of 28 Mg C ha^{-1}, a value which is an order of magnitude lower than that measured in the field (this study and Tran and others 2013a). *Melaleuca* wetlands have suffered from high deforestation rates with estimated losses of over half of their original area in the past century (Turner and others 1998). The underestimation of the C storage of *Melaleuca* wetlands results in the underestimation of their potential emissions arising from their loss, as well as the undervaluation of their protection. The results of this study could be used to incorporate the potential emissions derived from the deforestation and degradation of *Melaleuca* wetlands in Australia's C national reporting (Tran and others 2013a). Additionally, our results support the inclusion of *Melaleuca* wetlands as a potential blue carbon ecosystem and participate in C mitigation programmes such as the Emissions Reduction Fund (the Australian Government's primary C abatement mechanism) and voluntary carbon trading schemes. These schemes support land management activities for reducing C emission, such as the protection or restoration of wetlands (Kelleway and others 2017b).

In terms of N, *Melaleuca* wetlands have the potential to sequester and store large amounts of N, especially in their soils. Conversely, the deforestation, drainage, or degradation of these wetlands could release the N accumulated into adjacent waterways. In the Great Barrier Reef region, where this study was conducted, improving water quality is a government priority (Commonwealth of Australia 2014). The results from this study support the inclusion of *Melaleuca* wetlands for conservation and rehabilitation as a complementary strategy to minimise nitrogen inputs to waterways. In America, *Melaleuca* wetlands are burnt, cut, and flooded to control their spread into native wetland ecosystems (Turner and others 1998). The results of this study can be used to estimate the C and N releases resulting from this management practices, which should be accounted as trade-offs for the expected increase on biodiversity as a result of *Melaleuca* removal.

Finally, there is little understanding of the likely response of coastal *Melaleuca* wetlands to current acceleration in sea-level rise. Broadly, sea-level rise might result in their landward migration, their transition to other wetland ecosystem, or their complete disappearance (Krauss and others 2009; Tran and others 2013b). Recent analysis has shown that moderate rates of relative sea-level rise can enhance the accumulation of C within tidal wetlands by increasing their vertical accommodation space (Rogers and others 2019). However, it is not known to what extent this will apply to supratidal *Melaleuca* wetlands. The encroachment of *Melaleuca* wetland into cultivated lands could increase C and N stocks, their transition to marshes or mangroves will result in a similar C and N balance, and their disturbance or disappearance will result in the release of their large C and N stocks.

ACKNOWLEDGEMENTS

We acknowledge the Traditional Owners of the land in which the field study was conducted, especially the Nywaigi, Djiru, Girramay, and Gulnay people. We thank the Queensland Government through the Advance Queensland Fellowship granted to MFA, the Great Barrier Reef Water Quality Program for their financial support, and the Australian Government's National Environmental Science Program, Tropical Water Quality Hub (Project 3.3.2). Funding was provided to PM by the Generalitat de Catalunya (Grant 2017 SGR-1588) and through an Australian Research Council LIEF Project (LE170100219). This work is contributing to the ICTA ''Unit of Excellence'' (MinECo, MDM2015-0552).

REFERENCES

ABM, Australian Bureau of Meteorology, Viewed September 2018. http://www.bom.gov.au/

ABARES. 2016. Australian Bureau of Agricultural and Resource Economics and Sciences. Department of Agriculture and Water Resources. Australian Government. Australian forest profiles: Melaleuca. http://www.agriculture.gov.au/abares/research-topics/forests

Adame MF, Franklin H, Waltham N, Rodriguez S, Kavehei E, Turschwell M, Balcombe S, Kaniweska P, Burford M, Ronan M. 2019. Nitrogen removal by tropical floodplain wetlands through denitrification. Marine and Freshwater Research, in press.

Adame MF, Fry B. 2016. Source and stability of soil carbon in mangrove and freshwater wetlands of the Mexican Pacific coast. Wetland Ecoly and Management 24:129–37.

Adame MF, Kauffman JB, Medina I, Gamboa JN, Torres O, Caamal JP, Reza M, Herrera-Silveira JA. 2013. Carbon stocks of tropical coastal wetlands within the karstic landscape of the Mexican Caribbean. Chen HYH, editor. PLoS ONE 8:e56569.

Adame MF, Santini NS, Tovilla C, Vázquez-Lule A, Castro L, Guevara M. 2015. Carbon stocks and soil sequestration rates of tropical riverine wetlands. Biogeosciences 12:3805–18.

Appleby P, Oldfield F. 1978. The calculation of lead-210 dates assuming a constant rate of supply of unsupported 210Pb to the sediment. Catena 5:108.

Arias-Ortiz A, Masqué P, Garcia-Orellana J, Serrano O, Mazarrasa I, Marbà N, Lovelock CE, Lavery PS, Duarte CM. 2018. Reviews and syntheses: 210Pb-derived sediment and carbon accumulation rates in vegetated coastal ecosystems—setting the record straight. Biogeosciences 15:6791–818.

Atwood TB, Connolly RM, Almahasheer H, Carnell PE, Duarte CM, Ewers Lewis CJ, Irigoien X, Kelleway JJ, Lavery PS, Macreadie PI, Serrano O, Sanders CJ, Santos I, Steven ADL, Lovelock CE. 2017. Global patterns in mangrove soil carbon stocks and losses. Nature Climate Change 7:523–8.

Barlow B. 1988. Patterns of differentiation in tropical species of *Melaleuca* L. (Myrtaceae). Proceedings of the Ecology Society of Australia 15:239–47.

Boland DJ, Brooker MIH, Chippendale GM, Hall N, Hyland BPM, Johnson RD, Kleinig DA, McDonald MW, Turner JD. 2006. Forest trees of Australia. Collingwood: CSIRO Publishing.

Carsib CF, Hammer KA, Riley TV. 2006. *Melaleuca alternifolia* (Tea Tree) oil: a review of antimicrobial and other medicinal properties. Clinical Microbiol Rev 19:50–62.

Chmura GL, Anisfeld SC, Cahoon DR, Lynch JC. 2003. Global carbon sequestration in tidal, saline wetland soils. Biogeochem Cycles 17:1111–20.

Clough B. 1998. Mangrove forest productivity and biomass accumulation in Hinchinbrook. Mangroves and Salt Marshes 2:191–8.

Commonwealth of Australia. 2014. Reef 2050 Long-Term Sustainability Plan:1–111. https://www.environment.gov.au/marine/gbr/long-term-sustainability-plan

Finlayson CM. 2005. Plant ecology of Australia's tropical floodplain wetlands: a review. Annals of Botany 96:541–55.

Finlayson CM, Cowie ID, Bailey BJ. 1993. Biomass and litter dynamics in a Melaleuca forest on a seasonally inundated floodplain in tropical, northern Australia. Wetland Ecology and Management 2:177–88.

Fortier J, Truax B, Gagnon D, Lambert F. 2015. Biomass carbon, nitrogen and phosphorus stocks in hybrid poplar buffers, herbaceous buffers and natural woodlots in the riparian zone on agricultural land. Journal of Environmental Management 154:333–45.

Fourqurean JW, Duarte CM, Kennedy H, Marbà N, Holmer M, Mateo MA, Apostolaki ET, Kendrick GA, Krause-Jensen D, McGlathery KJ, Serrano O. 2012. Seagrass ecosystems as a globally significant carbon stock. Nature Geoscience 5:505–9.

Fry B. 2006. Isotope ecology. New York: Springer. p 295.

Geoscience Australia, 2005. Viewed March 2018. http://www.ga.gov.au/

Giri C, Ochieng E, Tieszen LL, Zhu Z, Singh A, Loveland T, Masek J, Duke N. 2011. Status and distribution of mangrove forests of the world using earth observation satellite data. Global Ecology and Biogeography 20:154–9.

Gong WK, Ong J-E. 1990. Plant biomass and nutrient flux in a managed mangrove forest in Malaysia. Estuarine Coastal and Shelf Science 31:519–30.

Greenway M. 1994. Litter accession and accumulation in a *Melaleuca quinquenervia* (Vac.)S.T. Blake wetland in south-eastern Queensland. Marine and Freshwater Research 45:1509–19.

Greenway M, Jenkins G. 2004. A comparative study of the effectiveness of wetlands and ponds in the treatment of stormwater in subtropical Australia. 9Th IWA Conference on Wetland Systems for Water Pollution Control, 1–12.

Hayes MA, Jesse A, Hawke B, Baldock J, Tabet B, Lockington D, Lovelock CE. 2017. Dynamics of sediment carbon stocks across intertidal wetland habitats of Moreton Bay, Australia. Global Change Biology 23:4222–34.

Hutchison J, Manica A, Swetnam R, Balmford A, Spalding M. 2014. Predicting global patterns in mangrove forest biomass. Conservation Letters 7:233–40.

Isbell R. 2002. The Australian Soil Classification. (Publishing C, editor.). Melbourne, Australia

Karim F, Kinsey-Henderson A, Wallace J, Arthington AH, Pearson RG. 2012. Modelling wetland connectivity during overbank flooding in a tropical floodplain in north Queensland, Australia. Hydrological Processes 26:2710–23.

Kelleway J, Jeffrey J, Saintilan N, Macreadie P, Ralph P. 2016. Sedimentary factors are key predictors of carbon storage in SE Australian saltmarshes. Ecosystems 19:865–80.

Kelleway JJ, Saintilan N, Macreadie PI, Baldock JA, Heijnis H, Zawadzki A, Gadd P, Jacobsen G, Ralph PJ. 2017a. Geochemical analyses reveal the importance of environmental history for blue carbon sequestration. Journal of Geophysical Research: Biogeosciences 122:1789–805.

Kelleway J, Serrano O, Baldock J, Cannard T, Lavery P, Lovelock C, Macreadie P, Masque P, Saintilan N, Steven A. 2017b. Technical review of opportunities for including Blue Carbon in the Australian government's Emissions Reduction Fund. Canberra: Department of Environment and Energy, Australian Government.

Krauss KW, Duberstein JA, Doyle TW, Conner WH, Day RH, Inabinette LW, Whitebeck JL. 2009. Site condition, structure, and growth of baldcypress along tidal/non-tidal salinity gradients. Wetlands 29:505–19.

Krauss KW, Noe GB, Duberstein JA, Conner WH, Stagg CL, Cormier N, Jones MC, Bernhardt CE, Lockaby BG, From AS, Doyle TW, Day RH, Ensign SH, Pierfelice KN, Hupp CR, Chow AT, Whitbeck JL. 2018. The role of the upper tidal estuary in wetland Blue Carbon storage and flux. Global Biogeochemical Cycles 32:817–39.

Krishnaswami S, Lal D, Marin J, Meybeck M. 1971. Geochronology of lake sediments. Earth and Planetary Science Letters 11:407–14.

Kulkarni MV, Groffman PM, Yavitt JB. 2008. Solving the global nitrogen problem: it's a gas!. Frontiers in Ecology and the Environment 6:199–206.

Lovelock CE, Duarte CM. 2019. Dimensions of Blue Carbon and emerging perspectives. Biology Letters, in press.

Macreadie PI, Ollivier QR, Kelleway JJ, Serrano O, Carnell PE, Ewers Lewis CJ, Atwood TB, Sanderman J, Baldock J, Connolly RM, Duarte CM, Lavery PS, Steven A, Lovelock CE. 2017. Carbon sequestration by Australian tidal marshes. Scientific Reports 7:1–10.

Maher DT, Santos IR, Schulz KG, Call M, Jacobsen Sanders CJ. 2017. Blue carbon oxidation revealed by radiogenic and stable isotopes in a mangrove system. Geophysical Research Letters 44:4889–96.

Meerts P. 2002. Mineral nutrient concentrations in sapwood and heartwood: a literature review. Annals of Forest Science 59:713–22.

Mensforth LS, Walker GR. 1996. Root dynamics of *Melaleuca halmaturorum* in response to fluctuating saline groundwater. Plant and Soil 184:75–84.

Murtha G, Smith C. 1994. Key to the soils and land suitability of the wet tropical coast: Cardwell – Cape Tribulation. Brisbane: CSIRO Division of Soils.

Nadelhoffer KJ, Fry B. 1988. Controls on Natural nitrogen-15 and Carbon-13 abundances in forest soil organic matter. Soil Science Society of American Journal 52:1633–40.

Rasiah V, Armour JD, Cogle AL, Florentine SK. 2010. Nitrate import-export dynamics in groundwater interacting with surface-water in a wet-tropical environment. Australian Journal of Soil Research 48:361–70.

Rayment G, Lyons D. 2001. Australian laboratory handbook of soil and water chemical methods. Australia: CSIRO Press.

Robertson MJ, Wood AW, Muchow RC. 1996. Growth of sugarcane under high input conditions in tropical Australia. III. Accumulation, partitioning and use of nitrogen. Field Crops Research 48:223–33.

Rogers K, Kelleway JJ, Saintilan N, Megonigal JP, Adams JB, Holmquist JR, Lu M, Schile-Beers L, Zawadzki A, Mazumder D, Woodroffe CD. 2019. Wetland carbon storage controlled by millennial-scale variation in relative sea-level rise. Nature Letters 567:91–5.

Saintilan N, Rogers K, Mazumder D, Woodroffe C. 2013. Allochthonous and autochthonous contributions to carbon accumulation and carbon store in southeastern Australian coastal wetlands. Estuarine Coastal and Shelf Science 128:84–92.

Sanchez-Cabeza J, Masque P, Ani-Ragolta I. 1998. 210Pb and 210Po analysis in sediments and soils by microwave acid digestion. Journal of Radioanalytical and Nuclear Chemistry 227:19–22.

State of Queensland. 2014. Environmental Protection (Water) Policy, 2009. Brisbane: Wet Tropics Groundwater Zones.

Tran DB, Dargusch P. 2016. Melaleuca forests in Australia have globally significant carbon stocks. Forest Ecology and Management 375:230–7.

Tran DB, Dargusch P, Herbohn J, Moss P. 2013a. Interventions to better manage the carbon stocks in Australian Melaleuca forests. Land Use Policy 35:417–20.

Tran DB, Dargusch P, Moss P, Hoang TV. 2013b. An assessment of potential responses of *Melaleuca* genus to global climate change. Mitigation and Adaptation Strategies for Global Change 18:851–67.

Tran DB, Hoang TV, Dargusch P. 2015. An assessment of the carbon stocks and sodicity tolerance of disturbed *Melaleuca* forests in Southern Vietnam. Carbon Balance and Management 10:15.

Turner CE, Center TD, Burrows DW, Buckingham GR. 1998. Ecology and management of *Melaleuca quinquenervia*, an invader of wetlands in Florida, U.S.A. Wetland Ecology and Management 5:165–78.

Wilson P, Baker D. 1990. Soils and agricultural land suitability of the wet tropical coast of North Queensland: Ingham area. Brisbane, Australia: Queensland Department of Primary Industries. Land Resources Bulletin. QV90001.



Reef & Rainforest
RESEARCH CENTRE

www.nesptropical.edu.au